

Search for resonances decaying into top-quark pairs using fully hadronic decays in pp collisions with ATLAS at $\sqrt{s} = 7$ TeV



The ATLAS collaboration

E-mail: atlas.publications@cern.ch

ABSTRACT: A search for resonances produced in 7 TeV proton-proton collisions and decaying into top-quark pairs is described. In this Letter events where the top-quark decay produces two massive jets with large transverse momenta recorded with the ATLAS detector at the Large Hadron Collider are considered. Two techniques that rely on jet substructure are used to separate top-quark jets from those arising from light quarks and gluons. In addition, each massive jet is required to have evidence of an associated bottom-quark decay. The data are consistent with the Standard Model, and limits can be set on the production cross section times branching fraction of a Z' boson and a Kaluza-Klein gluon resonance. These limits exclude, at the 95% credibility level, Z' bosons with masses 0.70-1.00 TeV as well as 1.28-1.32 TeV and Kaluza-Klein gluons with masses 0.70-1.62 TeV.

KEYWORDS: Hadron-Hadron Scattering

Contents

1	Introduction	1
2	ATLAS detector	3
3	Data and Monte Carlo samples	3
4	Event selection and physics object reconstruction	4
5	The HEPTopTagger algorithm	5
6	The Top Template Tagger method	9
7	Background estimates	12
	7.1 Background determination for the HEPTopTagger analysis	12
	7.2 Background determination in the Top Template Tagger analysis	15
8	Systematic uncertainties	19
9	Results	24
10	Conclusions	26
	The ATLAS collaboration	34

1 Introduction

Many models of new phenomena beyond the Standard Model (SM) predict resonances in the TeV mass range that decay primarily into top-antitop quark pairs¹ ($t\bar{t}$). This Letter reports on a search for such phenomena in proton-proton (pp) collisions at the Large Hadron Collider (LHC) where both top quarks are reconstructed in their fully hadronic final states and have large transverse momentum (p_T). The decay products of each high- p_T top quark are collimated and merge into one jet with large invariant mass.

Previous searches mostly considered cases where in one or both of the top-quark decays, the intermediate W boson decays leptonically and hence the top-quark decays result in one or two isolated leptons, missing energy from the neutrinos, and jets in the final state [1–8]. The requirements of a well-identified charged lepton isolated from nearby hadronic energy deposits and missing transverse energy reject a large fraction of background from multijet production. However, difficulties arise in these final states when the top-quark decay

¹In the following “top quark” refers to both the top quark and its anti-particle.

particles are collimated, since leptons from the top-quark decay are no longer isolated and thus background contributions with lepton candidates originating from hadronic jets are more difficult to distinguish from the signal.

An alternative approach that is reported in this Letter is to consider final states with high- p_T top quarks that decay hadronically and where the decay products are collimated in the direction of the top-quark. Such searches require the top quarks to have p_T in excess of 200-300 GeV and require rejection of the large background of gluon jets, light-quark jets, as well as c - and b -jets. The CMS Collaboration employed this technique in a recent study [9].

In the present analysis, two complementary algorithms are used to identify top-quark decays and reconstruct the top-quark momentum for data collected with the ATLAS detector at a centre-of-mass energy of 7 TeV. The first algorithm is the HEPTopTagger method [10, 11] that tests the substructure of a jet reconstructed with the Cambridge/Aachen (C/A) algorithm [12] with a large distance parameter $R = 1.5$ (“fat jets”) for its compatibility with a hadronic top-quark decay. This method is effective in identifying top-quark jets with $p_T > 200$ GeV. The second algorithm is the Top Template Tagger method [13, 14] that uses a large set of possible patterns of energy deposits (templates) from hadronic top-quark decays to identify the best match to the observed energy deposits. The quality of the match is used to reject light quark and gluon jets. The Top Template Tagger uses jets reconstructed with the anti- k_t algorithm [15] with a smaller distance parameter of $R = 1.0$ and is optimised to identify top quarks with $p_T > 450$ GeV. The invariant mass distributions of the $t\bar{t}$ pair candidates identified using each algorithm are examined for evidence of resonance structure.

Two specific models that predict resonances of masses m with narrow and broad decay widths Γ are considered: leptophobic topcolour Z' bosons with $\Gamma/m = 1.2\%$ [16] and Kaluza-Klein (KK) gluons from the bulk Randall-Sundrum model (RS)² with $\Gamma/m = 15.3\%$ [17–19]. The theoretical cross sections for the Z' boson model and the bulk Randall-Sundrum model (RS) are calculated with the PYTHIA v6.421 MC generator [20] and the MADGRAPH v4.4.51 [21] MC generator, respectively. A k-factor of 1.3 is applied to the Z' boson cross sections to account for NLO effects [22]. Recent results from the ATLAS Collaboration in the lepton plus jets channel [7, 8] exclude Z' bosons (KK gluons) with masses 0.5-1.15 TeV (0.5-1.5 TeV) at 95% credibility level (CL). The CMS Collaboration obtained similar results [9, 23] excluding 0.50-1.49 TeV for narrow ($\Gamma/m = 1.2\%$) Z' signals, 0.50-2.04 TeV for broad ($\Gamma/m = 10\%$) Z' signals, and 1.00-1.82 TeV for KK gluon signals.

This Letter is organised as follows: section 2 describes the ATLAS detector and section 3 summarises the data samples and Monte Carlo (MC) event generators used in the analysis. The event selection and the definition of the reconstructed objects are given in section 4. The HEPTopTagger and Top Template Tagger algorithms are described in section 5 and section 6, respectively. Estimates of the background rates and systematic uncertainties are given in section 7 and section 8, respectively. In section 9 the resulting $t\bar{t}$ mass spectrum and exclusion limits are presented.

²The left-handed (g_L) and right-handed (g_R) couplings to quarks in this model are: $g_L = g_R = -0.2g_S$ for light quarks including charm, where $g_S = \sqrt{4\pi\alpha_s}$; $g_L = g_S$ and $g_R = -0.2g_S$ for bottom quarks; and $g_L = g_S$ and $g_R = 4g_S$ for the top quark.

2 ATLAS detector

The ATLAS detector [24] at the LHC [25] covers nearly the entire solid angle³ around the pp collision point. The inner tracking detector (ID) comprises a silicon pixel detector, a silicon microstrip detector, and a transition radiation tracker, providing tracking capability within $|\eta| < 2.5$. The ID is surrounded by a thin superconducting solenoid providing a 2 T axial magnetic field and by liquid-argon (LAr) electromagnetic sampling calorimeters with high granularity. An iron/scintillator tile calorimeter provides hadronic energy measurements in the central rapidity range ($|\eta| < 1.7$). The end-cap and forward regions, covering $1.37 < |\eta| < 4.9$, are instrumented with LAr calorimeters for both electromagnetic and hadronic energy measurements. The calorimeter system is surrounded by a muon spectrometer incorporating three superconducting toroid magnet assemblies.

A three-level trigger system is used to select the events for subsequent analysis. The level-1 trigger is implemented in hardware and uses a subset of the detector information to reduce the rate to at most 75 kHz. This is followed by two software-based trigger levels that together reduce the event rate to a maximum of 400 Hz.

3 Data and Monte Carlo samples

The analysis is performed using pp collision data collected in 2011 corresponding to an integrated luminosity of $4.7 \pm 0.2 \text{ fb}^{-1}$ [26, 27]. With the increasing instantaneous luminosity of the LHC, the average number of simultaneous pp interactions per beam crossing (pile-up) at the beginning of a given fill of the LHC increased from about 6 to 17 during the 2011 data-taking period. The 2011 data pile-up conditions are included in the Monte Carlo simulation.

The main background contributions to a resonant signal in the $t\bar{t}$ channel consist of SM $t\bar{t}$ production and multijet events from gluon and non-top-quark production. Fully hadronic SM $t\bar{t}$ production is simulated using the MC@NLO v4.01 generator [28, 29] with CT10 parton distribution functions (PDFs) [30] and assuming a top-quark mass of 172.5 GeV. Final-state parton showers are simulated and hadronised using the HERWIG v6.5 [31] program in association with the JIMMY underlying event model [32]. A $t\bar{t}$ production cross section of 167 pb is used, calculated at approximate next-to-next-to-leading order (NNLO) in QCD using the HATHOR v1.2 Monte Carlo program [33]. This prediction employs the MSTW2008 NNLO PDF sets [34].

The other background contributions, dominated by multijet events arising from the production of light quarks and gluons, but also including smaller background contributions such as W +jets production and any remaining contributions from $t\bar{t}$ events where one of the top quarks decays semileptonically (lepton+jet events), are estimated from data in signal-depleted control regions. These are referred to as the multijet background in the

³ATLAS uses a right-handed coordinate system with its origin at the nominal interaction point (IP) in the centre of the detector and the z -axis along the beam pipe. The x -axis points from the IP to the centre of the LHC ring, and the y -axis points upward. Cylindrical coordinates (r, ϕ) are used in the transverse (x, y) plane, ϕ being the azimuthal angle around the beam pipe. The pseudorapidity is defined in terms of the polar angle θ as $\eta = -\ln \tan(\theta/2)$. Distances in (η, ϕ) space are given as $\Delta R = \sqrt{(\Delta\phi)^2 + (\Delta\eta)^2}$.

following. Cross-checks of these background estimates are performed using PYTHIA [35] MC dijet samples.

Simulated signal samples for the $pp \rightarrow Z' \rightarrow t\bar{t}$ process are produced using the PYTHIA v6.421 MC generator with MSTW2008 PDFs [34]. KK gluon final states are generated with the MADGRAPH v4.4.51 [21] MC generator with CTEQ6L1 PDFs [36] and using the PYTHIA MC to model the parton shower and hadronization. These are calculated with leading-order matrix elements. Possible interference effects between the $t\bar{t}$ resonances and the SM $t\bar{t}$ continuum are not taken into account.

The generated events are passed through a full simulation of the ATLAS detector [37] based on GEANT4 [38] and then processed with the same reconstruction algorithms used for the pp collision data events.

4 Event selection and physics object reconstruction

The events for this analysis are selected with triggers matched to efficiently identify collisions that meet the subsequent selection requirements. The trigger for the HEPTopTagger selection uses the logical OR of two triggers based on jets defined using the anti- k_t algorithm with a distance parameter $R = 0.4$. The first one requires the transverse energy (E_T) of at least one jet to satisfy $E_T > 100$ GeV and the scalar sum of all jets to satisfy $\sum E_T > 350$ GeV (> 400 GeV for later data-taking periods). The second trigger requires at least five jets with $E_T > 30$ GeV. The combined single-jet and $\sum E_T$ trigger is useful as it does not rely on the precise topology of the $t\bar{t}$ decay, which may change due to the splitting and merging of jets, but relies mainly on the total energy deposited in the calorimeter. The high-jet-multiplicity trigger is used to increase the efficiency at low $t\bar{t}$ invariant mass ($m_{t\bar{t}}$) where the top-quark decay products are often reconstructed individually at trigger level. The trigger for the Top Template Tagger selection requires an event to have at least one anti- k_t jet with a distance parameter $R = 1.0$ and $E_T > 240$ GeV.

The events for both tagger selections are required to have a primary vertex with at least five tracks with $p_T > 0.4$ GeV. In the case of multiple vertex candidates the primary vertex is defined as the one with the largest $\sum p_T^2$ of the tracks associated with it.

The analysis uses various jet-finder algorithms and distance parameters to reconstruct top-quark candidates and to suppress background. These jets are formed from topologically-related calorimeter energy deposits ('topoclusters') [39, 40] using the FAST-JET software [41, 42]. The topoclusters are calibrated using the local cluster weighting method (LCW [43]).

Events for the HEPTopTagger selection are required to contain at least two fat jets with $p_T > 200$ GeV and $|\eta| < 2.5$. Each of these fat jets is subjected to the HEPTopTagger algorithm (explained in detail in the following section), which either rejects the jet as being incompatible with a hadronic top-quark decay or reconstructs a top-quark candidate four-momentum. To ensure high reconstruction efficiency, only top-quark candidates with $p_T > 200$ GeV are considered in the following.

Events for the Top Template Tagger selection are required to have at least two jets reconstructed with the anti- k_t algorithm with a distance parameter of $R = 1.0$, with one jet with $p_T > 500$ GeV and $|\eta| < 2.0$, and a second jet with $p_T > 450$ GeV and $|\eta| < 2.0$.

In both selections, the leading and next-to-leading jets are required to satisfy one of the top-quark tagging algorithms. The $t\bar{t}$ invariant mass is constructed from the four-momenta of these two top-quark candidates.

To further suppress background events in which multiple light-quark and/or gluon jets satisfy the kinematic requirements, a neural-network-based b -tagging algorithm is used [44]. This algorithm uses information on the impact parameter, the secondary vertex, and the decay topology as its input.

Candidate b -quark jets are defined using the anti- k_t algorithm with a distance parameter $R = 0.4$, with each jet calibrated to the energy scale of hadronic jets [40]. These b -jets must satisfy the requirements $p_T > 25$ GeV and $|\eta| < 2.5$. In addition, more than 75% of the transverse momentum of the tracks associated with the jet must be carried by tracks with $p_T > 0.5$ GeV originating from the primary vertex. In the HEPTopTagger (Top Template Tagger) selection, the b -quark candidates must lie within $\Delta R = 1.4$ (1.0) of a fat jet axis such that each tagged top-quark jet is associated with a unique b -quark tagged jet. The b -tagging efficiency for b -jets from decays of high- p_T top quarks ranges from 50% to 70%, decreasing with increasing jet p_T because of the increasing collimation of the charged particles in the jet. With the same algorithm, about 3.5% (7%) of light-quark and gluon jets are mistagged as b -jets at $p_T = 200$ GeV ($p_T = 1$ TeV).

Additional data quality criteria are applied, rejecting events that contain anti- k_t $R = 0.4$ jets that are identified as likely resulting from instrumental failure or non-collision background (e.g. cosmic rays, beam gas and beam halo) [40].

The selected event samples are made complementary to samples used in searches for $t\bar{t}$ resonances in the lepton+jet and dilepton channels by rejecting events that contain at least one isolated electron (with $p_T > 25$ GeV) or muon candidate (with $p_T > 20$ GeV) [45].

5 The HEPTopTagger algorithm

The HEPTopTagger method is designed to reconstruct hadronically decaying top quarks that are sufficiently boosted for their decay products to lie inside a single fat jet. The performance of the HEPTopTagger has been studied extensively using ATLAS pp collision data and simulated events [46].

The HEPTopTagger method operates on a fat jet that has been constructed using the C/A jet algorithm. The same algorithm is employed to re-cluster the fat jet constituents into subjets. Previous studies [47] have shown that, compared to the k_t and SIScone [48] jet finders, the C/A algorithm provides the best signal efficiency and background rejection in the presence of underlying event activity for top-quark taggers like the HEPTopTagger. In the following the term “top-quark candidate” refers to the object resulting from the HEPTopTagger procedure.

The main steps of the method are described in the following; for a detailed description see ref. [11]. In a first phase, the input fat jet is split into subjets by undoing the last C/A clustering steps. This procedure is repeated until all subjet masses are below 50 GeV. These subjets form the basis of the substructure analysis. All combinations of three subjets (“triplets” in the following) are tested for compatibility with a hadronic top-quark decay using the following procedure. First, contributions from the underlying event and pile-up are removed in a filtering step: The C/A algorithm is re-run on the topoclusters of the triplet subjets with a distance parameter equal to half of the smallest pair-wise distance between the triplet subjets (but at most 0.3), and only the resulting five most energetic subjets are kept; the remaining activity is discarded. More than three subjets are potentially retained to account for possible QCD radiation in order to improve the reconstruction of the top-quark decay.

The constituents of those five subjets are then re-clustered exclusively [42, 49] into three subjets again using the C/A algorithm. The reconstructed energy of the subjets is calibrated to the energy of the incoming hadron jet using a simulation of the calorimeter response to particle jets [40]. The three sub-jets are then tested for compatibility with being products of a $t \rightarrow Wb \rightarrow q'\bar{q}b$ decay, using invariant mass ratios. If the mass ratio requirements are met, the top-quark candidate four-momentum is obtained by summing the four-momenta of the subjets. The invariant mass m_t of the top-quark candidate is required to lie in the range from 140 to 210 GeV, otherwise this triplet is discarded. If a top-quark candidate is found in more than one triplet, only the one with its mass closest to the measured top-quark mass [50] of 172.3 GeV is used.

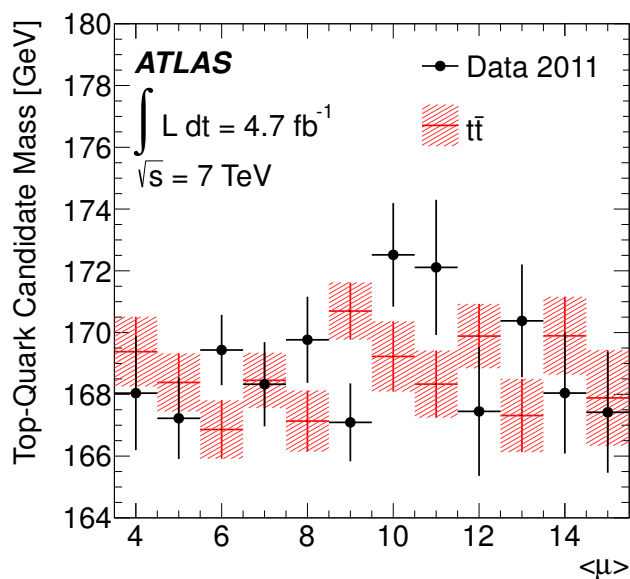
Distributions are shown in figure 1 of the mean reconstructed top-quark candidate mass (a) and the reconstructed $t\bar{t}$ mass averaged over the whole mass spectrum (b) as a function of the average number of interactions per bunch-crossing for data and simulated $t\bar{t}$ events. The events are required to satisfy the HEPTopTagger selection and to have two top-quark candidates. No systematic shift of the mass with increased pile-up is observed within the statistical uncertainties.

The reconstructed $t\bar{t}$ mass predicted by the MC simulations for various Z' and KK gluon masses is shown in figure 2.

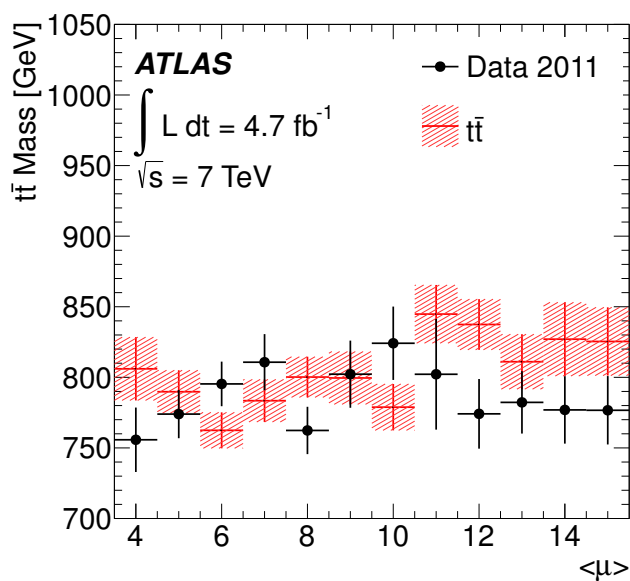
The total selection efficiency including both the HEPTopTagger and b -tagging requirements is given in table 1 for various Z' boson and KK gluon masses, in events where the top quarks decay hadronically. The efficiency is dominated by the top-tagging and b -tagging efficiencies, which vary as a function of the top- and bottom-quark momenta and are limited from above by

$$\varepsilon_{b\text{-tag, max}}^2 \cdot \varepsilon_{\text{top-tag, max}}^2 \approx 10\%, \tag{5.1}$$

where $\varepsilon_{b\text{-tag, max}}$ is the maximum b -tagging efficiency of 80% and $\varepsilon_{\text{top-tag, max}}$ is the maximum top-tagging efficiency of 40% for hadronically-decaying top quarks. The efficiency drops for higher masses because of the decreasing b -tagging efficiency.

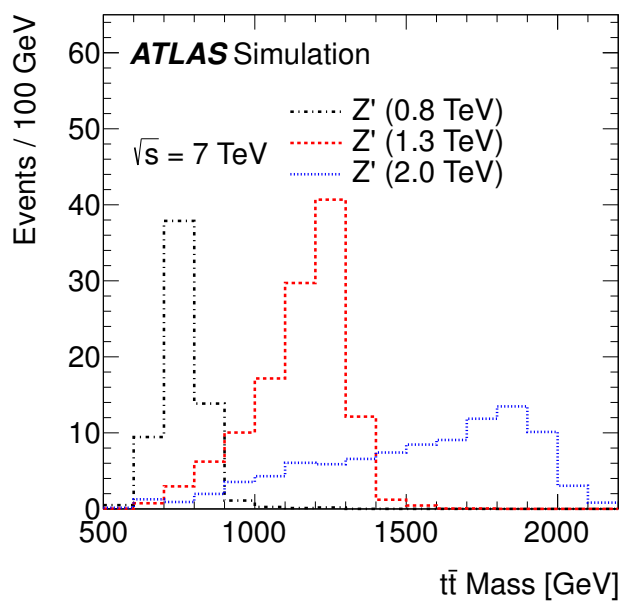


(a)

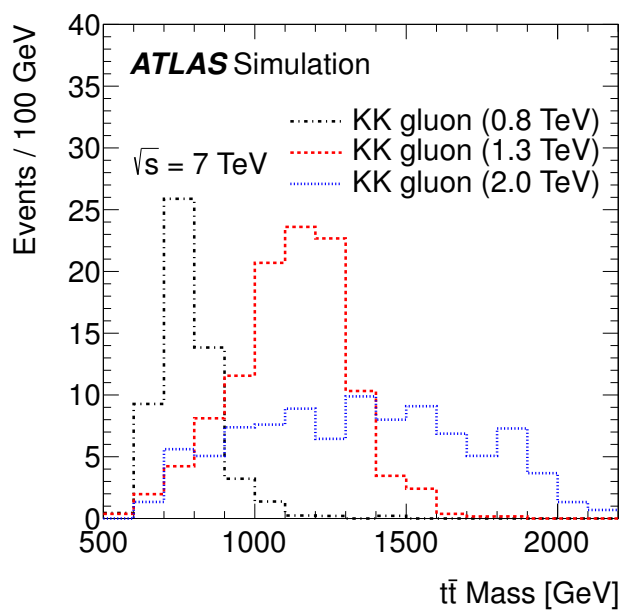


(b)

Figure 1. Distributions of (a) mean HEPTopTagger top-quark candidate mass and (b) mean reconstructed $t\bar{t}$ mass as a function of the average number of interactions per bunch-crossing, $\langle\mu\rangle$, for data and simulated $t\bar{t}$ events with the full selection applied. Only statistical uncertainties are shown.



(a)



(b)

Figure 2. Distributions of the reconstructed $t\bar{t}$ mass predicted by MC simulations for (a) Z' boson and (b) KK gluon benchmark models with various mass values for the HEPTopTagger analysis with the full selection applied. For each model, $\sigma(pp \rightarrow Z'/\text{KK gluon}) \times BR(Z'/\text{KK gluon} \rightarrow t\bar{t})$ is fixed to 1 pb and an integrated luminosity of 4.7 fb^{-1} is assumed.

Model	Total Efficiency (%)	
	HEPTopTagger	Template Tagger
Z' (0.5 TeV)	0.03 ± 0.01	—
Z' (0.8 TeV)	2.96 ± 0.08	—
Z' (1.0 TeV)	4.76 ± 0.09	0.48 ± 0.05
Z' (1.3 TeV)	5.67 ± 0.11	6.37 ± 0.13
Z' (1.6 TeV)	5.40 ± 0.10	8.13 ± 0.16
Z' (2.0 TeV)	4.44 ± 0.10	6.26 ± 0.13
g_{KK} (0.7 TeV)	1.70 ± 0.13	—
g_{KK} (1.0 TeV)	4.13 ± 0.21	0.74 ± 0.10
g_{KK} (1.3 TeV)	5.14 ± 0.23	5.02 ± 0.25
g_{KK} (1.6 TeV)	4.72 ± 0.22	6.43 ± 0.26
g_{KK} (2.0 TeV)	4.44 ± 0.22	5.22 ± 0.21

Table 1. Total efficiency (in %) for selecting Z' bosons and KK gluons (g_{KK}) that have decayed to $t\bar{t}$ pairs. These are the efficiencies determined by the MC calculations divided by the SM branching fraction of 46% for both top quarks to decay hadronically. All uncertainties are statistical only.

6 The Top Template Tagger method

The Top Template Tagger method [13, 14] is based on the concept that an infrared-safe set of observables can be defined that quantify the overlap between the observed energy flow inside a jet and the four-momenta of the partons arising from a top-quark decay. An “overlap function” ranging from 0 to 1 is defined that quantifies the agreement in energy flow between a given top-quark decay hypothesis (a template) and an observed jet. One then cycles over a large set of templates chosen to cover uniformly the 3-body phase space for a top-quark decay at a given p_T and finds the template that maximises this overlap, denoted as OV_3 . A requirement of $OV_3 > 0.7$ is made.

Sets (or “libraries”) of approximately 300,000 templates are generated in steps of top-quark p_T of 100 GeV starting from 450 GeV by calculating the parton-level daughters for a top quark in its rest frame and then boosting the daughters to the p_T of the given library. Studies of the top-quark jet tagging efficiency using MC data and of light quark/gluon jet rejection observed in the data were used to determine the size of the p_T steps and the minimum number of templates for each library that maximise the top-quark tagging efficiency while retaining high rejection against light quark/gluon jets. For each jet candidate, the overlap function is defined as

$$OV_3 = \max_{\{\tau_n\}} \exp \left[- \sum_{i=1}^3 \frac{1}{2\sigma_i^2} \left(E_i - \sum_{\substack{\Delta R(\text{topo},i) \\ < 0.2}} E_{\text{topo}} \right)^2 \right], \quad (6.1)$$

where $\{\tau_n\}$ is the set of templates defined for the given jet p_T , E_i are the parton energies of the top-quark decay daughters for the given template, E_{topo} is the energy of a topocluster,

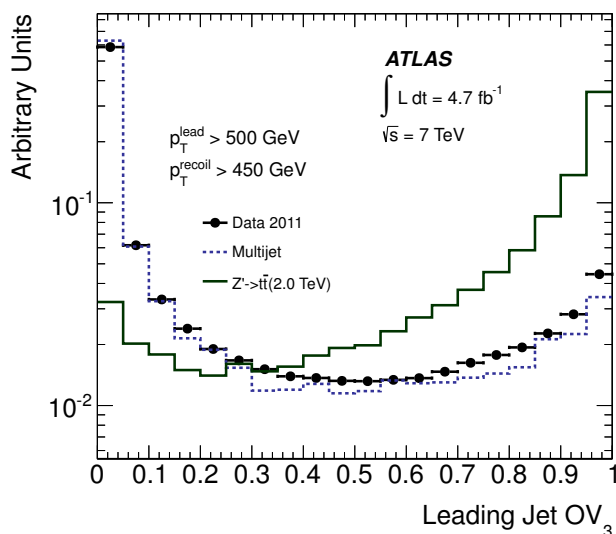


Figure 3. The OV_3 distributions for the leading jets in the 2 TeV $Z' \rightarrow t\bar{t}$ MC sample, a multijet-dominated 2011 data sample, and the multijet MC sample. The data and multijet MC distributions are from the samples prior to making any b -tagging or jet mass requirements on either jet, and so are dominated by light quark/gluon jets.

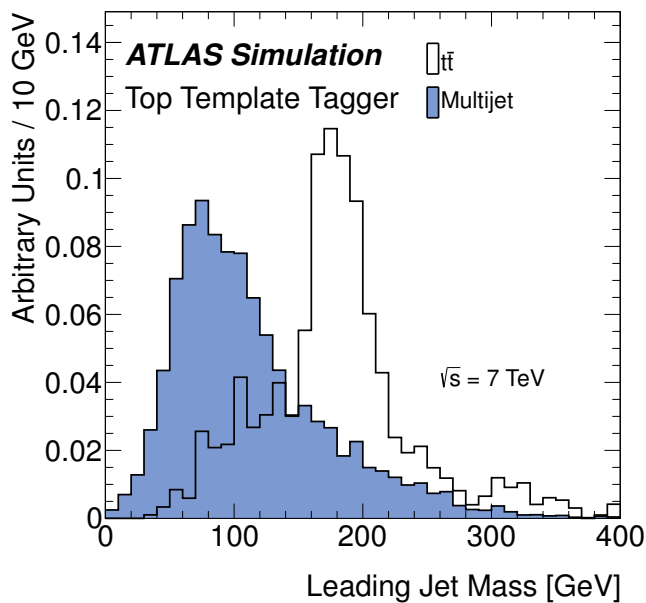
and $\Delta R(\text{topo}, i)$ is the $\eta - \phi$ distance between the i^{th} parton and a given topocluster. The first sum is over the three partons in the template and the second sum is over all topoclusters that are within $\Delta R(\text{topo}, i) = 0.2$ and that have $p_T > 2$ GeV. The weighting variable is

$$\sigma_i = E_i/3. \tag{6.2}$$

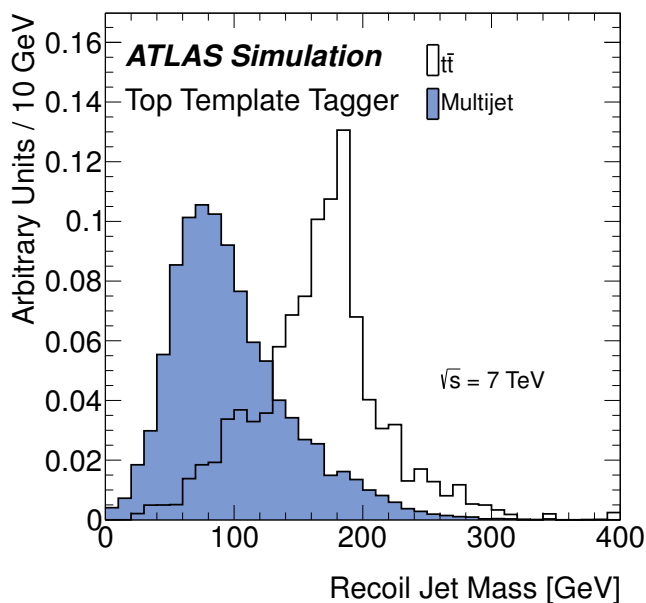
The three tunable parameters in the OV_3 calculation — the size of the cone used to match topoclusters with the parton, the minimum p_T requirement on the topocluster, and the weight σ_i — have been determined from studies of the tagger’s performance judged by tagging efficiency and background rejection. The overall performance is insensitive to the specific parameter values chosen. The OV_3 distributions for a Z' MC sample, a multijet-dominated 2011 data sample, and the multijet MC sample are shown in figure 3, illustrating the separation of top-quark jets from the light quark/gluon jets in the large OV_3 region.

The jet mass, m_j , defined as the invariant mass of the topoclusters added together as massless four-momenta [51], has been shown to be an effective discriminant between top-quark jets and light quark/gluon jets, even in the presence of multiple pp interactions [52, 53]. A data-driven pile-up correction scheme for the jet mass is used, which measures the average mass shift experienced by jets using the flow of energy far from the jet as a function of the number of multiple interactions in the event [54, 55]. The discrimination of the pile-up-corrected jet mass between light quark/gluon jets and top-quark jets is illustrated in figure 4 for the leading and next-to-leading (or recoil) jet in the MC events that satisfy the Top Template Tagger selection.

The jet mass m_j is required to be within ± 50 GeV of the top-quark mass.



(a)



(b)

Figure 4. Pile-up-corrected jet mass distribution in the multijet and $t\bar{t}$ MC samples for (a) the leading and (b) recoil jets. In both cases, the jet mass requirement has been applied on the opposing jet in the event. The distributions are independently normalised to unit area.

The jet mass and $OV_3 > 0.7$ requirements together have a rejection power of ~ 10 for light quark/gluon jets that satisfy the kinematic requirements imposed on the jets, based on studies of samples dominated by light quark/gluon jets, with an overall MC efficiency for selecting top-quark jets of $\sim 75\%$. Although OV_3 and m_j are found to be correlated for a given jet, the addition of the jet mass requirement increases the rejection against light quark/gluon jets after an OV_3 requirement by a factor of two. The combination of the OV_3 and m_j requirements is therefore the core element of the Top Template Tagger.

To verify that the tagger behaviour on top-quark jets is well modelled in the MC simulations, an auxiliary analysis of the Top Template Tagger sample is performed in which the m_j and OV_3 requirements are relaxed on the leading jet. The resulting jet mass distribution, shown in figure 5(a), illustrates a clear peak from top-quark jets on top of a large background from light quark/gluon jets. The number of top-quark jets in this sample is measured by performing a fit to the background and top-quark jet signal, where the background shape is determined from those events where the b -tag requirement has been removed from the recoil jet and the top-quark signal shape is obtained from the SM $t\bar{t}$ MC simulations. A smooth parameterisation has been used to describe the two distributions in the fit. The number of top-quark jets that survive the jet mass and OV_3 requirements on the leading jet is determined by subtracting the background in the signal region. This results in a measured efficiency of the jet mass and OV_3 requirement on top-quark jets of 0.81 ± 0.25 , which is in agreement with the estimate from the MC simulations of 0.75 ± 0.07 (both statistical and systematic sources of uncertainty are included).

A similar analysis can be performed, interchanging the role of the leading jet and the recoil jet in the event. This results in the jet mass distribution shown in figure 5(b), and in a top-quark tagging efficiency for the recoil jet of 0.62 ± 0.20 , to be compared with the MC prediction of 0.62 ± 0.05 .

The overall efficiency of the Top Template Tagger selection on various signal samples is summarized in table 1.

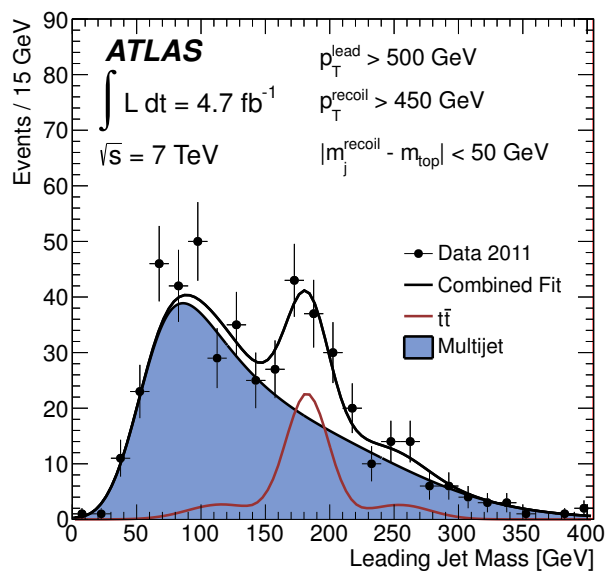
7 Background estimates

The background contributions for both tagging analyses are estimated using control regions defined by loosening the selection requirements for top-quark candidates and for associated b -tagged jets.

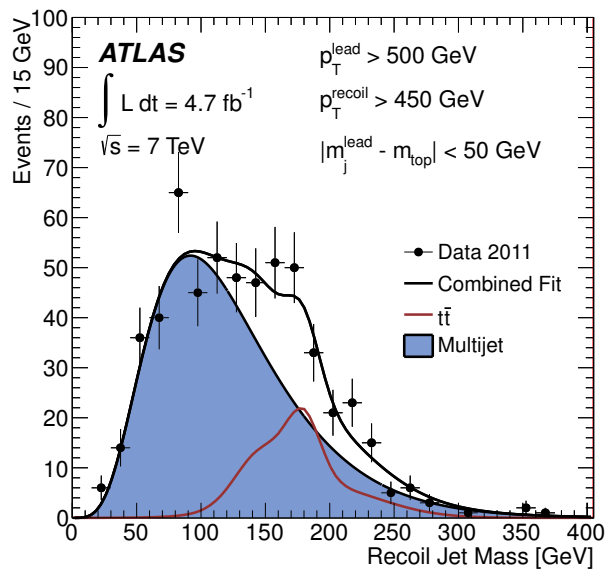
7.1 Background determination for the HEPTopTagger analysis

Six classes of events are created for the HEPTopTagger analysis, as outlined in table 2. They depend on the number of top-quark candidates and b -tagged jets. Regions Y and Z contain the events with at least two b -tags, with region Y (Z) additionally containing events with one (two or more) top-quark candidate(s). Region Z constitutes the signal region.

The contribution of SM $t\bar{t}$ production to each region is estimated from simulation and validated with data in region Y as follows: the top-quark candidate mass distribution in data, shown in figure 6, is fitted with the sum of a $t\bar{t}$ template and a multijet background template, to extract the $t\bar{t}$ background fraction, exploiting the different shapes. The $t\bar{t}$



(a)



(b)

Figure 5. The jet mass distributions for the leading (a) and for the recoil (b) jet when all other requirements have been made on the sample except the mass and OV_3 requirements on the jet being considered. The fits are described in the text.

	1 top-tag	≥ 2 top-tags
no b -tag	U(0.3%)	V(2.4%)
1 b -tag	W(3.2%)	X(24.3%)
≥ 2 b -tags	Y(22.5%)	Z(80.9%)

Table 2. The classes of events used to calculate the data-driven prediction for multijet background events in the HEPTopTagger analysis. The numbers in parentheses are the estimated $t\bar{t}$ purities in each region, given by the expected number of events arising from SM $t\bar{t}$ production divided by the number of observed events in that region.

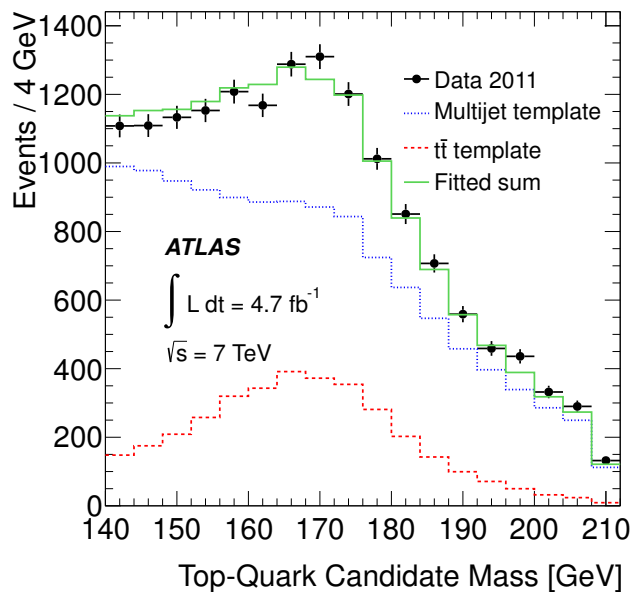


Figure 6. The distribution of the HEPTopTagger top-quark jet candidate mass in the sideband region Y for data, the templates for multijet background and SM $t\bar{t}$ production and the fitted sum.

template is taken from simulation. The multijet background template is defined as the data distribution in region W after subtracting the small contribution expected from SM $t\bar{t}$ production in that region.

The result is shown in figure 6. The selection of the top-quark candidate closest in mass to the top-quark mass when multiple top-quark candidates are reconstructed causes a small bias in the multijet background distribution, as seen in the figure. The ratio of the fitted $t\bar{t}$ event yield to the predicted yield is 1.01 ± 0.09 , where the uncertainty is statistical. This ratio is used to correct the normalisation of the SM $t\bar{t}$ contribution in the determination of the multijet background in the signal region. The resulting SM $t\bar{t}$ yield in signal region Z is estimated to be 770^{+220}_{-180} (stat. \oplus syst.) events.

The multijet background is estimated by exploiting the fact that the number of b -tags and the number of top-quark tags are uncorrelated for this background.⁴ The shape of the

⁴The HEPTopTagger does not use b -tagging information internally and hence the probability for a multijet background event to fake a top-quark signal is independent of the probability for it to fake a

multijet background for a given variable (e.g. $m_{t\bar{t}}$) is estimated from the weighted average of the distribution of that variable in regions V and X, normalised by the yields in regions U and W respectively, and scaled by the event count in region Y:

$$\frac{dn_Z}{dm_{t\bar{t}}} = \left(\frac{1}{n_U} \times \frac{dn_V}{dm_{t\bar{t}}} + \frac{1}{n_W} \times \frac{dn_X}{dm_{t\bar{t}}} \right) \times \frac{n_Y}{2}, \quad (7.1)$$

in which n_i is the number of events in region i after subtracting the expected SM $t\bar{t}$ background normalised to the observed $t\bar{t}$ yield. Hence the $t\bar{t}$ and multijet background contributions are anti-correlated. The resulting estimate for the multijet background in the signal region is 130 ± 70 (stat. \oplus syst.) events.

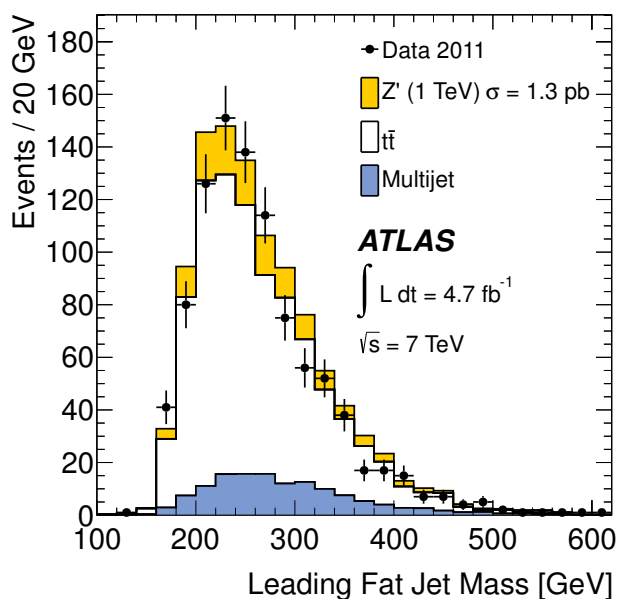
To check that the multijet and SM $t\bar{t}$ background predictions are consistent with the data and to illustrate that the HEPTopTagger identifies top-quark jets effectively, figures 7 and 8 show comparisons of predicted and observed distributions in the signal region: of the fat-jet mass (figure 7(a)), the top-quark candidate mass (figure 7(b)), and the substructure variables m_{23}/m_{123} (figure 8(a)) and $\arctan(m_{13}/m_{12})$ (figure 8(b)). In these ratios m_{123} is the invariant mass of all three subjets and m_{ij} is the invariant mass of subjets i and j , where the subjets have been sorted by p_T in descending order. The data are consistent with the sum of the multijet and SM $t\bar{t}$ background predictions for all distributions.

7.2 Background determination in the Top Template Tagger analysis

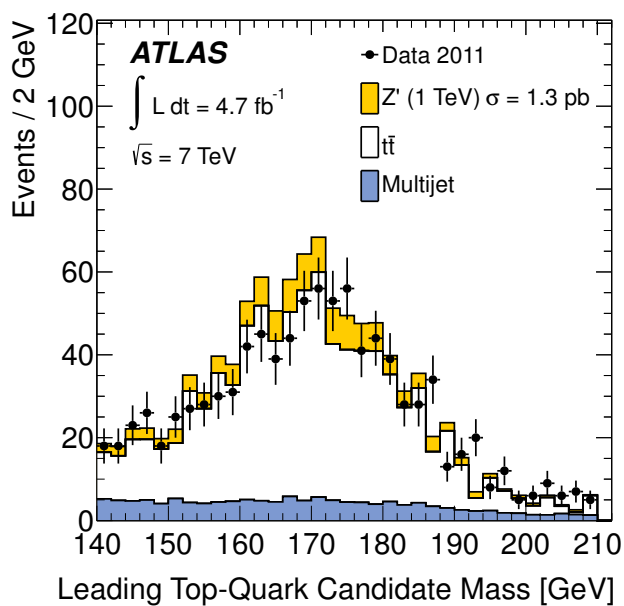
The multijet background for the Top Template Tagger analysis is estimated in a manner similar to the HEPTopTagger analysis. Various control regions are used in order to reduce biases resulting from the observed correlations in Top Template Tagger tagging efficiencies between the recoil and leading jet.

The sample of events in the Top Template Tagger analysis prior to requiring either top-quark tags or b -quark tags is divided into 16 discrete and non-overlapping subsamples, as shown in figure 9. The jet mass requirement has been applied to both the leading and recoil jets in all subsamples. An expected correlation in the masses of the leading and recoil jets [56] leads to a non-negligible correlation in the top-quark tagging efficiency for the two jets in dijet events. On the other hand, the b -quark tagging efficiency of the two jets is uncorrelated. Jets produced from $b\bar{b}$ pairs would create a small correlation, but their overall rate is expected to be negligible in the samples used below to calculate the multijet background.

The rate of multijet background events in the signal region (subsample P) is calculated with an iterative method that uses the lack of correlation in b -tagging efficiencies between the leading and recoil jets. In its simple form, a two-dimensional-sideband counting technique for background estimation requires events to be selected using pairs of uncorrelated variables. For example, in our subsample grid, the top-tagging state of the leading jet is not correlated to the b -tagging state of the recoil jet in multijet background events. Therefore, the ratio of background events in region D to region C should be the same as the ratio of background events in region B to region A. This relation can be used to predict the background rate in region D using the observed rates in the other three regions. The predicted b -quark signal. This is verified using dijet MC samples.

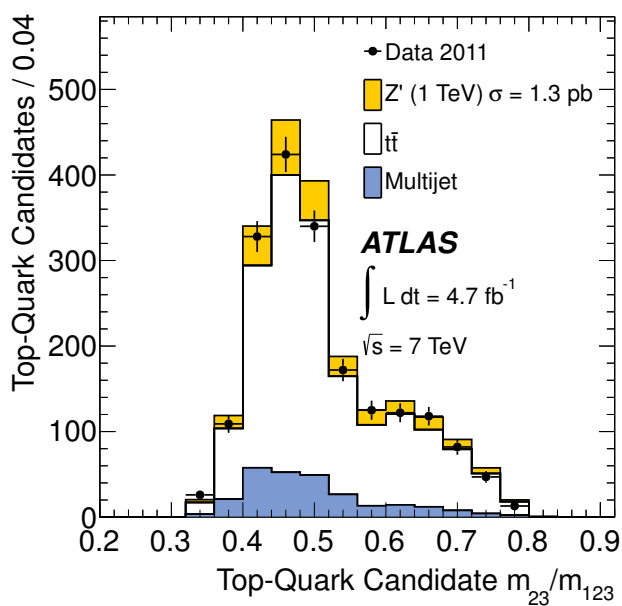


(a)

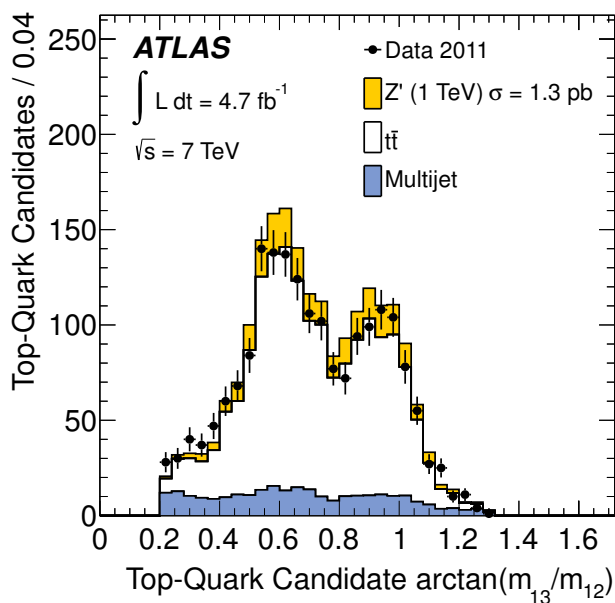


(b)

Figure 7. Signal region distributions of (a) the mass of the leading p_T fat jet and (b) the mass of the leading p_T top-quark candidate. Also shown are the prediction for SM $t\bar{t}$ production, the multijet background contribution as estimated from data, and a hypothetical Z' boson signal.



(a)



(b)

Figure 8. Signal region distributions of the top-quark candidate substructure variables m_{23}/m_{123} (a) and $\arctan(m_{13}/m_{12})$ (b). Also shown are the prediction for SM $t\bar{t}$ production, the multijet background contribution as estimated from data, and a hypothetical Z' boson signal.

P = signal region

		P = signal region			
		t + b	J	K	L
Recoil Jet	b	B	D	H	N
	t	E	F	G	M
	no-tag	A	C	I	O
			no-tag	t	b
		Leading Jet			

Figure 9. The 16 subsamples into which the Top Template Tagger data are divided, based on whether the leading and recoil jets have a b -quark tag, and on whether they satisfy the Top Template tag requirements of $OV_3 > 0.7$. The jet mass requirement of $|m_j - m_t| < 50$ GeV is applied to both jets for all subsamples. The colour coding (in the online version) reflects the anticipated level of expected signal from both SM $t\bar{t}$ production and possible production of $t\bar{t}$ states through resonant production: $< 0.25\%$ (light green: A,C,E), $0.25 - 10\%$ (shades of yellow: B, D, F-J, O), and $> 10\%$ (red: K-N).

number of SM $t\bar{t}$ events in each subsample (which is of order 1% or less for each region used in the background calculation) is subtracted before this calculation is performed.

A number of the subsamples (regions K, L, M, and N) can contain potential $t\bar{t}$ contributions from beyond-the-SM processes and therefore cannot be used in this method. Furthermore, the AJOP grid cannot be used to predict the background rate in region P, due to the correlation in the top-tagging rates for the leading and recoil jets. An iterative calculation is performed: background rates in subsamples K and M are determined with subsamples not potentially contaminated with top-quark jets, and these predicted rates are then used in a subsequent step to predict the background rate in the Top Template Tagger signal region:

$$K' = N_J \times \frac{N_F}{N_E} \quad (7.2)$$

$$M' = N_F \times \frac{N_O}{N_C} \quad (7.3)$$

$$P' = K' \times \frac{M'}{N_F} = \frac{N_J \times N_O \times N_F}{N_E \times N_C}, \quad (7.4)$$

where the N_X in these equations are the observed number of events in subsample X and K' , M' , and P' are the predicted multijet background contributions in the associated subsample.

Subsamples	Predicted Events
$(J \times F \times O)/(E \times C)$	51 ± 3
$(J \times F \times H \times O)/(E \times D \times I)$	56 ± 6
$(J \times F \times H \times O)/(B \times C \times G)$	54 ± 6
$(J \times F \times I \times O)/(A \times C \times G)$	51 ± 4
$(J \times F \times B \times O)/(A \times E \times D)$	52 ± 4
<i>Average</i>	53 ± 3

Table 3. Results of the different predictions for the multijet background rates in the Top Template Tagger signal region. The table lists the calculation performed and the corresponding predicted number of multijet background events. The uncertainties shown are statistical.

The prediction is verified through similar calculations using different combinations of subsamples, as shown in table 3. The corresponding average of the predictions for the dijet mass distribution from these calculations is shown in figure 10. The results from the different calculations are in good agreement with one another, as shown by the envelope of predictions in figure 10. The averages of the individual predictions as a function of the dijet mass are used as the estimate of the rate and shape of the multijet background in the signal region. An independent check of this multijet background estimate is made by using the observed rate of jets in the events prior to making the Top Template Tagger requirements, as shown in figure 5, and then using the measured rejection of light quark/gluon jets to estimate the final background rate. The result, 55 ± 5 (stat.) events, is in excellent agreement with the background estimate from the iterative calculation.

The SM $t\bar{t}$ background in the signal region has been modelled using the SM Monte Carlo calculation. This leads to an expected yield of 59_{-26}^{+27} (stat. \oplus syst.) events.

Figures 11 and 12 show the predicted and observed p_T and jet mass distributions in the Top Template Tagger signal region. There is good agreement between the observed data and predicted background-only distributions.

8 Systematic uncertainties

The following systematic uncertainties are considered and propagated to the predicted $m_{t\bar{t}}$ distributions for both analyses. These are presented in order of their relative size, with the b -tagging efficiency and the jet energy scale being the two largest sources of systematic uncertainty.

The uncertainty due to the b -tagging efficiency [44, 57, 58] is evaluated by re-weighting MC events according to uncertainties on the tagging efficiency and mistag rate for b -jets, c -jets, and light-quark and gluon jets. The b -tagging efficiency has a maximum at $p_T \sim 100$ GeV. The b -tagging efficiency uncertainty in the region $p_T < 200$ GeV is determined from data using muon-tagged b -jet candidates [44]. An additional systematic uncertainty that can be as large as 50% for jets with $p_T > 800$ GeV results from limitations in the understanding of the tracking response in dense tracking environments. This additional uncertainty is added in quadrature to the uncertainty measured from data for lower p_T .

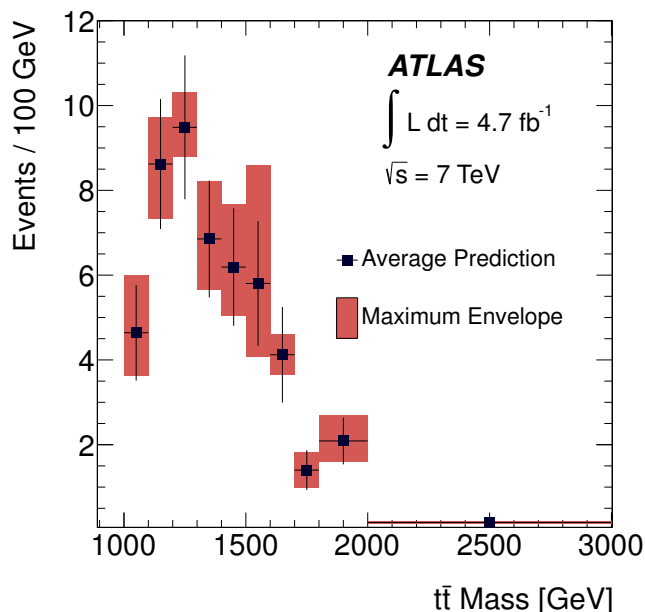
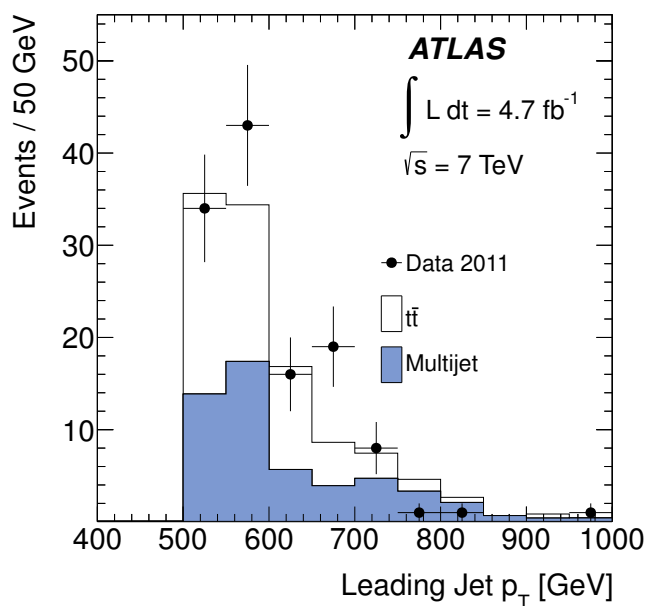


Figure 10. The data-driven prediction of the $t\bar{t}$ mass distribution for the multijet background in the Top Template Tagger signal region. The points are the average prediction and statistical uncertainties from the five calculations, and the envelope is the range of the predictions in each bin.

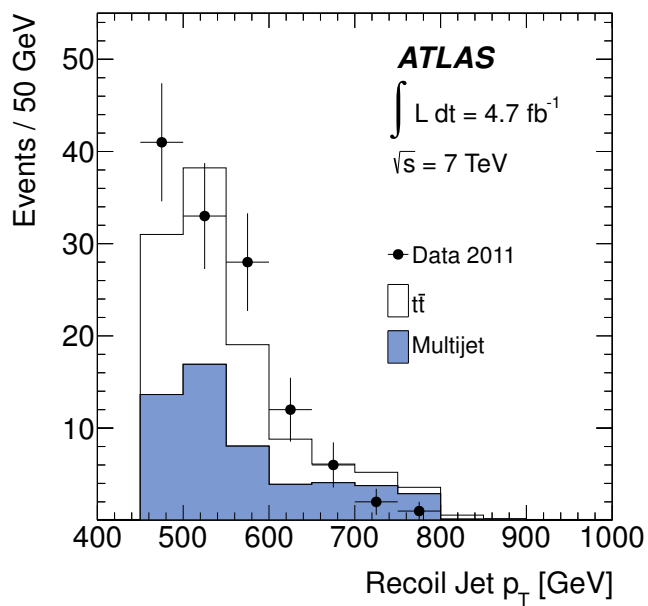
For the HEPTopTagger analysis differences in the jet energy scale (JES) between data and simulation are determined from a comparison of the jet energy measured with the calorimeter and the energy measured with charged tracks associated with the jet. The differences vary between 2.3% and 6.8%, depending on the jet distance parameter, jet p_T and η . The differences have been studied independently in a sample of QCD dijet events in which jets originate mainly from light quarks and gluons, and in a sample enriched in $t\bar{t}$ events. For the latter sample, a lepton+jet $t\bar{t}$ selection is made as described in ref. [46] and a fat jet is required with $p_T > 200$ GeV. According to simulation this sample consists of 40% $t\bar{t}$ events. The remaining events are characterised by the production of W bosons in association with light-quark and gluon jets. This sample has a mix of quark flavours similar to the final sample in the present analysis and also exhibits the same boosted top-quark decay topology in which the jets are close-by. A similar uncertainty is found for the QCD dijet and $t\bar{t}$ -enhanced samples; the maximum value is used. The jet energy resolution (JER) for the HEPTopTagger jets has been measured using the p_T asymmetry in dijet events. The impact of differences between data and simulation is evaluated by worsening the resolution in simulation such that it corresponds to that measured in data.

The JES uncertainty for the jets used in the Top Template Tagger analysis ranges between 4% and 5%, depending on the jet p_T and η . The JER uncertainty has been increased by 50% of that predicted by MC simulations to account for differences in the JER measured in data and the simulations.

The PDF eigenvector approach is applied to determine the sensitivity of the resulting invariant mass distribution to the PDF uncertainties. The envelope of the CT10 [30],

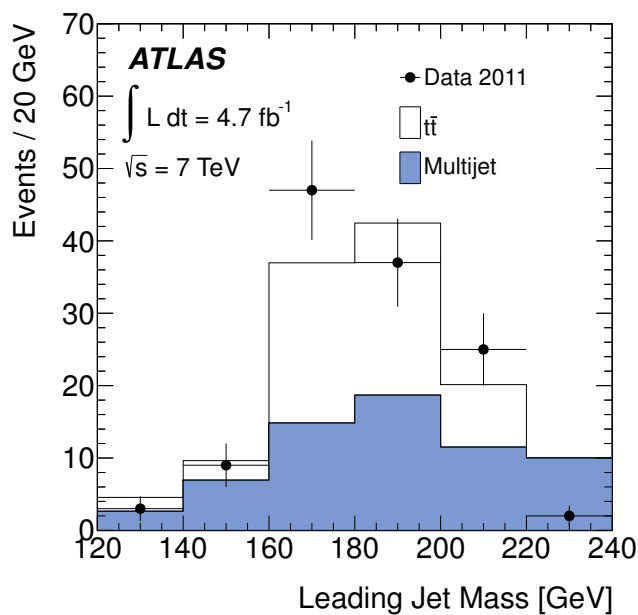


(a)

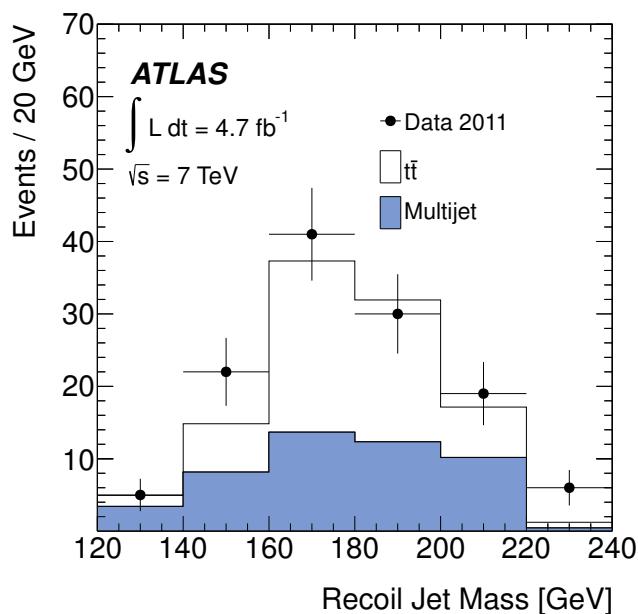


(b)

Figure 11. Transverse momentum distributions for the leading (a) and recoil (b) jets in the Top Template Tagger signal region. Shown are the data distribution, the predicted SM $t\bar{t}$ contribution and the multijet background contributions as estimated from data.



(a)



(b)

Figure 12. Jet mass distributions (a) for the leading and (b) recoil jets in the Top Template Tagger signal region. Shown are the data distribution, the predicted SM $t\bar{t}$ contribution and the multijet background contributions as estimated from data.

MSTW2008 [59] and NNPDF2.0 [60] next-to-leading-order (NLO) PDF sets is used in this procedure [61]. The uncertainty on the integrated luminosity is 3.9% [26, 27], which affects the uncertainty on the resonance yield and the SM $t\bar{t}$ background.

The uncertainty due to higher-order QCD corrections to the SM $t\bar{t}$ background prediction is assessed by using two alternative samples produced with the MC@NLO generator in which the renormalisation and factorisation scales have been simultaneously increased or decreased by a factor of two.

The impact on the shape of the $m_{t\bar{t}}$ distribution of the choice of models for QCD initial and final state radiation (ISR/FSR) and for parton showers is evaluated for the $t\bar{t}$ sample by comparing two different simulated samples. The differences between the distributions are symmetrised and taken as the systematic uncertainty. The variations considered are:

- ISR/FSR: ACERMC simulated [62, 63] samples with two different PYTHIA tunes for the simulation of ISR/FSR.
- Parton shower model: two POWHEG MC [64] simulated samples, one created using the HERWIG parton shower and hadronisation models and the other created with the PYTHIA model.

The uncertainty on the $m_{t\bar{t}}$ distribution due to electroweak virtual corrections is estimated by adding an additional uncertainty on the SM $t\bar{t}$ differential cross section that is the size of the expected reduction in the SM $t\bar{t}$ production cross section as a function of $m_{t\bar{t}}$ [65].

The SM $t\bar{t}$ normalisation uncertainty is treated differently in the two analyses due to the different kinematic reach. In the statistical analysis of the HEPTopTagger results, the normalisation of the $t\bar{t}$ contribution is left to be constrained in the limit-setting procedure within a variation from +100% to -50%. The width of the posterior variation is much smaller. In the Top Template Tagger analysis the uncertainty on the SM $t\bar{t}$ rate and the $m_{t\bar{t}}$ shape uncertainty are estimated for each systematic source. The theoretical uncertainty on the SM $t\bar{t}$ contribution is constrained to the 10% uncertainty on the production cross section, convolved with the uncertainty arising from the virtual electroweak corrections.

The cross-checks described in section 5 and section 6 show that the internal variables used for the top-quark tagging methods model the data well. In addition, as all uncertainties on the input objects (such as the JES) are fully propagated into the two analyses no additional uncertainty for the modelling of top-tagging variables is added.

The trigger efficiency in the simulation is found to agree well with data, within the uncertainty of the jet energy scale, such that no additional trigger efficiency uncertainty is needed.

The multijet background is estimated in a data-driven procedure that includes subtraction of the predicted SM $t\bar{t}$ contribution as described in section 7. The systematic uncertainties on the $t\bar{t}$ contribution are propagated to the multijet estimate. An additional uncertainty on the multijet background is obtained by comparing the $m_{t\bar{t}}$ predictions using the various subsamples as described in section 7.

9 Results

There are 953 and 123 events observed in the HEPTopTagger and Top Template Tagger signal regions, respectively. For the HEPTopTagger selection, the SM $t\bar{t}$ background is 770_{-180}^{+220} (stat. \oplus syst.) events and the multijet background is 130 ± 70 (stat. \oplus syst.) events. For the Top Template Tagger selection, the SM $t\bar{t}$ background is 59_{-26}^{+27} (stat. \oplus syst.) events and the multijet background is 53 ± 6 (stat. \oplus syst.) events. The predicted SM event rates are in good agreement with the observation.

The $t\bar{t}$ mass distributions for the data and the expected backgrounds are shown in figure 13. The $t\bar{t}$ mass binning at the lower masses is chosen to correspond approximately to the $t\bar{t}$ mass resolution. For illustration, a hypothetical Z' boson signal with mass 1 TeV is shown for the HEPTopTagger $t\bar{t}$ mass distribution and a hypothetical KK gluon signal with mass 1.6 TeV is shown for the Top Template Tagger $t\bar{t}$ mass distribution. No statistically significant excess over the SM $t\bar{t}$ expectation plus multijet background is observed at any mass value.

As no signal is observed in either selection, 95% CL upper limits are set on the production cross section times branching ratio to $t\bar{t}$ final states for each model using a Bayesian approach [66]. A binned likelihood function based on Poisson distributions for each $t\bar{t}$ invariant mass bin is used.

The limits are determined for resonance masses ranging from 0.5 to 2.0 TeV for the Z' boson model and 0.7 to 2.0 TeV for the KK gluon model. The systematic uncertainties are treated as nuisance parameters with Gaussian prior distributions reflecting their uncertainty and are then marginalised to set credibility intervals.

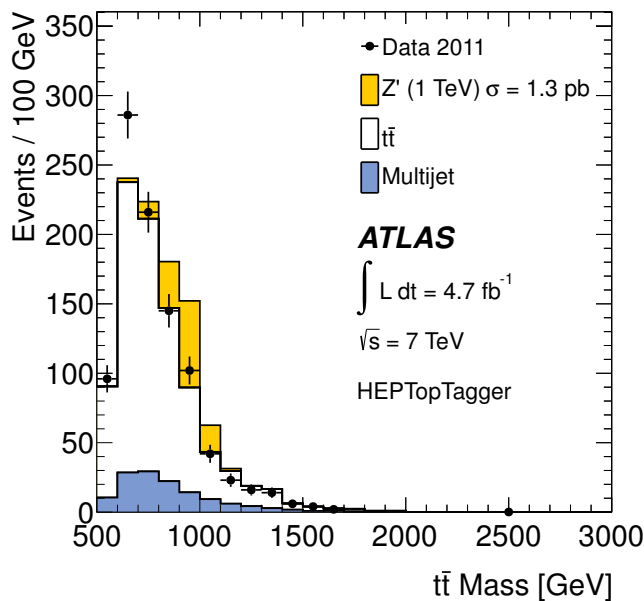
The large uncertainty on the SM $t\bar{t}$ normalisation in the HEPTopTagger selection by construction precludes other nuisance parameters that are sensitive to this normalisation to be strongly constrained. To prevent regions with low $m_{t\bar{t}}$, where high event yields result in small statistical uncertainties, constraining regions with high $m_{t\bar{t}}$, the jet energy scale uncertainty is treated as being uncorrelated between different bins in jet p_T . Studies of the posterior distributions of the nuisance parameters have been performed to ensure that the uncertainties arising from the parton shower model and ISR/FSR do not over-constrain the uncertainties.

To estimate the *a priori* sensitivity of this search, background-only pseudo-experiments are randomly drawn from the background prediction. All nuisance parameters are allowed to vary in a manner consistent with their prior distributions for each pseudo-experiment.

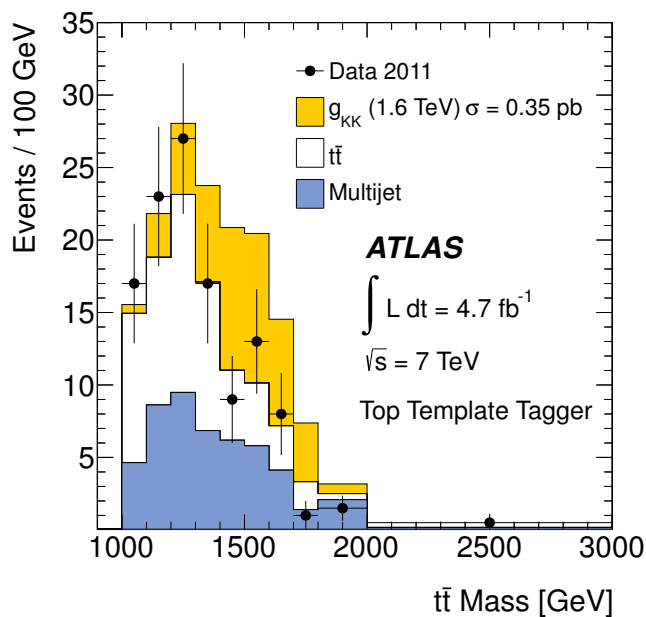
The median of the distribution is chosen to represent the expected limit. The ensemble of limits is also used to define the 68% and 95% CL envelope of limits as a function of resonance mass.

The dominant systematic uncertainties in both analyses come from the uncertainties on b -tagging efficiency, jet energy scale and SM $t\bar{t}$ normalisation.

Figures 14 and 15 show the HEPTopTagger and Top Template Tagger 95% CL exclusion limits on the cross section times branching ratio for the two models. They are interpreted as mass limits by comparing the cross-section limits to theoretical cross-section



(a)



(b)

Figure 13. Distributions of the $t\bar{t}$ invariant mass $m_{t\bar{t}}$. The HEPTopTagger data, the SM $t\bar{t}$ background prediction, the multijet background prediction and a hypothetical Z' signal with $m_{Z'} = 1$ TeV are shown in (a). The Top Template Tagger data, the SM $t\bar{t}$ background prediction, the multijet background prediction and a hypothetical KK gluon signal with $m_{KKg} = 1.6$ TeV are shown in (b). Data points show statistical uncertainties only.

Model	Obs. Limit (TeV)	Exp. Limit (TeV)
HEPTopTagger		
Z'	$0.70 < m_{Z'} < 1.00$ $1.28 < m_{Z'} < 1.32$	$0.68 < m_{Z'} < 1.16$
KK gluon	$0.70 < m_{g_{KK}} < 1.48$	$0.70 < m_{g_{KK}} < 1.52$
Top Template Tagger		
KK gluon	$1.02 < m_{g_{KK}} < 1.62$	$1.08 < m_{g_{KK}} < 1.62$

Table 4. Expected (Exp.) and observed (Obs.) exclusion regions on the leptophobic Z' boson mass and on the KK gluon mass in the Randall-Sundrum model.

predictions as a function of mass from specific benchmark models. The expected and observed mass limits are shown in table 4.

As described in ref. [67], the colour structure of the KK resonance can affect the tagging efficiency. This effect is small, but the results presented here are valid only for resonances with the same colour structure as the KK gluon (e.g., the sensitivity for a KK photon with the same mass and width as a KK gluon will differ by $\approx 10\%$).

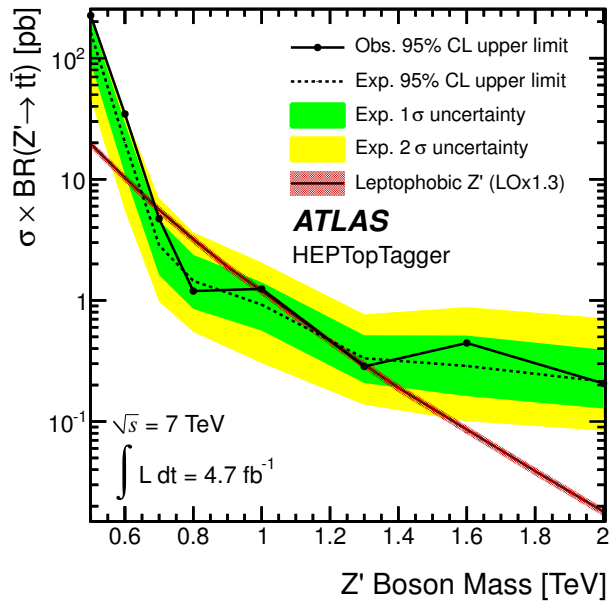
The data samples for the two analyses are statistically correlated. However, the expected limits are different for the two analyses and illustrate their complementarity: The HEPTopTagger selection is able to exclude Z' boson resonances over part of the mass range between 0.70 and 1.32 TeV and KK gluons with masses between 0.70 and 1.48 TeV. The Top Template Tagger selection is not able to set an exclusion limit on Z' boson resonances but is able to exclude the wider-width KK gluon resonances for masses between 1.02 and 1.62 TeV.

To combine the limits from these two analyses, the results from the tagger with the lower expected exclusion limit are selected. The HEPTopTagger selection provides lower expected limits for Z' boson masses up to 1.3 TeV, and for KK gluons with masses between 0.7 and 1.3 TeV. The Top Template Tagger selection provides the lower expected limits for both Z' bosons and KK gluons with masses above 1.4 TeV. These two analyses together are able to exclude the Z' boson model with masses $0.70 < m_{Z'} < 1.00$ TeV and $1.28 < m_{Z'} < 1.32$ TeV, and KK gluons with masses $0.70 < m_{g_{KK}} < 1.62$ TeV, all at 95% CL.

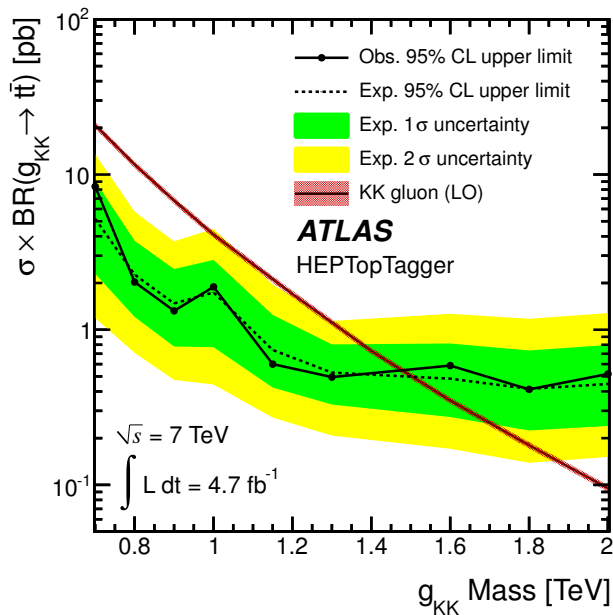
10 Conclusions

A search for massive resonances, characterised by a narrow state such as a Z' boson or a wider object such as a KK gluon, decaying into $t\bar{t}$ pairs in the fully hadronic final state is presented. The analysis uses a dataset corresponding to 4.7fb^{-1} , collected with the ATLAS detector during the 2011 pp run of the LHC at a centre-of-mass energy of 7 TeV. Two top-quark tagging schemes, the HEPTopTagger and Top Template Tagger methods, are used to identify and reconstruct top-quark pairs in their hadronic decay mode for boosted top quarks with transverse momenta between 200 GeV and approximately 1 TeV.

The reconstructed $m_{t\bar{t}}$ spectra are compared to predictions for SM $t\bar{t}$ production and background from massive jets produced through QCD interactions. No evidence for res-

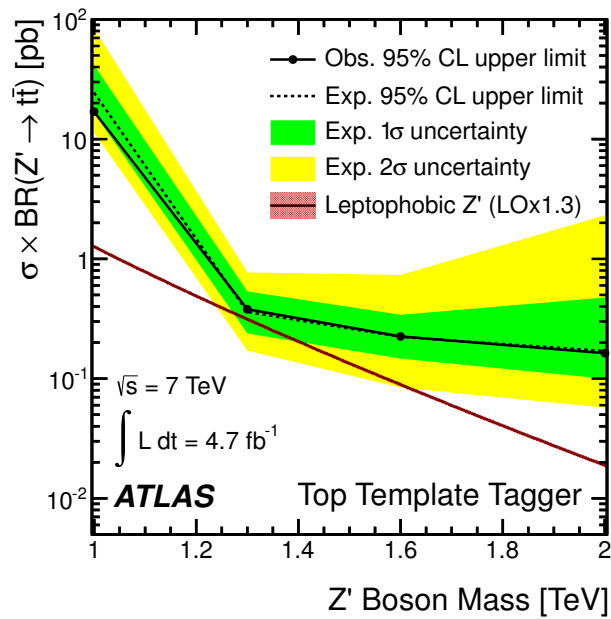


(a)

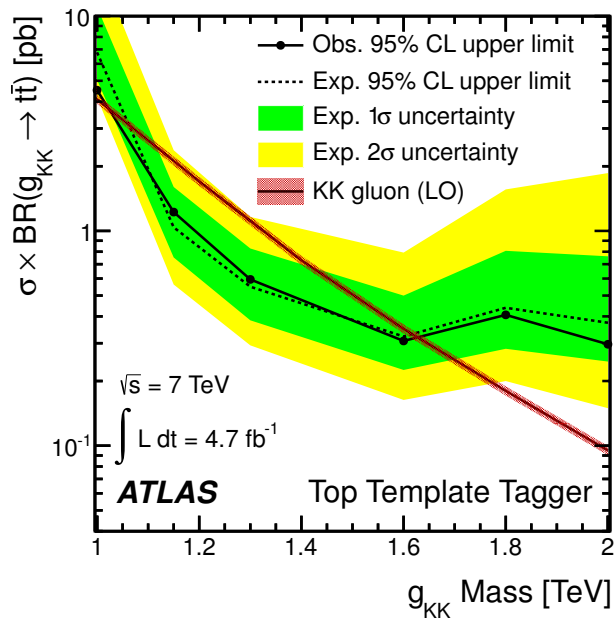


(b)

Figure 14. Expected and observed 95% CL upper limits on the production cross section times branching fraction $\sigma \times BR$ as a function of (a) the Z' boson mass and (b) the KK gluon mass for the HEPTopTagger selection. The red bands are the model predictions including theoretical uncertainties. The Z' boson leading-order (LO) cross section is multiplied by 1.3 to account for expected higher-order corrections. The KK gluon LO cross section is used.



(a)



(b)

Figure 15. Expected and observed 95% CL upper limits on the production cross section times branching fraction $\sigma \times BR$ as a function of (a) the Z' boson mass and (b) the KK gluon mass for the Top Template Tagger selection. The red bands are the model predictions including theoretical uncertainties. The Z' boson LO cross section is multiplied by 1.3 to account for expected higher order corrections. The KK gluon LO cross section is used.

onant $t\bar{t}$ production is found using either top-quark tagging method. These two analyses together exclude the Z' boson model with masses $0.70 < m_{Z'} < 1.00$ TeV and $1.28 < m_{Z'} < 1.32$ TeV, and KK gluons with masses $0.70 < m_{g_{KK}} < 1.62$ TeV, all at 95% CL. These results extend the previous ATLAS limits on Z' bosons and KK gluons production that were based on the lepton plus jets final state.

Acknowledgments

We acknowledge the contributions of Jose Juknevich and Mihailo Backovic, Weizmann Institute of Science, for insights and calculations. We thank CERN for the very successful operation of the LHC, as well as the support staff from our institutions without whom ATLAS could not be operated efficiently.

We acknowledge the support of ANPCyT, Argentina; YerPhI, Armenia; ARC, Australia; BMWF and FWF, Austria; ANAS, Azerbaijan; SSTC, Belarus; CNPq and FAPESP, Brazil; NSERC, NRC and CFI, Canada; CERN; CONICYT, Chile; CAS, MOST and NSFC, China; COLCIENCIAS, Colombia; MSMT CR, MPO CR and VSC CR, Czech Republic; DNRF, DNSRC and Lundbeck Foundation, Denmark; EPLANET, ERC and NSRF, European Union; IN2P3-CNRS, CEA-DSM/IRFU, France; GNSF, Georgia; BMBF, DFG, HGF, MPG and AvH Foundation, Germany; GSRT and NSRF, Greece; ISF, MINERVA, GIF, DIP and Benoziyo Center, Israel; INFN, Italy; MEXT and JSPS, Japan; CNRST, Morocco; FOM and NWO, Netherlands; BRF and RCN, Norway; MNiSW, Poland; GRICES and FCT, Portugal; MERYS (MECTS), Romania; MES of Russia and ROSATOM, Russian Federation; JINR; MSTD, Serbia; MSSR, Slovakia; ARRS and MVZT, Slovenia; DST/NRF, South Africa; MICINN, Spain; SRC and Wallenberg Foundation, Sweden; SER, SNSF and Cantons of Bern and Geneva, Switzerland; NSC, Taiwan; TAEK, Turkey; STFC, the Royal Society and Leverhulme Trust, United Kingdom; DOE and NSF, United States of America.

The crucial computing support from all WLCG partners is acknowledged gratefully, in particular from CERN and the ATLAS Tier-1 facilities at TRIUMF (Canada), NDGF (Denmark, Norway, Sweden), CC-IN2P3 (France), KIT/GridKA (Germany), INFN-CNAF (Italy), NL-T1 (Netherlands), PIC (Spain), ASGC (Taiwan), RAL (U.K.) and BNL (U.S.A.) and in the Tier-2 facilities worldwide.

Open Access. This article is distributed under the terms of the Creative Commons Attribution License which permits any use, distribution and reproduction in any medium, provided the original author(s) and source are credited.

References

- [1] CDF collaboration, *Limits on the production of narrow $t\bar{t}$ resonances in $p\bar{p}$ collisions at $\sqrt{s} = 1.96$ TeV*, *Phys. Rev. D* **77** (2008) 051102 [[arXiv:0710.5335](#)] [[INSPIRE](#)].
- [2] CDF collaboration, *Search for resonant $t\bar{t}$ production in $p\bar{p}$ collisions at $\sqrt{s} = 1.96$ TeV*, *Phys. Rev. Lett.* **100** (2008) 231801 [[arXiv:0709.0705](#)] [[INSPIRE](#)].

- [3] D0 collaboration, *Search for $t\bar{t}$ resonances in the lepton plus jets final state in $p\bar{p}$ collisions at $\sqrt{s} = 1.96$ TeV*, *Phys. Lett. B* **668** (2008) 98 [[arXiv:0804.3664](#)] [[INSPIRE](#)].
- [4] CDF collaboration, *Search for new color-octet vector particle decaying to $t\bar{t}$ in $p\bar{p}$ collisions at $\sqrt{s} = 1.96$ TeV*, *Phys. Lett. B* **691** (2010) 183 [[arXiv:0911.3112](#)] [[INSPIRE](#)].
- [5] CDF collaboration, *A search for resonant production of $t\bar{t}$ pairs in 4.8 fb^{-1} of integrated luminosity of $p\bar{p}$ collisions at $\sqrt{s} = 1.96$ TeV*, *Phys. Rev. D* **84** (2011) 072004 [[arXiv:1107.5063](#)] [[INSPIRE](#)].
- [6] D0 collaboration, *Search for a narrow $t\bar{t}$ resonance in $p\bar{p}$ collisions at $\sqrt{s} = 1.96$ TeV*, *Phys. Rev. D* **85** (2012) 051101 [[arXiv:1111.1271](#)] [[INSPIRE](#)].
- [7] ATLAS collaboration, *A search for $t\bar{t}$ resonances with the ATLAS detector in 2.05 fb^{-1} of proton-proton collisions at $\sqrt{s} = 7$ TeV*, *Eur. Phys. J. C* **72** (2012) 2083 [[arXiv:1205.5371](#)] [[INSPIRE](#)].
- [8] ATLAS collaboration, *A search for $t\bar{t}$ resonances in lepton+jet events with highly boosted top quarks collected in pp collisions at $\sqrt{s} = 7$ TeV with the ATLAS detector*, *JHEP* **09** (2012) 041 [[arXiv:1207.2409](#)] [[INSPIRE](#)].
- [9] CMS collaboration, *Search for anomalous $t\bar{t}$ production in the highly-boosted all-hadronic final state*, *JHEP* **09** (2012) 029 [[arXiv:1204.2488](#)] [[INSPIRE](#)].
- [10] T. Plehn, G.P. Salam and M. Spannowsky, *Fat jets for a light Higgs*, *Phys. Rev. Lett.* **104** (2010) 111801 [[arXiv:0910.5472](#)] [[INSPIRE](#)].
- [11] T. Plehn, M. Spannowsky, M. Takeuchi and D. Zerwas, *Stop reconstruction with tagged tops*, *JHEP* **10** (2010) 078 [[arXiv:1006.2833](#)] [[INSPIRE](#)].
- [12] Y.L. Dokshitzer, G. Leder, S. Moretti and B. Webber, *Better jet clustering algorithms*, *JHEP* **08** (1997) 001 [[hep-ph/9707323](#)] [[INSPIRE](#)].
- [13] L.G. Almeida, S.J. Lee, G. Perez, G. Sterman and I. Sung, *Template overlap method for massive jets*, *Phys. Rev. D* **82** (2010) 054034 [[arXiv:1006.2035](#)] [[INSPIRE](#)].
- [14] L.G. Almeida, O. Erdogan, J. Juknevich, S.J. Lee, G. Perez, et al., *Three-particle templates for a boosted Higgs boson*, *Phys. Rev. D* **85** (2012) 114046 [[arXiv:1112.1957](#)] [[INSPIRE](#)].
- [15] M. Cacciari, G.P. Salam and G. Soyez, *The \bar{k}_t jet clustering algorithm*, *JHEP* **4** (2008) 63 [[arXiv:0802.1189](#)].
- [16] R.M. Harris, C.T. Hill and S.J. Parke, *Cross section for topcolor Z' decaying to top-antitop*, [hep-ph/9911288](#).
- [17] K. Agashe, A. Belyaev, T. Krupovnickas, G. Perez and J. Virzi, *LHC signals from warped extra dimensions*, *Phys. Rev. D* **77** (2008) 015003 [[hep-ph/0612015](#)] [[INSPIRE](#)].
- [18] B. Lillie, L. Randall and L.-T. Wang, *The bulk RS KK-gluon at the LHC*, *JHEP* **09** (2007) 074 [[hep-ph/0701166](#)] [[INSPIRE](#)].
- [19] B. Lillie, J. Shu and T.M. Tait, *Kaluza-Klein gluons as a diagnostic of warped models*, *Phys. Rev. D* **76** (2007) 115016 [[arXiv:0706.3960](#)] [[INSPIRE](#)].
- [20] T. Sjöstrand, S. Mrenna and P.Z. Skands, *A brief introduction to PYTHIA 8.1*, *Comput. Phys. Commun.* **178** (2008) 852 [[arXiv:0710.3820](#)] [[INSPIRE](#)].
- [21] J. Alwall, P. Demin, S. de Visscher, R. Frederix, M. Herquet, F. Maltoni, T. Plehn, D.L. Rainwater and T. Stelzer, *MadGraph/MadEvent v4: the new web generation*, *JHEP* **9** (2007) 28 [[arXiv:0706.2334](#)].

- [22] J. Gao, C.S. Li, B.H. Li, H.X. Zhu and C.-P. Yuan, *Next-to-leading order QCD corrections to a heavy resonance production and decay into top quark pair at the LHC*, *Phys. Rev. D* **82** (2010) 014020 [[arXiv:1004.0876](#)].
- [23] CMS collaboration, *Search for resonant $t\bar{t}$ production in lepton+jets events in pp collisions at $\sqrt{s} = 7$ TeV*, *JHEP* **12** (2012) 015 [[arXiv:1209.4397](#)] [[INSPIRE](#)].
- [24] ATLAS collaboration, *The ATLAS experiment at the CERN large hadron collider*, *2008 JINST* **3** S08003 [[INSPIRE](#)].
- [25] L. Evans and P. Bryant, *The LHC machine*, *2008 JINST* **3** S08001 [[INSPIRE](#)].
- [26] ATLAS collaboration, *Improved luminosity determination in pp collisions at $\sqrt{s} = 7$ TeV using the ATLAS detector at the LHC*, *ATLAS-CONF-2012-080* (2012).
- [27] ATLAS collaboration, *Luminosity determination in pp collisions at $\sqrt{s} = 7$ TeV using the ATLAS detector at the LHC*, *Eur. Phys. J. C* **71** (2011) 1630 [[arXiv:1101.2185](#)] [[INSPIRE](#)].
- [28] S. Frixione and B.R. Webber, *Matching NLO QCD computations and parton shower simulations*, *JHEP* **06** (2002) 029 [[hep-ph/0204244](#)] [[INSPIRE](#)].
- [29] S. Frixione, P. Nason and B.R. Webber, *Matching NLO QCD and parton showers in heavy flavor production*, *JHEP* **08** (2003) 007 [[hep-ph/0305252](#)] [[INSPIRE](#)].
- [30] H.-L. Lai, M. Guzzi, J. Huston, Z. Li, P.M. Nadolsky, et al., *New parton distributions for collider physics*, *Phys. Rev. D* **82** (2010) 074024 [[arXiv:1007.2241](#)] [[INSPIRE](#)].
- [31] G. Corcella, I. Knowles, G. Marchesini, S. Moretti, K. Odagiri, et al., *HERWIG 6.5 release note*, [hep-ph/0210213](#) [[INSPIRE](#)].
- [32] J.M. Butterworth, J.R. Forshaw and M.H. Seymour, *Multiparton interactions in photoproduction at HERA*, *Zeit. Phys. C* **72** (1996) 637 [[hep-ph/9601371](#)].
- [33] M. Aliev, H. Lacker, U. Langenfeld, S. Moch, P. Uwer and M. Wiedermann, *HATHOR — Hadronic top and heavy quarks cross section calculator*, *Comp. Phys. Comm.* **182** (2011) 1034 [[arXiv:1007.1327](#)].
- [34] A. Martin, W. Stirling, R. Thorne and G. Watt, *Parton distributions for the LHC*, *Eur. Phys. J. C* **63** (2009) 189 [[arXiv:0901.0002](#)] [[INSPIRE](#)].
- [35] T. Sjöstrand, S. Mrenna and P.Z. Skands, *PYTHIA 6.4 physics and manual*, *JHEP* **05** (2006) 026 [[hep-ph/0603175](#)] [[INSPIRE](#)].
- [36] J. Pumplin, D. Stump, J. Huston, H. Lai, P.M. Nadolsky, et al., *New generation of parton distributions with uncertainties from global QCD analysis*, *JHEP* **07** (2002) 012 [[hep-ph/0201195](#)] [[INSPIRE](#)].
- [37] ATLAS collaboration, *The ATLAS simulation infrastructure*, *Eur. Phys. J. C* **70** (2010) 823 [[arXiv:1005.4568](#)] [[INSPIRE](#)].
- [38] GEANT4 collaboration, S. Agostinelli et al., *GEANT4: a simulation toolkit*, *Nucl. Instrum. Meth. A* **506** (2003) 250 [[INSPIRE](#)].
- [39] W. Lampl et al., *Calorimeter clustering algorithms: description and performance*, *ATL-LARG-PUB-2008-002* (2008).
- [40] ATLAS collaboration, *Jet energy measurement with the ATLAS detector in proton-proton collisions at $\sqrt{s} = 7$ TeV*, [arXiv:1112.6426](#) [[INSPIRE](#)].

- [41] M. Cacciari, G.P. Salam and G. Soyez, *The \bar{k}_t jet clustering algorithm*, *JHEP* **04** (2008) 063 [[arXiv:0802.1189](#)] [[INSPIRE](#)].
- [42] M. Cacciari, G.P. Salam and G. Soyez, *FastJet user manual*, *Eur. Phys. J. C* **72** (2012) 1896 [[arXiv:1111.6097](#)] [[INSPIRE](#)].
- [43] ATLAS collaboration, *Properties of jets and inputs to jet reconstruction and calibration with the atlas detector using proton-proton collisions at $\sqrt{s} = 7$ TeV*, *ATLAS-CONF-2010-053* (2010).
- [44] ATLAS collaboration, *Measurement of the b -tag efficiency in a sample of jets containing muons with 5fb^{-1} of data from the ATLAS detector*, *ATLAS-CONF-2012-043* (2012).
- [45] ATLAS collaboration, *A search for $t\bar{t}$ resonances in the lepton plus jets final state using 4.66fb^{-1} of pp collisions at $\sqrt{s} = 7$ TeV*, *ATLAS-CONF-2012-136* (2012).
- [46] ATLAS collaboration, *Performance of large- R jets and jet substructure reconstruction with the ATLAS detector*, *ATLAS-CONF-2012-065* (2012).
- [47] J.M. Butterworth, A.R. Davison, M. Rubin and G.P. Salam, *Jet substructure as a new Higgs search channel at the LHC*, *Phys. Rev. Lett.* **100** (2008) 242001 [[arXiv:0802.2470](#)] [[INSPIRE](#)].
- [48] G.P. Salam and G. Soyez, *A practical seedless infrared-safe cone jet algorithm*, *JHEP* **05** (2007) 086 [[arXiv:0704.0292](#)] [[INSPIRE](#)].
- [49] S. Catani, Y.L. Dokshitzer, M. Seymour and B. Webber, *Longitudinally invariant K_t clustering algorithms for hadron hadron collisions*, *Nucl. Phys. B* **406** (1993) 187 [[INSPIRE](#)].
- [50] TEVATRON ELECTROWEAK WORKING GROUP, CDF, D0 collaborations, *Combination of CDF and D0 results on the mass of the top quark using up to 5.8fb^{-1} of data*, [arXiv:1107.5255](#) [[INSPIRE](#)].
- [51] G.C. Blazey, J.R. Dittmann, S.D. Ellis, V.D. Elvira, K. Frame, et al., *Run II jet physics*, [hep-ex/0005012](#) [[INSPIRE](#)].
- [52] ATLAS collaboration, *Jet mass and substructure of inclusive jets in $\sqrt{s} = 7$ TeV pp collisions with the ATLAS experiment*, *JHEP* **5** (2012) 128 [[arXiv:1203.4606](#)].
- [53] ATLAS collaboration, *ATLAS measurements of the properties of jets for boosted particle searches*, *Phys. Rev. D* **86** (2012) 072006 [[arXiv:1206.5369](#)] [[INSPIRE](#)].
- [54] R. Alon, E. Duchovni, G. Perez, A.P. Pranko and P.K. Sinervo, *Data-driven method of pile-up correction for the substructure of massive jets*, *Phys. Rev. D* **84** (2011) 114025 [[arXiv:1101.3002](#)].
- [55] CDF collaboration, *Study of substructure of high transverse momentum jets produced in proton-antiproton collisions at $\sqrt{s} = 1.96$ TeV*, *Phys. Rev. D* **85** (2012) 091101 [[arXiv:1106.5952](#)] [[INSPIRE](#)].
- [56] K. Blum, C. Delaunay, O. Gedalia, Y. Hochberg, S.J. Lee, et al., *Implications of the CDF $t\bar{t}$ forward-backward asymmetry for boosted top physics*, *Phys. Lett. B* **702** (2011) 364 [[arXiv:1102.3133](#)] [[INSPIRE](#)].
- [57] ATLAS collaboration, *Measurement of the mistag rate with 5fb^{-1} of data collected by the ATLAS detector*, *ATLAS-CONF-2012-040* (2012).
- [58] ATLAS collaboration, *Measuring the b -tag efficiency in a top-pair sample with 4.7fb^{-1} of data from the ATLAS detector*, *ATLAS-CONF-2012-097* (2012).

- [59] A. Martin, W. Stirling, R. Thorne and G. Watt, *Uncertainties on α_s in global PDF analyses and implications for predicted hadronic cross sections*, *Eur. Phys. J. C* **64** (2009) 653 [[arXiv:0905.3531](#)] [[INSPIRE](#)].
- [60] NNPDF collaboration, R.D. Ball et al., *Unbiased global determination of parton distributions and their uncertainties at NNLO and at LO*, *Nucl. Phys. B* **855** (2012) 153 [[arXiv:1107.2652](#)] [[INSPIRE](#)].
- [61] M. Botje, J. Butterworth, A. Cooper-Sarkar, A. de Roeck, J. Feltesse, et al., *The PDF4LHC working group interim recommendations*, [arXiv:1101.0538](#) [[INSPIRE](#)].
- [62] B.P. Kersevan and E. Richter-Was, *The Monte Carlo event generator AcerMC version 2.0 with interfaces to PYTHIA 6.2 and HERWIG 6.5*, [hep-ph/0405247](#) [[INSPIRE](#)].
- [63] ATLAS collaboration, *Measurement of $t\bar{t}$ production with a veto on additional central jet activity in pp collisions at $\sqrt{s} = 7$ TeV using the ATLAS detector*, *Eur. Phys. J. C* **72** (2012) 2043 [[arXiv:1203.5015](#)] [[INSPIRE](#)].
- [64] S. Frixione, P. Nason and C. Oleari, *Matching NLO QCD computations with parton shower simulations: the POWHEG method*, *JHEP* **11** (2007) 070 [[arXiv:0709.2092](#)] [[INSPIRE](#)].
- [65] A.V. Manohar and M. Trott, *Electroweak Sudakov corrections and the top quark forward-backward asymmetry*, *Phys. Lett. B* **711** (2012) 313 [[arXiv:1201.3926](#)] [[INSPIRE](#)].
- [66] D0 collaboration, *A recipe for the construction of confidence limits*, FERMILAB-TM-2104 (2000).
- [67] K. Joshi, A.D. Pilkington and M. Spannowsky, *The dependency of boosted tagging algorithms on the event colour structure*, *Phys. Rev. D* **86** (2012) 114016 [[arXiv:1207.6066](#)] [[INSPIRE](#)].

The ATLAS collaboration

G. Aad⁴⁸, T. Abajyan²¹, B. Abbott¹¹¹, J. Abdallah¹², S. Abdel Khalek¹¹⁵, A.A. Abdelalim⁴⁹, O. Abidinov¹¹, R. Aben¹⁰⁵, B. Abi¹¹², M. Abolins⁸⁸, O.S. AbouZeid¹⁵⁸, H. Abramowicz¹⁵³, H. Abreu¹³⁶, B.S. Acharya^{164a,164b}, L. Adamczyk³⁸, D.L. Adams²⁵, T.N. Addy⁵⁶, J. Adelman¹⁷⁶, S. Adomeit⁹⁸, P. Adragna⁷⁵, T. Adye¹²⁹, S. Aefsky²³, J.A. Aguilar-Saavedra^{124b,a}, M. Agustoni¹⁷, M. Aharrouche⁸¹, S.P. Ahlen²², F. Ahles⁴⁸, A. Ahmad¹⁴⁸, M. Ahsan⁴¹, G. Aielli^{133a,133b}, T.P.A. Åkesson⁷⁹, G. Akimoto¹⁵⁵, A.V. Akimov⁹⁴, M.S. Alam², M.A. Alam⁷⁶, J. Albert¹⁶⁹, S. Albrand⁵⁵, M. Aleksa³⁰, I.N. Aleksandrov⁶⁴, F. Alessandria^{89a}, C. Alexa^{26a}, G. Alexander¹⁵³, G. Alexandre⁴⁹, T. Alexopoulos¹⁰, M. Alhroob^{164a,164c}, M. Aliev¹⁶, G. Alimonti^{89a}, J. Alison¹²⁰, B.M.M. Allbrooke¹⁸, P.P. Allport⁷³, S.E. Allwood-Spiers⁵³, J. Almond⁸², A. Aloisio^{102a,102b}, R. Alon¹⁷², A. Alonso⁷⁹, F. Alonso⁷⁰, A. Altheimer³⁵, B. Alvarez Gonzalez⁸⁸, M.G. Alvigi^{102a,102b}, K. Amako⁶⁵, C. Amelung²³, V.V. Ammosov^{128,*}, S.P. Amor Dos Santos^{124a}, A. Amorim^{124a,b}, N. Amram¹⁵³, C. Anastopoulos³⁰, L.S. Ancu¹⁷, N. Andari¹¹⁵, T. Andeen³⁵, C.F. Anders^{58b}, G. Anders^{58a}, K.J. Anderson³¹, A. Andreazza^{89a,89b}, V. Andrei^{58a}, M-L. Andrieux⁵⁵, X.S. Anduaga⁷⁰, S. Angelidakis⁹, P. Anger⁴⁴, A. Angerami³⁵, F. Anghinolfi³⁰, A. Anisenkov¹⁰⁷, N. Anjos^{124a}, A. Annovi⁴⁷, A. Antonaki⁹, M. Antonelli⁴⁷, A. Antonov⁹⁶, J. Antos^{144b}, F. Anulli^{132a}, M. Aoki¹⁰¹, S. Aoun⁸³, L. Aperio Bella⁵, R. Apolle^{118,c}, G. Arabidze⁸⁸, I. Aracena¹⁴³, Y. Arai⁶⁵, A.T.H. Arce⁴⁵, S. Arfaoui¹⁴⁸, J-F. Arguin⁹³, S. Argyropoulos⁴², E. Arik^{19a,*}, M. Arik^{19a}, A.J. Armbruster⁸⁷, O. Arnaez⁸¹, V. Arnal⁸⁰, C. Arnault¹¹⁵, A. Artamonov⁹⁵, G. Artoni^{132a,132b}, D. Arutinov²¹, S. Asai¹⁵⁵, S. Ask²⁸, B. Åsman^{146a,146b}, L. Asquith⁶, K. Assamagan^{25,d}, A. Astbury¹⁶⁹, M. Atkinson¹⁶⁵, B. Aubert⁵, E. Auge¹¹⁵, K. Augsten¹²⁷, M. Aurousseau^{145a}, G. Avolio³⁰, R. Avramidou¹⁰, D. Axen¹⁶⁸, G. Azuelos^{93,e}, Y. Azuma¹⁵⁵, M.A. Baak³⁰, G. Baccaglioni^{89a}, C. Bacci^{134a,134b}, A.M. Bach¹⁵, H. Bachacou¹³⁶, K. Bachas³⁰, M. Backes⁴⁹, M. Backhaus²¹, J. Backus Mayes¹⁴³, E. Badescu^{26a}, P. Bagnaia^{132a,132b}, S. Bahinipati³, Y. Bai^{33a}, D.C. Bailey¹⁵⁸, T. Bain¹⁵⁸, J.T. Baines¹²⁹, O.K. Baker¹⁷⁶, M.D. Baker²⁵, S. Baker⁷⁷, P. Balek¹²⁶, E. Banas³⁹, P. Banerjee⁹³, Sw. Banerjee¹⁷³, D. Banfi³⁰, A. Bangert¹⁵⁰, V. Bansal¹⁶⁹, H.S. Bansil¹⁸, L. Barak¹⁷², S.P. Baranov⁹⁴, A. Barbaro Galtieri¹⁵, T. Barber⁴⁸, E.L. Barberio⁸⁶, D. Barberis^{50a,50b}, M. Barbero²¹, D.Y. Bardin⁶⁴, T. Barillari⁹⁹, M. Barisonzi¹⁷⁵, T. Barklow¹⁴³, N. Barlow²⁸, B.M. Barnett¹²⁹, R.M. Barnett¹⁵, A. Baroncelli^{134a}, G. Barone⁴⁹, A.J. Barr¹¹⁸, F. Barreiro⁸⁰, J. Barreiro Guimarães da Costa⁵⁷, P. Barrillon¹¹⁵, R. Bartoldus¹⁴³, A.E. Barton⁷¹, V. Bartsch¹⁴⁹, A. Basye¹⁶⁵, R.L. Bates⁵³, L. Batkova^{144a}, J.R. Batley²⁸, A. Battaglia¹⁷, M. Battistin³⁰, F. Bauer¹³⁶, H.S. Bawa^{143,f}, S. Beale⁹⁸, T. Beau⁷⁸, P.H. Beauchemin¹⁶¹, R. Beccherle^{50a}, P. Bechtel²¹, H.P. Beck¹⁷, K. Becker¹⁷⁵, S. Becker⁹⁸, M. Beckingham¹³⁸, K.H. Becks¹⁷⁵, A.J. Beddall^{19c}, A. Beddall^{19c}, S. Bedikian¹⁷⁶, V.A. Bednyakov⁶⁴, C.P. Bee⁸³, L.J. Beemster¹⁰⁵, M. Begel²⁵, S. Behar Harpaz¹⁵², P.K. Behera⁶², M. Beimforde⁹⁹, C. Belanger-Champagne⁸⁵, P.J. Bell⁴⁹, W.H. Bell⁴⁹, G. Bella¹⁵³, L. Bellagamba^{20a}, M. Bellomo³⁰, A. Belloni⁵⁷, O. Beloborodova^{107,g}, K. Belotskiy⁹⁶, O. Beltramello³⁰, O. Benary¹⁵³, D. Benchekroun^{135a}, K. Bendtz^{146a,146b}, N. Benekos¹⁶⁵, Y. Benhammou¹⁵³, E. Benhar Nocchioli⁴⁹, J.A. Benitez Garcia^{159b}, D.P. Benjamin⁴⁵, M. Benoit¹¹⁵, J.R. Bensinger²³, K. Benslama¹³⁰, S. Bentvelsen¹⁰⁵, D. Berge³⁰, E. Bergeas Kuutmann⁴², N. Berger⁵, F. Berghaus¹⁶⁹, E. Berglund¹⁰⁵, J. Beringer¹⁵, P. Bernat⁷⁷, R. Bernhard⁴⁸, C. Bernius²⁵, T. Berry⁷⁶, C. Bertella⁸³, A. Bertin^{20a,20b}, F. Bertolucci^{122a,122b}, M.I. Besana^{89a,89b}, G.J. Besjes¹⁰⁴, N. Besson¹³⁶, S. Bethke⁹⁹, W. Bhimji⁴⁶, R.M. Bianchi³⁰, L. Bianchini²³, M. Bianco^{72a,72b}, O. Biebel⁹⁸, S.P. Bieniek⁷⁷, K. Bierwagen⁵⁴, J. Biesiada¹⁵, M. Biglietti^{134a}, H. Bilokon⁴⁷, M. Bindi^{20a,20b}, S. Binet¹¹⁵, A. Bingul^{19c}, C. Bini^{132a,132b}, C. Biscarat¹⁷⁸, B. Bittner⁹⁹, C.W. Black¹⁵⁰, K.M. Black²², R.E. Blair⁶, J.-B. Blanchard¹³⁶, G. Blanchot³⁰, T. Blazek^{144a}, I. Bloch⁴²,

C. Blocker²³, J. Blocki³⁹, A. Blondel⁴⁹, W. Blum⁸¹, U. Blumenschein⁵⁴, G.J. Bobbink¹⁰⁵,
 V.S. Bobrovnikov¹⁰⁷, S.S. Bocchetta⁷⁹, A. Bocci⁴⁵, C.R. Boddy¹¹⁸, M. Boehler⁴⁸, J. Boek¹⁷⁵,
 T.T. Boek¹⁷⁵, N. Boelaert³⁶, J.A. Bogaerts³⁰, A. Bogdanchikov¹⁰⁷, A. Bogouch^{90,*}, C. Boehm^{146a},
 J. Bohm¹²⁵, V. Boisvert⁷⁶, T. Bold³⁸, V. Boldea^{26a}, N.M. Bolnet¹³⁶, M. Bomben⁷⁸, M. Bona⁷⁵,
 M. Boonekamp¹³⁶, S. Bordoni⁷⁸, C. Borer¹⁷, A. Borisov¹²⁸, G. Borissov⁷¹, I. Borjanovic^{13a},
 M. Borri⁸², S. Borroni⁸⁷, J. Bortfeldt⁹⁸, V. Bortolotto^{134a,134b}, K. Bos¹⁰⁵, D. Boscherini^{20a},
 M. Bosman¹², H. Boterenbrood¹⁰⁵, J. Bouchami⁹³, J. Boudreau¹²³, E.V. Bouhova-Thacker⁷¹,
 D. Boumediene³⁴, C. Bourdarios¹¹⁵, N. Bousson⁸³, A. Boveia³¹, J. Boyd³⁰, I.R. Boyko⁶⁴,
 I. Bozovic-Jelisavcic^{13b}, J. Bracinik¹⁸, P. Branchini^{134a}, A. Brandt⁸, G. Brandt¹¹⁸, O. Brandt⁵⁴,
 U. Bratzler¹⁵⁶, B. Brau⁸⁴, J.E. Brau¹¹⁴, H.M. Braun^{175,*}, S.F. Brazzale^{164a,164c}, B. Brelier¹⁵⁸,
 J. Bremer³⁰, K. Brendlinger¹²⁰, R. Brenner¹⁶⁶, S. Bressler¹⁷², D. Britton⁵³, F.M. Brochu²⁸,
 I. Brock²¹, R. Brock⁸⁸, F. Broggi^{89a}, C. Bromberg⁸⁸, J. Bronner⁹⁹, G. Brooijmans³⁵, T. Brooks⁷⁶,
 W.K. Brooks^{32b}, G. Brown⁸², H. Brown⁸, P.A. Bruckman de Renstrom³⁹, D. Bruncko^{144b},
 R. Bruneliere⁴⁸, S. Brunet⁶⁰, A. Bruni^{20a}, G. Bruni^{20a}, M. Bruschi^{20a}, T. Buanes¹⁴, Q. Buat⁵⁵,
 F. Bucci⁴⁹, J. Buchanan¹¹⁸, P. Buchholz¹⁴¹, R.M. Buckingham¹¹⁸, A.G. Buckley⁴⁶, S.I. Buda^{26a},
 I.A. Budagov⁶⁴, B. Budick¹⁰⁸, V. Buescher⁸¹, L. Bugge¹¹⁷, O. Bulekov⁹⁶, A.C. Bundock⁷³,
 M. Bunse⁴³, T. Buran¹¹⁷, H. Burckhart³⁰, S. Burdin⁷³, T. Burgess¹⁴, S. Burke¹²⁹, E. Busato³⁴,
 P. Bussey⁵³, C.P. Buszello¹⁶⁶, B. Butler¹⁴³, J.M. Butler²², C.M. Buttar⁵³, J.M. Butterworth⁷⁷,
 W. Buttinger²⁸, M. Byszewski³⁰, S. Cabrera Urbán¹⁶⁷, D. Caforio^{20a,20b}, O. Cakir^{4a},
 P. Calafura¹⁵, G. Calderini⁷⁸, P. Calfayan⁹⁸, R. Calkins¹⁰⁶, L.P. Caloba^{24a}, R. Caloi^{132a,132b},
 D. Calvet³⁴, S. Calvet³⁴, R. Camacho Toro³⁴, P. Camarri^{133a,133b}, D. Cameron¹¹⁷,
 L.M. Caminada¹⁵, R. Caminal Armadans¹², S. Campana³⁰, M. Campanelli⁷⁷, V. Canale^{102a,102b},
 F. Canelli³¹, A. Canepa^{159a}, J. Cantero⁸⁰, R. Cantrill⁷⁶, L. Capasso^{102a,102b},
 M.D.M. Capeans Garrido³⁰, I. Caprini^{26a}, M. Caprini^{26a}, D. Capriotti⁹⁹, M. Capua^{37a,37b},
 R. Caputo⁸¹, R. Cardarelli^{133a}, T. Carli³⁰, G. Carlino^{102a}, L. Carminati^{89a,89b}, B. Caron⁸⁵,
 S. Caron¹⁰⁴, E. Carquin^{32b}, G.D. Carrillo-Montoya^{145b}, A.A. Carter⁷⁵, J.R. Carter²⁸,
 J. Carvalho^{124a,h}, D. Casadei¹⁰⁸, M.P. Casado¹², M. Cascella^{122a,122b}, C. Caso^{50a,50b,*},
 A.M. Castaneda Hernandez^{173,i}, E. Castaneda-Miranda¹⁷³, V. Castillo Gimenez¹⁶⁷,
 N.F. Castro^{124a}, G. Cataldi^{72a}, P. Catastini⁵⁷, A. Catinaccio³⁰, J.R. Catmore³⁰, A. Cattai³⁰,
 G. Cattani^{133a,133b}, S. Caughron⁸⁸, V. Cavaliere¹⁶⁵, P. Cavalleri⁷⁸, D. Cavalli^{89a},
 M. Cavalli-Sforza¹², V. Cavalinni^{122a,122b}, F. Ceradini^{134a,134b}, A.S. Cerqueira^{24b}, A. Cerri³⁰,
 L. Cerrito⁷⁵, F. Cerutti⁴⁷, S.A. Cetin^{19b}, A. Chafaq^{135a}, D. Chakraborty¹⁰⁶, I. Chalupkova¹²⁶,
 K. Chan³, P. Chang¹⁶⁵, B. Chapleau⁸⁵, J.D. Chapman²⁸, J.W. Chapman⁸⁷, E. Chareyre⁷⁸,
 D.G. Charlton¹⁸, V. Chavda⁸², C.A. Chavez Barajas³⁰, S. Cheatham⁸⁵, S. Chekanov⁶,
 S.V. Chekulaev^{159a}, G.A. Chelkov⁶⁴, M.A. Chelstowska¹⁰⁴, C. Chen⁶³, H. Chen²⁵, S. Chen^{33c},
 X. Chen¹⁷³, Y. Chen³⁵, Y. Cheng³¹, A. Cheplakov⁶⁴, R. Cherkaoui El Moursli^{135e},
 V. Chernyatin²⁵, E. Cheu⁷, S.L. Cheung¹⁵⁸, L. Chevalier¹³⁶, G. Chiefari^{102a,102b},
 L. Chikovani^{51a,*}, J.T. Childers³⁰, A. Chilingarov⁷¹, G. Chiodini^{72a}, A.S. Chisholm¹⁸,
 R.T. Chislett⁷⁷, A. Chitan^{26a}, M.V. Chizhov⁶⁴, G. Choudalakis³¹, S. Chouridou¹³⁷,
 I.A. Christidi⁷⁷, A. Christov⁴⁸, D. Chromek-Burckhart³⁰, M.L. Chu¹⁵¹, J. Chudoba¹²⁵,
 G. Ciapetti^{132a,132b}, A.K. Ciftci^{4a}, R. Ciftci^{4a}, D. Cinca³⁴, V. Cindro⁷⁴, C. Ciocca^{20a,20b},
 A. Ciochio¹⁵, M. Cirilli⁸⁷, P. Cirkovic^{13b}, Z.H. Citron¹⁷², M. Citterio^{89a}, M. Ciubancan^{26a},
 A. Clark⁴⁹, P.J. Clark⁴⁶, R.N. Clarke¹⁵, W. Cleland¹²³, J.C. Clemens⁸³, B. Clement⁵⁵,
 C. Clement^{146a,146b}, Y. Coadou⁸³, M. Cobal^{164a,164c}, A. Coccaro¹³⁸, J. Cochran⁶³, L. Coffey²³,
 J.G. Cogan¹⁴³, J. Coggeshall¹⁶⁵, E. Cogneras¹⁷⁸, J. Colas⁵, S. Cole¹⁰⁶, A.P. Colijn¹⁰⁵,
 N.J. Collins¹⁸, C. Collins-Tooth⁵³, J. Collot⁵⁵, T. Colombo^{119a,119b}, G. Colon⁸⁴,
 G. Compostella⁹⁹, P. Conde Muiño^{124a}, E. Coniavitis¹⁶⁶, M.C. Conidi¹², S.M. Consonni^{89a,89b},
 V. Consorti⁴⁸, S. Constantinescu^{26a}, C. Conta^{119a,119b}, G. Conti⁵⁷, F. Conventi^{102a,j}, M. Cooke¹⁵,

B.D. Cooper⁷⁷, A.M. Cooper-Sarkar¹¹⁸, K. Copic¹⁵, T. Cornelissen¹⁷⁵, M. Corradi^{20a},
F. Corriveau^{85,k}, A. Cortes-Gonzalez¹⁶⁵, G. Cortiana⁹⁹, G. Costa^{89a}, M.J. Costa¹⁶⁷,
D. Costanzo¹³⁹, D. Côté³⁰, L. Courneyea¹⁶⁹, G. Cowan⁷⁶, C. Cowden²⁸, B.E. Cox⁸²,
K. Cranmer¹⁰⁸, F. Crescioli⁷⁸, M. Cristinziani²¹, G. Crosetti^{37a,37b}, S. Crépe-Renaudin⁵⁵,
C.-M. Cuciuc^{26a}, C. Cuenca Almenar¹⁷⁶, T. Cuhadar Donszelmann¹³⁹, J. Cummings¹⁷⁶,
M. Curatolo⁴⁷, C.J. Curtis¹⁸, C. Cuthbert¹⁵⁰, P. Cwetanski⁶⁰, H. Czirr¹⁴¹, P. Czodrowski⁴⁴,
Z. Czyczula¹⁷⁶, S. D'Auria⁵³, M. D'Onofrio⁷³, A. D'Orazio^{132a,132b},
M.J. Da Cunha Sargedas De Sousa^{124a}, C. Da Via⁸², W. Dabrowski³⁸, A. Dafinca¹¹⁸, T. Dai⁸⁷,
C. Dallapiccola⁸⁴, M. Dam³⁶, M. Dameri^{50a,50b}, D.S. Damiani¹³⁷, H.O. Danielsson³⁰, V. Dao⁴⁹,
G. Darbo^{50a}, G.L. Darlea^{26b}, J.A. Dassoulas⁴², W. Davey²¹, T. Davidek¹²⁶, N. Davidson⁸⁶,
R. Davidson⁷¹, E. Davies^{118,c}, M. Davies⁹³, O. Davignon⁷⁸, A.R. Davison⁷⁷, Y. Davygora^{58a},
E. Dawe¹⁴², I. Dawson¹³⁹, R.K. Daya-Ishmukhametova²³, K. De⁸, R. de Asmundis^{102a},
S. De Castro^{20a,20b}, S. De Cecco⁷⁸, J. de Graat⁹⁸, N. De Groot¹⁰⁴, P. de Jong¹⁰⁵,
C. De La Taille¹¹⁵, H. De la Torre⁸⁰, F. De Lorenzi⁶³, L. de Mora⁷¹, L. De Nooij¹⁰⁵,
D. De Pedis^{132a}, A. De Salvo^{132a}, U. De Sanctis^{164a,164c}, A. De Santo¹⁴⁹,
J.B. De Vivie De Regie¹¹⁵, G. De Zorzi^{132a,132b}, W.J. Dearnaley⁷¹, R. Debbé²⁵, C. Debenedetti⁴⁶,
B. Dechenaux⁵⁵, D.V. Dedovich⁶⁴, J. Degenhardt¹²⁰, J. Del Peso⁸⁰, T. Del Prete^{122a,122b},
T. Delemontex⁵⁵, M. Deliyergiyev⁷⁴, A. Dell'Acqua³⁰, L. Dell'Asta²², M. Della Pietra^{102a,j},
D. della Volpe^{102a,102b}, M. Delmastro⁵, P.A. Delsart⁵⁵, C. Deluca¹⁰⁵, S. Demers¹⁷⁶,
M. Demichev⁶⁴, B. Demirköz^{12,l}, S.P. Denisov¹²⁸, D. Derendarz³⁹, J.E. Derkaoui^{135d}, F. Derue⁷⁸,
P. Dervan⁷³, K. Desch²¹, E. Devetak¹⁴⁸, P.O. Deviveiros¹⁰⁵, A. Dewhurst¹²⁹, B. DeWilde¹⁴⁸,
S. Dhaliwal¹⁵⁸, R. Dhullipudi^{25,m}, A. Di Ciaccio^{133a,133b}, L. Di Ciaccio⁵, C. Di Donato^{102a,102b},
A. Di Girolamo³⁰, B. Di Girolamo³⁰, S. Di Luise^{134a,134b}, A. Di Mattia¹⁷³, B. Di Micco³⁰,
R. Di Nardo⁴⁷, A. Di Simone^{133a,133b}, R. Di Sipio^{20a,20b}, M.A. Diaz^{32a}, E.B. Diehl⁸⁷,
J. Dietrich⁴², T.A. Dietzsch^{58a}, S. Diglio⁸⁶, K. Dindar Yagci⁴⁰, J. Dingfelder²¹, F. Dinut^{26a},
C. Dionisi^{132a,132b}, P. Dita^{26a}, S. Dita^{26a}, F. Dittus³⁰, F. Djama⁸³, T. Djobava^{51b},
M.A.B. do Vale^{24c}, A. Do Valle Wemans^{124a,n}, T.K.O. Doan⁵, M. Dobbs⁸⁵, D. Dobos³⁰,
E. Dobson^{30,o}, J. Dodd³⁵, C. Doglioni⁴⁹, T. Doherty⁵³, Y. Doi^{65,*}, J. Dolejsi¹²⁶, I. Dolenc⁷⁴,
Z. Dolezal¹²⁶, B.A. Dolgoshein^{96,*}, T. Dohmae¹⁵⁵, M. Donadelli^{24d}, J. Donini³⁴, J. Dopke³⁰,
A. Doria^{102a}, A. Dos Anjos¹⁷³, A. Dotti^{122a,122b}, M.T. Dova⁷⁰, A.D. Doxiadis¹⁰⁵, A.T. Doyle⁵³,
N. Dressnandt¹²⁰, M. Dris¹⁰, J. Dubbert⁹⁹, S. Dube¹⁵, E. Duchovni¹⁷², G. Duckeck⁹⁸, D. Duda¹⁷⁵,
A. Dudarev³⁰, F. Dudziak⁶³, M. Dührssen³⁰, I.P. Duerdoth⁸², L. Dufflot¹¹⁵, M-A. Dufour⁸⁵,
L. Duguid⁷⁶, M. Dunford^{58a}, H. Duran Yildiz^{4a}, R. Duxfield¹³⁹, M. Dwuznik³⁸, M. Düren⁵²,
W.L. Ebenstein⁴⁵, J. Ebke⁹⁸, S. Eckweiler⁸¹, K. Edmonds⁸¹, W. Edson², C.A. Edwards⁷⁶,
N.C. Edwards⁵³, W. Ehrenfeld⁴², T. Eifert¹⁴³, G. Eigen¹⁴, K. Einsweiler¹⁵, E. Eisenhandler⁷⁵,
T. Ekelof¹⁶⁶, M. El Kacimi^{135c}, M. Ellert¹⁶⁶, S. Elles⁵, F. Ellinghaus⁸¹, K. Ellis⁷⁵, N. Ellis³⁰,
J. Elmsheuser⁹⁸, M. Elsing³⁰, D. Emeliyanov¹²⁹, R. Engelmann¹⁴⁸, A. Engl⁹⁸, B. Epp⁶¹,
J. Erdmann⁵⁴, A. Ereditato¹⁷, D. Eriksson^{146a}, J. Ernst², M. Ernst²⁵, J. Ernwein¹³⁶,
D. Errede¹⁶⁵, S. Errede¹⁶⁵, E. Ertel⁸¹, M. Escalier¹¹⁵, H. Esch⁴³, C. Escobar¹²³,
X. Espinal Curull¹², B. Esposito⁴⁷, F. Etienne⁸³, A.I. Etievre¹³⁶, E. Etzion¹⁵³,
D. Evangelakou⁵⁴, H. Evans⁶⁰, L. Fabbri^{20a,20b}, C. Fabre³⁰, R.M. Fakhruddinov¹²⁸,
S. Falciano^{132a}, Y. Fang^{33a}, M. Fanti^{89a,89b}, A. Farbin⁸, A. Farilla^{134a}, J. Farley¹⁴⁸,
T. Farooque¹⁵⁸, S. Farrell¹⁶³, S.M. Farrington¹⁷⁰, P. Farthouat³⁰, F. Fassi¹⁶⁷, P. Fassnacht³⁰,
D. Fassouliotis⁹, B. Fatholahzadeh¹⁵⁸, A. Favareto^{89a,89b}, L. Fayard¹¹⁵, S. Fazio^{37a,37b},
R. Febbraro³⁴, P. Federic^{144a}, O.L. Fedin¹²¹, W. Fedorko⁸⁸, M. Fehling-Kaschek⁴⁸, L. Feligioni⁸³,
C. Feng^{33d}, E.J. Feng⁶, A.B. Fenyuk¹²⁸, J. Ferencei^{144b}, W. Fernando⁶, S. Ferrag⁵³, J. Ferrando⁵³,
V. Ferrara⁴², A. Ferrari¹⁶⁶, P. Ferrari¹⁰⁵, R. Ferrari^{119a}, D.E. Ferreira de Lima⁵³, A. Ferrer¹⁶⁷,
D. Ferrere⁴⁹, C. Ferretti⁸⁷, A. Ferretto Parodi^{50a,50b}, M. Fiascaris³¹, F. Fiedler⁸¹, A. Filipčić⁷⁴,

F. Filthaut¹⁰⁴, M. Fincke-Keeler¹⁶⁹, M.C.N. Fiolhais^{124a,h}, L. Fiorini¹⁶⁷, A. Firan⁴⁰, G. Fischer⁴², M.J. Fisher¹⁰⁹, M. Flechl¹⁴⁸, I. Fleck¹⁴¹, J. Fleckner⁸¹, P. Fleischmann¹⁷⁴, S. Fleischmann¹⁷⁵, T. Flick¹⁷⁵, A. Floderus⁷⁹, L.R. Flores Castillo¹⁷³, M.J. Flowerdew⁹⁹, T. Fonseca Martin¹⁷, A. Formica¹³⁶, A. Forti⁸², D. Fortin^{159a}, D. Fournier¹¹⁵, A.J. Fowler⁴⁵, H. Fox⁷¹, P. Francavilla¹², M. Franchini^{20a,20b}, S. Franchino^{119a,119b}, D. Francis³⁰, T. Frank¹⁷², M. Franklin⁵⁷, S. Franz³⁰, M. Fraternali^{119a,119b}, S. Fratina¹²⁰, S.T. French²⁸, C. Friedrich⁴², F. Friedrich⁴⁴, R. Froeschl³⁰, D. Froidevaux³⁰, J.A. Frost²⁸, C. Fukunaga¹⁵⁶, E. Fullana Torregrosa³⁰, B.G. Fulson¹⁴³, J. Fuster¹⁶⁷, C. Gabaldon³⁰, O. Gabizon¹⁷², T. Gadfort²⁵, S. Gadomski⁴⁹, G. Gagliardi^{50a,50b}, P. Gagnon⁶⁰, C. Galea⁹⁸, B. Galhardo^{124a}, E.J. Gallas¹¹⁸, V. Gallo¹⁷, B.J. Gallop¹²⁹, P. Gallus¹²⁵, K.K. Gan¹⁰⁹, Y.S. Gao^{143,f}, A. Gaponenko¹⁵, F. Garberon¹⁷⁶, M. Garcia-Sciveres¹⁵, C. García¹⁶⁷, J.E. García Navarro¹⁶⁷, R.W. Gardner³¹, N. Garelli³⁰, H. Garitaonandia¹⁰⁵, V. Garonne³⁰, C. Gatti⁴⁷, G. Gaudio^{119a}, B. Gaur¹⁴¹, L. Gauthier¹³⁶, P. Gauzzi^{132a,132b}, I.L. Gavrilenko⁹⁴, C. Gay¹⁶⁸, G. Gaycken²¹, E.N. Gazis¹⁰, P. Ge^{33d}, Z. Gecse¹⁶⁸, C.N.P. Gee¹²⁹, D.A.A. Geerts¹⁰⁵, Ch. Geich-Gimbel²¹, K. Gellerstedt^{146a,146b}, C. Gemme^{50a}, A. Gemmell⁵³, M.H. Genest⁵⁵, S. Gentile^{132a,132b}, M. George⁵⁴, S. George⁷⁶, P. Gerlach¹⁷⁵, A. Gershon¹⁵³, C. Geweniger^{58a}, H. Ghazlane^{135b}, N. Ghodbane³⁴, B. Giacobbe^{20a}, S. Giagu^{132a,132b}, V. Giakoumopoulou⁹, V. Giangiobbe¹², F. Gianotti³⁰, B. Gibbard²⁵, A. Gibson¹⁵⁸, S.M. Gibson³⁰, M. Gilchriese¹⁵, D. Gillberg²⁹, A.R. Gillman¹²⁹, D.M. Gingrich^{3,e}, J. Ginzburg¹⁵³, N. Giokaris⁹, M.P. Giordani^{164c}, R. Giordano^{102a,102b}, F.M. Giorgi¹⁶, P. Giovannini⁹⁹, P.F. Giraud¹³⁶, D. Giugni^{89a}, M. Giunta⁹³, B.K. Gjelsten¹¹⁷, L.K. Gladilin⁹⁷, C. Glasman⁸⁰, J. Glatzer²¹, A. Glazov⁴², K.W. Glitza¹⁷⁵, G.L. Glonti⁶⁴, J.R. Goddard⁷⁵, J. Godfrey¹⁴², J. Godlewski³⁰, M. Goebel⁴², T. Göpfert⁴⁴, C. Goeringer⁸¹, C. Gössling⁴³, S. Goldfarb⁸⁷, T. Golling¹⁷⁶, A. Gomes^{124a,b}, L.S. Gomez Fajardo⁴², R. Gonçalo⁷⁶, J. Goncalves Pinto Firmino Da Costa⁴², L. Gonella²¹, S. González de la Hoz¹⁶⁷, G. Gonzalez Parra¹², M.L. Gonzalez Silva²⁷, S. Gonzalez-Sevilla⁴⁹, J.J. Goodson¹⁴⁸, L. Goossens³⁰, P.A. Gorbounov⁹⁵, H.A. Gordon²⁵, I. Gorelov¹⁰³, G. Gorfine¹⁷⁵, B. Gorini³⁰, E. Gorini^{72a,72b}, A. Gorišek⁷⁴, E. Gornicki³⁹, A.T. Goshaw⁶, M. Gosselink¹⁰⁵, M.I. Gostkin⁶⁴, I. Gough Eschrich¹⁶³, M. Gouighri^{135a}, D. Goujdami^{135c}, M.P. Goulette⁴⁹, A.G. Goussiou¹³⁸, C. Goy⁵, S. Gozpinar²³, I. Grabowska-Bold³⁸, P. Grafström^{20a,20b}, K.-J. Grah⁴², E. Gramstad¹¹⁷, F. Grancagnolo^{72a}, S. Grancagnolo¹⁶, V. Grassi¹⁴⁸, V. Gratchev¹²¹, N. Grau³⁵, H.M. Gray³⁰, J.A. Gray¹⁴⁸, E. Graziani^{134a}, O.G. Grebenyuk¹²¹, T. Greenshaw⁷³, Z.D. Greenwood^{25,m}, K. Gregersen³⁶, I.M. Gregor⁴², P. Grenier¹⁴³, J. Griffiths⁸, N. Grigalashvili⁶⁴, A.A. Grillo¹³⁷, S. Grinstein¹², Ph. Gris³⁴, Y.V. Grishkevich⁹⁷, J.-F. Grivaz¹¹⁵, E. Gross¹⁷², J. Grosse-Knetter⁵⁴, J. Groth-Jensen¹⁷², K. Grybel¹⁴¹, D. Guest¹⁷⁶, C. Guicheney³⁴, E. Guido^{50a,50b}, S. Guindon⁵⁴, U. Gul⁵³, J. Gunther¹²⁵, B. Guo¹⁵⁸, J. Guo³⁵, P. Gutierrez¹¹¹, N. Guttman¹⁵³, O. Gutzwiller¹⁷³, C. Guyot¹³⁶, C. Gwenlan¹¹⁸, C.B. Gwilliam⁷³, A. Haas¹⁰⁸, S. Haas³⁰, C. Haber¹⁵, H.K. Hadavand⁸, D.R. Hadley¹⁸, P. Haefner²¹, F. Hahn³⁰, Z. Hajduk³⁹, H. Hakobyan¹⁷⁷, D. Hall¹¹⁸, K. Hamacher¹⁷⁵, P. Hamal¹¹³, K. Hamano⁸⁶, M. Hamer⁵⁴, A. Hamilton^{145b,p}, S. Hamilton¹⁶¹, L. Han^{33b}, K. Hanagaki¹¹⁶, K. Hanawa¹⁶⁰, M. Hance¹⁵, C. Handel⁸¹, P. Hanke^{58a}, J.R. Hansen³⁶, J.B. Hansen³⁶, J.D. Hansen³⁶, P.H. Hansen³⁶, P. Hansson¹⁴³, K. Hara¹⁶⁰, T. Harenberg¹⁷⁵, S. Harkusha⁹⁰, D. Harper⁸⁷, R.D. Harrington⁴⁶, O.M. Harris¹³⁸, J. Hartert⁴⁸, F. Hartjes¹⁰⁵, T. Haruyama⁶⁵, A. Harvey⁵⁶, S. Hasegawa¹⁰¹, Y. Hasegawa¹⁴⁰, S. Hassani¹³⁶, S. Haug¹⁷, M. Hauschild³⁰, R. Hauser⁸⁸, M. Havranek²¹, C.M. Hawkes¹⁸, R.J. Hawkings³⁰, A.D. Hawkins⁷⁹, T. Hayakawa⁶⁶, T. Hayashi¹⁶⁰, D. Hayden⁷⁶, C.P. Hays¹¹⁸, H.S. Hayward⁷³, S.J. Haywood¹²⁹, S.J. Head¹⁸, V. Hedberg⁷⁹, L. Heelan⁸, S. Heim¹²⁰, B. Heinemann¹⁵, S. Heisterkamp³⁶, L. Helary²², C. Heller⁹⁸, M. Heller³⁰, S. Hellman^{146a,146b}, D. Hellmich²¹, C. Helsen¹², R.C.W. Henderson⁷¹, M. Henke^{58a}, A. Henrichs¹⁷⁶, A.M. Henriques Correia³⁰, S. Henrot-Versille¹¹⁵, C. Hensel⁵⁴, C.M. Hernandez⁸, Y. Hernández Jiménez¹⁶⁷, R. Herrberg¹⁶,

G. Herten⁴⁸, R. Hertenberger⁹⁸, L. Hervas³⁰, G.G. Hesketh⁷⁷, N.P. Hessey¹⁰⁵,
E. Higón-Rodríguez¹⁶⁷, J.C. Hill²⁸, K.H. Hiller⁴², S. Hillert²¹, S.J. Hillier¹⁸, I. Hinchliffe¹⁵,
E. Hines¹²⁰, M. Hirose¹¹⁶, F. Hirsch⁴³, D. Hirschbuehl¹⁷⁵, J. Hobbs¹⁴⁸, N. Hod¹⁵³,
M.C. Hodgkinson¹³⁹, P. Hodgson¹³⁹, A. Hoecker³⁰, M.R. Hoferkamp¹⁰³, J. Hoffman⁴⁰,
D. Hoffmann⁸³, M. Hohlfeld⁸¹, M. Holder¹⁴¹, S.O. Holmgren^{146a}, T. Holy¹²⁷, J.L. Holzbauer⁸⁸,
T.M. Hong¹²⁰, L. Hooft van Huysduynen¹⁰⁸, S. Horner⁴⁸, J.-Y. Hostachy⁵⁵, S. Hou¹⁵¹,
A. Hoummada^{135a}, J. Howard¹¹⁸, J. Howarth⁸², I. Hristova¹⁶, J. Hrivnac¹¹⁵, T. Hryn'ova⁵,
P.J. Hsu⁸¹, S.-C. Hsu¹⁵, D. Hu³⁵, Z. Hubacek¹²⁷, F. Hubaut⁸³, F. Huegging²¹, A. Huettmann⁴²,
T.B. Huffman¹¹⁸, E.W. Hughes³⁵, G. Hughes⁷¹, M. Huhtinen³⁰, M. Hurwitz¹⁵, N. Huseynov^{64,g},
J. Huston⁸⁸, J. Huth⁵⁷, G. Iacobucci⁴⁹, G. Iakovidis¹⁰, M. Ibbotson⁸², I. Ibragimov¹⁴¹,
L. Iconomidou-Fayard¹¹⁵, J. Idarraga¹¹⁵, P. Iengo^{102a}, O. Igonkina¹⁰⁵, Y. Ikegami⁶⁵, M. Ikeno⁶⁵,
D. Iliadis¹⁵⁴, N. Ilic¹⁵⁸, T. Ince⁹⁹, P. Ioannou⁹, M. Iodice^{134a}, K. Iordanidou⁹, V. Ippolito^{132a,132b},
A. Irles Quiles¹⁶⁷, C. Isaksson¹⁶⁶, M. Ishino⁶⁷, M. Ishitsuka¹⁵⁷, R. Ishmukhametov¹⁰⁹,
C. Issever¹¹⁸, S. Istin^{19a}, A.V. Ivashin¹²⁸, W. Iwanski³⁹, H. Iwasaki⁶⁵, J.M. Izen⁴¹, V. Izzo^{102a},
B. Jackson¹²⁰, J.N. Jackson⁷³, P. Jackson¹, M.R. Jaekel³⁰, V. Jain⁶⁰, K. Jakobs⁴⁸, S. Jakobsen³⁶,
T. Jakoubek¹²⁵, J. Jakubek¹²⁷, D.O. Jamin¹⁵¹, D.K. Jana¹¹¹, E. Jansen⁷⁷, H. Jansen³⁰,
J. Janssen²¹, A. Jantsch⁹⁹, M. Janus⁴⁸, R.C. Jared¹⁷³, G. Jarlskog⁷⁹, L. Jeanty⁵⁷,
I. Jen-La Plante³¹, D. Jennens⁸⁶, P. Jenni³⁰, A.E. Loevschall-Jensen³⁶, P. Jež³⁶, S. Jézéquel⁵,
M.K. Jha^{20a}, H. Ji¹⁷³, W. Ji⁸¹, J. Jia¹⁴⁸, Y. Jiang^{33b}, M. Jimenez Belenguer⁴², S. Jin^{33a},
O. Jinnouchi¹⁵⁷, M.D. Joergensen³⁶, D. Joffe⁴⁰, M. Johansen^{146a,146b}, K.E. Johansson^{146a},
P. Johansson¹³⁹, S. Johnert⁴², K.A. Johns⁷, K. Jon-And^{146a,146b}, G. Jones¹⁷⁰, R.W.L. Jones⁷¹,
T.J. Jones⁷³, C. Joram³⁰, P.M. Jorge^{124a}, K.D. Joshi⁸², J. Jovicevic¹⁴⁷, T. Jovin^{13b}, X. Ju¹⁷³,
C.A. Jung⁴³, R.M. Jungst³⁰, V. Juranek¹²⁵, P. Jussel⁶¹, A. Juste Rozas¹², S. Kabana¹⁷,
M. Kaci¹⁶⁷, A. Kaczmarska³⁹, P. Kadlecik³⁶, M. Kado¹¹⁵, H. Kagan¹⁰⁹, M. Kagan⁵⁷,
E. Kajomovitz¹⁵², S. Kalinin¹⁷⁵, L.V. Kalinovskaya⁶⁴, S. Kama⁴⁰, N. Kanaya¹⁵⁵, M. Kaneda³⁰,
S. Kaneti²⁸, T. Kanno¹⁵⁷, V.A. Kantserov⁹⁶, J. Kanzaki⁶⁵, B. Kaplan¹⁰⁸, A. Kapliy³¹,
J. Kaplon³⁰, D. Kar⁵³, M. Karagounis²¹, K. Karakostas¹⁰, M. Karnevskiy⁴², V. Kartvelishvili⁷¹,
A.N. Karyukhin¹²⁸, L. Kashif¹⁷³, G. Kasieczka^{58b}, R.D. Kass¹⁰⁹, A. Kastanas¹⁴, M. Kataoka⁵,
Y. Kataoka¹⁵⁵, E. Katsoufis¹⁰, J. Katzy⁴², V. Kaushik⁷, K. Kawagoe⁶⁹, T. Kawamoto¹⁵⁵,
G. Kawamura⁸¹, M.S. Kayl¹⁰⁵, S. Kazama¹⁵⁵, V.F. Kazanin¹⁰⁷, M.Y. Kazarinov⁶⁴, R. Keeler¹⁶⁹,
P.T. Keener¹²⁰, R. Kehoe⁴⁰, M. Keil⁵⁴, G.D. Kekelidze⁶⁴, J.S. Keller¹³⁸, M. Kenyon⁵³,
O. Kepka¹²⁵, N. Kerschen³⁰, B.P. Kerševan⁷⁴, S. Kersten¹⁷⁵, K. Kessoku¹⁵⁵, J. Keung¹⁵⁸,
F. Khalil-zada¹¹, H. Khandanyan^{146a,146b}, A. Khanov¹¹², D. Kharchenko⁶⁴, A. Khodinov⁹⁶,
A. Khomich^{58a}, T.J. Khoo²⁸, G. Khoriali²¹, A. Khoroshilov¹⁷⁵, V. Khovanskiy⁹⁵, E. Khramov⁶⁴,
J. Khubua^{51b}, H. Kim^{146a,146b}, S.H. Kim¹⁶⁰, N. Kimura¹⁷¹, O. Kind¹⁶, B.T. King⁷³, M. King⁶⁶,
R.S.B. King¹¹⁸, J. Kirk¹²⁹, A.E. Kiryunin⁹⁹, T. Kishimoto⁶⁶, D. Kisielewska³⁸, T. Kitamura⁶⁶,
T. Kittelmann¹²³, K. Kiuchi¹⁶⁰, E. Kladiva^{144b}, M. Klein⁷³, U. Klein⁷³, K. Kleinknecht⁸¹,
M. Klemetti⁸⁵, A. Klier¹⁷², P. Klimek^{146a,146b}, A. Klimentov²⁵, R. Klingenberg⁴³, J.A. Klinger⁸²,
E.B. Klinkby³⁶, T. Klioutchnikova³⁰, P.F. Klok¹⁰⁴, S. Klous¹⁰⁵, E.-E. Kluge^{58a}, T. Kluge⁷³,
P. Kluit¹⁰⁵, S. Kluth⁹⁹, E. Kneringer⁶¹, E.B.F.G. Knoops⁸³, A. Knue⁵⁴, B.R. Ko⁴⁵,
T. Kobayashi¹⁵⁵, M. Kobel⁴⁴, M. Kocian¹⁴³, P. Kodys¹²⁶, K. Köneke³⁰, A.C. König¹⁰⁴,
S. Koenig⁸¹, L. Köpke⁸¹, F. Koetsveld¹⁰⁴, P. Koevesarki²¹, T. Koffas²⁹, E. Koffeman¹⁰⁵,
L.A. Kogan¹¹⁸, S. Kohlmann¹⁷⁵, F. Kohn⁵⁴, Z. Kohout¹²⁷, T. Kohriki⁶⁵, T. Koi¹⁴³,
G.M. Kolachev^{107,*}, H. Kolanoski¹⁶, V. Kolesnikov⁶⁴, I. Koletsou^{89a}, J. Koll⁸⁸, A.A. Komar⁹⁴,
Y. Komori¹⁵⁵, T. Kondo⁶⁵, T. Kono^{42,r}, A.I. Kononov⁴⁸, R. Konoplich^{108,s}, N. Konstantinidis⁷⁷,
R. Kopeliansky¹⁵², S. Koperny³⁸, K. Korcyl³⁹, K. Kordas¹⁵⁴, A. Korn¹¹⁸, A. Korol¹⁰⁷,
I. Korolkov¹², E.V. Korolkova¹³⁹, V.A. Korotkov¹²⁸, O. Kortner⁹⁹, S. Kortner⁹⁹,
V.V. Kostyukhin²¹, S. Kotov⁹⁹, V.M. Kotov⁶⁴, A. Kotwal⁴⁵, C. Kourkoumelis⁹, V. Kouskoura¹⁵⁴,

A. Koutsman^{159a}, R. Kowalewski¹⁶⁹, T.Z. Kowalski³⁸, W. Kozanecki¹³⁶, A.S. Kozhin¹²⁸,
 V. Kral¹²⁷, V.A. Kramarenko⁹⁷, G. Kramberger⁷⁴, M.W. Krasny⁷⁸, A. Krasznahorkay¹⁰⁸,
 J.K. Kraus²¹, S. Kreiss¹⁰⁸, F. Krejci¹²⁷, J. Kretzschmar⁷³, N. Krieger⁵⁴, P. Krieger¹⁵⁸,
 K. Kroeninger⁵⁴, H. Kroha⁹⁹, J. Kroll¹²⁰, J. Kroseberg²¹, J. Krstic^{13a}, U. Kruchonak⁶⁴,
 H. Krüger²¹, T. Kruker¹⁷, N. Krumnack⁶³, Z.V. Krumshteyn⁶⁴, M.K. Kruse⁴⁵, T. Kubota⁸⁶,
 S. Kuday^{4a}, S. Kuehn⁴⁸, A. Kugel^{58c}, T. Kuhl⁴², D. Kuhn⁶¹, V. Kukhtin⁶⁴, Y. Kulchitsky⁹⁰,
 S. Kuleshov^{32b}, C. Kummer⁹⁸, M. Kuna⁷⁸, J. Kunkle¹²⁰, A. Kupco¹²⁵, H. Kurashige⁶⁶,
 M. Kurata¹⁶⁰, Y.A. Kurochkin⁹⁰, V. Kus¹²⁵, E.S. Kuwertz¹⁴⁷, M. Kuze¹⁵⁷, J. Kvita¹⁴²,
 R. Kwee¹⁶, A. La Rosa⁴⁹, L. La Rotonda^{37a,37b}, L. Labarga⁸⁰, J. Labbe⁵, S. Lablak^{135a},
 C. Lacasta¹⁶⁷, F. Lacava^{132a,132b}, J. Lacey²⁹, H. Lacker¹⁶, D. Lacour⁷⁸, V.R. Lacuesta¹⁶⁷,
 E. Ladygin⁶⁴, R. Lafaye⁵, B. Laforge⁷⁸, T. Lagouri¹⁷⁶, S. Lai⁴⁸, E. Laisne⁵⁵, L. Lambourne⁷⁷,
 C.L. Lampen⁷, W. Lampl⁷, E. Lancon¹³⁶, U. Landgraf⁴⁸, M.P.J. Landon⁷⁵, V.S. Lang^{58a},
 C. Lange⁴², A.J. Lankford¹⁶³, F. Lanni²⁵, K. Lantzsich¹⁷⁵, A. Lanza^{119a}, S. Laplace⁷⁸,
 C. Lapoire²¹, J.F. Laporte¹³⁶, T. Lari^{89a}, A. Lerner¹¹⁸, M. Lassnig³⁰, P. Laurelli⁴⁷,
 V. Lavorini^{37a,37b}, W. Lavrijsen¹⁵, P. Laycock⁷³, O. Le Dortz⁷⁸, E. Le Guirriec⁸³,
 E. Le Menedeu¹², T. LeCompte⁶, F. Ledroit-Guillon⁵⁵, H. Lee¹⁰⁵, J.S.H. Lee¹¹⁶, S.C. Lee¹⁵¹,
 L. Lee¹⁷⁶, M. Lefebvre¹⁶⁹, M. Legendre¹³⁶, F. Legger⁹⁸, C. Leggett¹⁵, M. Lehmacher²¹,
 G. Lehmann Miotto³⁰, A.G. Leister¹⁷⁶, M.A.L. Leite^{24d}, R. Leitner¹²⁶, D. Lellouch¹⁷²,
 B. Lemmer⁵⁴, V. Lendermann^{58a}, K.J.C. Leney^{145b}, T. Lenz¹⁰⁵, G. Lenzen¹⁷⁵, B. Lenzi³⁰,
 K. Leonhardt⁴⁴, S. Leontsinis¹⁰, F. Lepold^{58a}, C. Leroy⁹³, J-R. Lessard¹⁶⁹, C.G. Lester²⁸,
 C.M. Lester¹²⁰, J. Levêque⁵, D. Levin⁸⁷, L.J. Levinson¹⁷², A. Lewis¹¹⁸, G.H. Lewis¹⁰⁸,
 A.M. Leyko²¹, M. Leyton¹⁶, B. Li^{33b}, B. Li⁸³, H. Li¹⁴⁸, H.L. Li³¹, S. Li^{33b,t}, X. Li⁸⁷,
 Z. Liang^{118,u}, H. Liao³⁴, B. Liberti^{133a}, P. Lichard³⁰, M. Lichtnecker⁹⁸, K. Lie¹⁶⁵, W. Liebig¹⁴,
 C. Limbach²¹, A. Limosani⁸⁶, M. Limper⁶², S.C. Lin^{151,v}, F. Linde¹⁰⁵, J.T. Linnemann⁸⁸,
 E. Lipeles¹²⁰, A. Lipniacka¹⁴, T.M. Liss¹⁶⁵, D. Lissauer²⁵, A. Lister⁴⁹, A.M. Litke¹³⁷, C. Liu²⁹,
 D. Liu¹⁵¹, H. Liu⁸⁷, J.B. Liu⁸⁷, L. Liu⁸⁷, M. Liu^{33b}, Y. Liu^{33b}, M. Livan^{119a,119b},
 S.S.A. Livermore¹¹⁸, A. Lleres⁵⁵, J. Llorente Merino⁸⁰, S.L. Lloyd⁷⁵, E. Lobodzinska⁴², P. Loch⁷,
 W.S. Lockman¹³⁷, T. Loddenkoetter²¹, F.K. Loebinger⁸², A. Loginov¹⁷⁶, C.W. Loh¹⁶⁸,
 T. Lohse¹⁶, K. Lohwasser⁴⁸, M. Lokajicek¹²⁵, V.P. Lombardo⁵, R.E. Long⁷¹, L. Lopes^{124a},
 D. Lopez Mateos⁵⁷, J. Lorenz⁹⁸, N. Lorenzo Martinez¹¹⁵, M. Losada¹⁶², P. Loscutoff¹⁵,
 F. Lo Sterzo^{132a,132b}, M.J. Losty^{159a,*}, X. Lou⁴¹, A. Lounis¹¹⁵, K.F. Loureiro¹⁶², J. Love⁶,
 P.A. Love⁷¹, A.J. Lowe^{143,f}, F. Lu^{33a}, H.J. Lubatti¹³⁸, C. Luci^{132a,132b}, A. Lucotte⁵⁵,
 A. Ludwig⁴⁴, D. Ludwig⁴², I. Ludwig⁴⁸, J. Ludwig⁴⁸, F. Luehring⁶⁰, G. Luijckx¹⁰⁵, W. Lukas⁶¹,
 L. Luminari^{132a}, E. Lund¹¹⁷, B. Lund-Jensen¹⁴⁷, B. Lundberg⁷⁹, J. Lundberg^{146a,146b},
 O. Lundberg^{146a,146b}, J. Lundquist³⁶, M. Lungwitz⁸¹, D. Lynn²⁵, E. Lytken⁷⁹, H. Ma²⁵,
 L.L. Ma¹⁷³, G. Maccarrone⁴⁷, A. Macchiolo⁹⁹, B. Maček⁷⁴, J. Machado Miguens^{124a}, D. Macina³⁰,
 R. Mackeprang³⁶, R.J. Madaras¹⁵, H.J. Maddocks⁷¹, W.F. Mader⁴⁴, R. Maenner^{58c}, T. Maeno²⁵,
 P. Mättig¹⁷⁵, S. Mättig⁴², L. Magnoni¹⁶³, E. Magradze⁵⁴, K. Mahboubi⁴⁸, J. Mahlstedt¹⁰⁵,
 S. Mahmoud⁷³, G. Mahout¹⁸, C. Maiani¹³⁶, C. Maidantchik^{24a}, A. Maio^{124a,b}, S. Majewski²⁵,
 Y. Makida⁶⁵, N. Makovec¹¹⁵, P. Mal¹³⁶, B. Malaescu³⁰, Pa. Malecki³⁹, P. Malecki³⁹,
 V.P. Maleev¹²¹, F. Malek⁵⁵, U. Mallik⁶², D. Malon⁶, C. Malone¹⁴³, S. Maltezos¹⁰,
 V. Malyshev¹⁰⁷, S. Malyukov³⁰, R. Mameghani⁹⁸, J. Mamuzic^{13b}, A. Manabe⁶⁵, L. Mandelli^{89a},
 I. Mandić⁷⁴, R. Mandrysch¹⁶, J. Maneira^{124a}, A. Manfredini⁹⁹, L. Manhaes de Andrade Filho^{24b},
 J.A. Manjarres Ramos¹³⁶, A. Mann⁵⁴, P.M. Manning¹³⁷, A. Manousakis-Katsikakis⁹,
 B. Mansoulie¹³⁶, A. Mapelli³⁰, L. Mapelli³⁰, L. March¹⁶⁷, J.F. Marchand²⁹, F. Marchese^{133a,133b},
 G. Marchiori⁷⁸, M. Marcisovskey¹²⁵, C.P. Marino¹⁶⁹, F. Marroquim^{24a}, Z. Marshall³⁰,
 L.F. Marti¹⁷, S. Marti-Garcia¹⁶⁷, B. Martin³⁰, B. Martin⁸⁸, J.P. Martin⁹³, T.A. Martin¹⁸,
 V.J. Martin⁴⁶, B. Martin dit Latour⁴⁹, S. Martin-Haugh¹⁴⁹, M. Martinez¹²,

V. Martinez Outschoorn⁵⁷, A.C. Martyniuk¹⁶⁹, M. Marx⁸², F. Marzano^{132a}, A. Marzin¹¹¹,
L. Masetti⁸¹, T. Mashimo¹⁵⁵, R. Mashinistov⁹⁴, J. Masik⁸², A.L. Maslennikov¹⁰⁷, I. Massa^{20a,20b},
G. Massaro¹⁰⁵, N. Massol⁵, P. Mastrandrea¹⁴⁸, A. Mastroberardino^{37a,37b}, T. Masubuchi¹⁵⁵,
P. Matricon¹¹⁵, H. Matsunaga¹⁵⁵, T. Matsushita⁶⁶, C. Mattravers^{118,c}, J. Maurer⁸³,
S.J. Maxfield⁷³, D.A. Maximov^{107,g}, A. Mayne¹³⁹, R. Mazini¹⁵¹, M. Mazur²¹,
L. Mazzaferro^{133a,133b}, M. Mazzanti^{89a}, J. Mc Donald⁸⁵, S.P. Mc Kee⁸⁷, A. McCarn¹⁶⁵,
R.L. McCarthy¹⁴⁸, T.G. McCarthy²⁹, N.A. McCubbin¹²⁹, K.W. McFarlane^{56,*}, J.A. McFayden¹³⁹,
G. Mchedlidze^{51b}, T. Mclaughlan¹⁸, S.J. McMahon¹²⁹, R.A. McPherson^{169,k}, A. Meade⁸⁴,
J. Mechnich¹⁰⁵, M. Mechtel¹⁷⁵, M. Medinnis⁴², S. Meehan³¹, R. Meera-Lebbai¹¹¹, T. Meguro¹¹⁶,
S. Mehlhase³⁶, A. Mehta⁷³, K. Meier^{58a}, B. Meirose⁷⁹, C. Melachrinou³¹, B.R. Mellado Garcia¹⁷³,
F. Meloni^{89a,89b}, L. Mendoza Navas¹⁶², Z. Meng^{151,w}, A. Mengarelli^{20a,20b}, S. Menke⁹⁹,
E. Meoni¹⁶¹, K.M. Mercurio⁵⁷, P. Mermod⁴⁹, L. Merola^{102a,102b}, C. Meroni^{89a}, F.S. Merritt³¹,
H. Merritt¹⁰⁹, A. Messina^{30,x}, J. Metcalfe²⁵, A.S. Mete¹⁶³, C. Meyer⁸¹, C. Meyer³¹,
J.-P. Meyer¹³⁶, J. Meyer¹⁷⁴, J. Meyer⁵⁴, S. Michal³⁰, L. Micu^{26a}, R.P. Middleton¹²⁹, S. Migas⁷³,
L. Mijovic¹³⁶, G. Mikenberg¹⁷², M. Mikestikova¹²⁵, M. Mikuš⁷⁴, D.W. Miller³¹, R.J. Miller⁸⁸,
W.J. Mills¹⁶⁸, C. Mills⁵⁷, A. Milov¹⁷², D.A. Milstead^{146a,146b}, D. Milstein¹⁷², A.A. Minaenko¹²⁸,
M. Miñano Moya¹⁶⁷, I.A. Minashvili⁶⁴, A.I. Mincer¹⁰⁸, B. Mindur³⁸, M. Mineev⁶⁴, Y. Ming¹⁷³,
L.M. Mir¹², G. Mirabelli^{132a}, J. Mitrevski¹³⁷, V.A. Mitsou¹⁶⁷, S. Mitsui⁶⁵, P.S. Miyagawa¹³⁹,
J.U. Mjörnmark⁷⁹, T. Moe^{146a,146b}, V. Moeller²⁸, K. Mönig⁴², N. Möser²¹, S. Mohapatra¹⁴⁸,
W. Mohr⁴⁸, R. Moles-Valls¹⁶⁷, A. Molfetis³⁰, J. Monk⁷⁷, E. Monnier⁸³, J. Montejo Berlingen¹²,
F. Monticelli⁷⁰, S. Monzani^{20a,20b}, R.W. Moore³, G.F. Moorhead⁸⁶, C. Mora Herrera⁴⁹,
A. Moraes⁵³, N. Morange¹³⁶, J. Morel⁵⁴, G. Morello^{37a,37b}, D. Moreno⁸¹, M. Moreno Llácer¹⁶⁷,
P. Morettini^{50a}, M. Morgenstern⁴⁴, M. Morii⁵⁷, A.K. Morley³⁰, G. Mornacchi³⁰, J.D. Morris⁷⁵,
L. Morvaj¹⁰¹, H.G. Moser⁹⁹, M. Mosidze^{51b}, J. Moss¹⁰⁹, R. Mount¹⁴³, E. Mountricha^{10,y},
S.V. Mouraviev^{94,*}, E.J.W. Moyses⁸⁴, F. Mueller^{58a}, J. Mueller¹²³, K. Mueller²¹, T.A. Müller⁹⁸,
T. Mueller⁸¹, D. Muenstermann³⁰, Y. Munwes¹⁵³, W.J. Murray¹²⁹, I. Mussche¹⁰⁵, E. Musto¹⁵²,
A.G. Myagkov¹²⁸, M. Myska¹²⁵, O. Nackenhorst⁵⁴, J. Nadal¹², K. Nagai¹⁶⁰, R. Nagai¹⁵⁷,
K. Nagano⁶⁵, A. Nagarkar¹⁰⁹, Y. Nagasaka⁵⁹, M. Nagel⁹⁹, A.M. Nairz³⁰, Y. Nakahama³⁰,
K. Nakamura¹⁵⁵, T. Nakamura¹⁵⁵, I. Nakano¹¹⁰, G. Nanava²¹, A. Napier¹⁶¹, R. Narayan^{58b},
M. Nash^{77,c}, T. Nattermann²¹, T. Naumann⁴², G. Navarro¹⁶², H.A. Neal⁸⁷, P.Yu. Nechaeva⁹⁴,
T.J. Neep⁸², A. Negri^{119a,119b}, G. Negri³⁰, M. Negrini^{20a}, S. Nektarijevic⁴⁹, A. Nelson¹⁶³,
T.K. Nelson¹⁴³, S. Nemecek¹²⁵, P. Nemethy¹⁰⁸, A.A. Nepomuceno^{24a}, M. Nessi^{30,z},
M.S. Neubauer¹⁶⁵, M. Neumann¹⁷⁵, A. Neusiedl⁸¹, R.M. Neves¹⁰⁸, P. Nevski²⁵,
F.M. Newcomer¹²⁰, P.R. Newman¹⁸, V. Nguyen Thi Hong¹³⁶, R.B. Nickerson¹¹⁸,
R. Nicolaidou¹³⁶, B. Niquevert³⁰, F. Niedercorn¹¹⁵, J. Nielsen¹³⁷, N. Nikiforou³⁵, A. Nikiforov¹⁶,
V. Nikolaenko¹²⁸, I. Nikolic-Audit⁷⁸, K. Nikolics⁴⁹, K. Nikolopoulos¹⁸, H. Nilsen⁴⁸, P. Nilsson⁸,
Y. Ninomiya¹⁵⁵, A. Nisati^{132a}, R. Nisius⁹⁹, T. Nobe¹⁵⁷, L. Nodulman⁶, M. Nomachi¹¹⁶,
I. Nomidis¹⁵⁴, S. Norberg¹¹¹, M. Nordberg³⁰, P.R. Norton¹²⁹, J. Novakova¹²⁶, M. Nozaki⁶⁵,
L. Nozka¹¹³, I.M. Nugent^{159a}, A.-E. Nuncio-Quiroz²¹, G. Nunes Hanninger⁸⁶, T. Nunnemann⁹⁸,
E. Nurse⁷⁷, B.J. O'Brien⁴⁶, D.C. O'Neil¹⁴², V. O'Shea⁵³, L.B. Oakes⁹⁸, F.G. Oakham^{29,e},
H. Oberlack⁹⁹, J. Ocariz⁷⁸, A. Ochi⁶⁶, S. Oda⁶⁹, S. Odaka⁶⁵, J. Odier⁸³, H. Ogren⁶⁰, A. Oh⁸²,
S.H. Oh⁴⁵, C.C. Ohm³⁰, T. Ohshima¹⁰¹, W. Okamura¹¹⁶, H. Okawa²⁵, Y. Okumura³¹,
T. Okuyama¹⁵⁵, A. Olariu^{26a}, A.G. Olchevski⁶⁴, S.A. Olivares Pino^{32a}, M. Oliveira^{124a,h},
D. Oliveira Damazio²⁵, E. Oliver Garcia¹⁶⁷, D. Olivito¹²⁰, A. Olszewski³⁹, J. Olszowska³⁹,
A. Onofre^{124a,aa}, P.U.E. Onyisi³¹, C.J. Oram^{159a}, M.J. Oreglia³¹, Y. Oren¹⁵³,
D. Orestano^{134a,134b}, N. Orlando^{72a,72b}, I. Orlov¹⁰⁷, C. Oropeza Barrera⁵³, R.S. Orr¹⁵⁸,
B. Osculati^{50a,50b}, R. Ospanov¹²⁰, C. Osuna¹², G. Otero y Garzon²⁷, J.P. Ottersbach¹⁰⁵,
M. Ouchrif^{135d}, E.A. Ouellette¹⁶⁹, F. Ould-Saada¹¹⁷, A. Ouraou¹³⁶, Q. Ouyang^{33a},

A. Ovcharova¹⁵, M. Owen⁸², S. Owen¹³⁹, V.E. Ozcan^{19a}, N. Ozturk⁸, A. Pacheco Pages¹²,
 C. Padilla Aranda¹², S. Pagan Griso¹⁵, E. Paganis¹³⁹, C. Pahl⁹⁹, F. Paige²⁵, P. Pais⁸⁴,
 K. Pajchel¹¹⁷, G. Palacino^{159b}, C.P. Palestini⁷, S. Palestini³⁰, D. Pallin³⁴, A. Palma^{124a},
 J.D. Palmer¹⁸, Y.B. Pan¹⁷³, E. Panagiotopoulou¹⁰, J.G. Panduro Vazquez⁷⁶, P. Pani¹⁰⁵,
 N. Panikashvili⁸⁷, S. Panitkin²⁵, D. Pantea^{26a}, A. Papadelis^{146a}, Th.D. Papadopoulou¹⁰,
 A. Paramonov⁶, D. Paredes Hernandez³⁴, W. Park^{25,ab}, M.A. Parker²⁸, F. Parodi^{50a,50b},
 J.A. Parsons³⁵, U. Parzefall⁴⁸, S. Pashapour⁵⁴, E. Pasqualucci^{132a}, S. Passaggio^{50a}, A. Passeri^{134a},
 F. Pastore^{134a,134b,*}, Fr. Pastore⁷⁶, G. Pásztor^{49,ac}, S. Pataraiia¹⁷⁵, N. Patel¹⁵⁰, J.R. Pater⁸²,
 S. Patricelli^{102a,102b}, T. Pauly³⁰, M. Pecsý^{144a}, S. Pedraza Lopez¹⁶⁷, M.I. Pedraza Morales¹⁷³,
 S.V. Peleganchuk¹⁰⁷, D. Pelikan¹⁶⁶, H. Peng^{33b}, B. Penning³¹, A. Penson³⁵, J. Penwell⁶⁰,
 M. Perantoni^{24a}, G. Perez^{172,ad}, K. Perez^{35,ae}, T. Perez Cavalcanti⁴², E. Perez Codina^{159a},
 M.T. Pérez García-Estañ¹⁶⁷, V. Perez Reale³⁵, L. Perini^{89a,89b}, H. Pernegger³⁰, R. Perrino^{72a},
 P. Perrodo⁵, V.D. Peshekhonov⁶⁴, K. Peters³⁰, B.A. Petersen³⁰, J. Petersen³⁰, T.C. Petersen³⁶,
 E. Petit⁵, A. Petridis¹⁵⁴, C. Petridou¹⁵⁴, E. Petrolo^{132a}, F. Petrucci^{134a,134b}, D. Petschull⁴²,
 M. Petteni¹⁴², R. Pezoa^{32b}, A. Phan⁸⁶, P.W. Phillips¹²⁹, G. Piacquadio³⁰, A. Picazio⁴⁹,
 E. Piccaro⁷⁵, M. Piccinini^{20a,20b}, S.M. Piec⁴², R. Piegaiia²⁷, D.T. Pignotti¹⁰⁹, J.E. Pilcher³¹,
 A.D. Pilkington⁸², J. Pina^{124a,b}, M. Pinamonti^{164a,164c}, A. Pinder¹¹⁸, J.L. Pinfold³, B. Pinto^{124a},
 C. Pizio^{89a,89b}, M. Plamondon¹⁶⁹, M.-A. Pleier²⁵, E. Plotnikova⁶⁴, A. Poblaguev²⁵, S. Poddar^{58a},
 F. Podlyski³⁴, L. Poggioli¹¹⁵, D. Pohl²¹, M. Pohl⁴⁹, G. Polesello^{119a}, A. Policicchio^{37a,37b},
 A. Polini^{20a}, J. Poll⁷⁵, V. Polychronakos²⁵, D. Pomeroy²³, K. Pommès³⁰, L. Pontecorvo^{132a},
 B.G. Pope⁸⁸, G.A. Popeneciu^{26a}, D.S. Popovic^{13a}, A. Poppleton³⁰, X. Portell Bueso³⁰,
 G.E. Pospelov⁹⁹, S. Pospisil¹²⁷, I.N. Potrap⁹⁹, C.J. Potter¹⁴⁹, C.T. Potter¹¹⁴, G. Poulard³⁰,
 J. Poveda⁶⁰, V. Pozdnyakov⁶⁴, R. Prabhu⁷⁷, P. Pralavorio⁸³, A. Pranko¹⁵, S. Prasad³⁰,
 R. Pravahan²⁵, S. Prell⁶³, K. Pretzl¹⁷, D. Price⁶⁰, J. Price⁷³, L.E. Price⁶, D. Prieur¹²³,
 M. Primavera^{72a}, K. Prokofiev¹⁰⁸, F. Prokoshin^{32b}, S. Protopopescu²⁵, J. Proudfoot⁶,
 X. Prudent⁴⁴, M. Przybycien³⁸, H. Przysiezniak⁵, S. Psoroulas²¹, E. Ptacek¹¹⁴, E. Pueschel⁸⁴,
 J. Purdham⁸⁷, M. Purohit^{25,ab}, P. Puzo¹¹⁵, Y. Pylypchenko⁶², J. Qian⁸⁷, A. Quadt⁵⁴,
 D.R. Quarrie¹⁵, W.B. Quayle¹⁷³, F. Quinonez^{32a}, M. Raas¹⁰⁴, V. Radeka²⁵, V. Radescu⁴²,
 P. Radloff¹¹⁴, F. Ragusa^{89a,89b}, G. Rahal¹⁷⁸, A.M. Rahimi¹⁰⁹, D. Rahm²⁵, S. Rajagopalan²⁵,
 M. Rammensee⁴⁸, M. Rammes¹⁴¹, A.S. Randle-Conde⁴⁰, K. Randrianarivony²⁹, F. Rauscher⁹⁸,
 T.C. Rave⁴⁸, M. Raymond³⁰, A.L. Read¹¹⁷, D.M. Rebutti^{119a,119b}, A. Redelbach¹⁷⁴,
 G. Redlinger²⁵, R. Reece¹²⁰, K. Reeves⁴¹, A. Reinsch¹¹⁴, I. Reisinger⁴³, C. Rembser³⁰,
 Z.L. Ren¹⁵¹, A. Renaud¹¹⁵, M. Rescigno^{132a}, S. Resconi^{89a}, B. Resende¹³⁶, P. Reznicek⁹⁸,
 R. Rezvani¹⁵⁸, R. Richter⁹⁹, E. Richter-Was^{5,af}, M. Ridel⁷⁸, M. Rijpstra¹⁰⁵, M. Rijssenbeek¹⁴⁸,
 A. Rimoldi^{119a,119b}, L. Rinaldi^{20a}, R.R. Rios⁴⁰, I. Riu¹², G. Rivoltella^{89a,89b}, F. Rizatdinova¹¹²,
 E. Rizvi⁷⁵, S.H. Robertson^{85,k}, A. Robichaud-Veronneau¹¹⁸, D. Robinson²⁸, J.E.M. Robinson⁸²,
 A. Robson⁵³, J.G. Rocha de Lima¹⁰⁶, C. Roda^{122a,122b}, D. Roda Dos Santos³⁰, A. Roe⁵⁴,
 S. Roe³⁰, O. Røhne¹¹⁷, S. Rolli¹⁶¹, A. Romaniouk⁹⁶, M. Romano^{20a,20b}, G. Romeo²⁷,
 E. Romero Adam¹⁶⁷, N. Rompotis¹³⁸, L. Roos⁷⁸, E. Ros¹⁶⁷, S. Rosati^{132a}, K. Rosbach⁴⁹,
 A. Rose¹⁴⁹, M. Rose⁷⁶, G.A. Rosenbaum¹⁵⁸, E.I. Rosenberg⁶³, P.L. Rosendahl¹⁴, O. Rosenthal¹⁴¹,
 L. Rosselet⁴⁹, V. Rossetti¹², E. Rossi^{132a,132b}, L.P. Rossi^{50a}, M. Rotaru^{26a}, I. Roth¹⁷²,
 J. Rothberg¹³⁸, D. Rousseau¹¹⁵, C.R. Royon¹³⁶, A. Rozanov⁸³, Y. Rozen¹⁵², X. Ruan^{33a,ag},
 F. Rubbo¹², I. Rubinskiy⁴², N. Ruckstuhl¹⁰⁵, V.I. Rud⁹⁷, C. Rudolph⁴⁴, G. Rudolph⁶¹, F. Rühr⁷,
 A. Ruiz-Martinez⁶³, L. Rummyantsev⁶⁴, Z. Rurikova⁴⁸, N.A. Rusakovich⁶⁴, A. Ruschke⁹⁸,
 J.P. Rutherford⁷, P. Ruzicka¹²⁵, Y.F. Ryabov¹²¹, M. Rybar¹²⁶, G. Rybkin¹¹⁵, N.C. Ryder¹¹⁸,
 A.F. Saavedra¹⁵⁰, I. Sadeh¹⁵³, H.F-W. Sadrozinski¹³⁷, R. Sadykov⁶⁴, F. Safai Tehrani^{132a},
 H. Sakamoto¹⁵⁵, G. Salamanna⁷⁵, A. Salamon^{133a}, M. Saleem¹¹¹, D. Salek³⁰, D. Salihagic⁹⁹,
 A. Salnikov¹⁴³, J. Salt¹⁶⁷, B.M. Salvachua Ferrando⁶, D. Salvatore^{37a,37b}, F. Salvatore¹⁴⁹,

A. Salvucci¹⁰⁴, A. Salzburger³⁰, D. Sampsonidis¹⁵⁴, B.H. Samset¹¹⁷, A. Sanchez^{102a,102b},
 V. Sanchez Martinez¹⁶⁷, H. Sandaker¹⁴, H.G. Sander⁸¹, M.P. Sanders⁹⁸, M. Sandhoff¹⁷⁵,
 T. Sandoval²⁸, C. Sandoval¹⁶², R. Sandstroem⁹⁹, D.P.C. Sankey¹²⁹, A. Sansoni⁴⁷,
 C. Santamarina Rios⁸⁵, C. Santoni³⁴, R. Santonico^{133a,133b}, H. Santos^{124a}, I. Santoyo Castillo¹⁴⁹,
 J.G. Saraiva^{124a}, T. Sarangi¹⁷³, E. Sarkisyan-Grinbaum⁸, B. Sarrazin²¹, F. Sarri^{122a,122b},
 G. Sartisohn¹⁷⁵, O. Sasaki⁶⁵, Y. Sasaki¹⁵⁵, N. Sasao⁶⁷, I. Satsounkevitch⁹⁰, G. Sauvage^{5,*},
 E. Sauvan⁵, J.B. Sauvan¹¹⁵, P. Savard^{158,e}, V. Savinov¹²³, D.O. Savu³⁰, L. Sawyer^{25,m},
 D.H. Saxon⁵³, J. Saxon¹²⁰, C. Sbarra^{20a}, A. Sbrizzi^{20a,20b}, D.A. Scannicchio¹⁶³, M. Scarcella¹⁵⁰,
 J. Schaarschmidt¹¹⁵, P. Schacht⁹⁹, D. Schaefer¹²⁰, U. Schäfer⁸¹, A. Schaelicke⁴⁶, S. Schaepe²¹,
 S. Schaetzel^{58b}, A.C. Schaffer¹¹⁵, D. Schaile⁹⁸, R.D. Schamberger¹⁴⁸, A.G. Schamov¹⁰⁷,
 V. Scharf^{58a}, V.A. Schegelsky¹²¹, D. Scheirich⁸⁷, M. Schernau¹⁶³, M.I. Scherzer³⁵,
 C. Schiavi^{50a,50b}, J. Schieck⁹⁸, M. Schioppa^{37a,37b}, S. Schlenker³⁰, E. Schmidt⁴⁸, K. Schmieden²¹,
 C. Schmitt⁸¹, S. Schmitt^{58b}, B. Schneider¹⁷, U. Schnoor⁴⁴, L. Schoeffel¹³⁶, A. Schoening^{58b},
 A.L.S. Schorlemmer⁵⁴, M. Schott³⁰, D. Schouten^{159a}, J. Schovancova¹²⁵, M. Schram⁸⁵,
 C. Schroeder⁸¹, N. Schroer^{58c}, M.J. Schultens²¹, J. Schultes¹⁷⁵, H.-C. Schultz-Coulon^{58a},
 H. Schulz¹⁶, M. Schumacher⁴⁸, B.A. Schumm¹³⁷, Ph. Schune¹³⁶, C. Schwanenberger⁸²,
 A. Schwartzman¹⁴³, Ph. Schwegler⁹⁹, Ph. Schwemling⁷⁸, R. Schwienhorst⁸⁸, R. Schwierz⁴⁴,
 J. Schwindling¹³⁶, T. Schwindt²¹, M. Schwoerer⁵, F.G. Sciacca¹⁷, G. Sciolla²³, W.G. Scott¹²⁹,
 J. Searcy¹¹⁴, G. Sedov⁴², E. Sedykh¹²¹, S.C. Seidel¹⁰³, A. Seiden¹³⁷, F. Seifert⁴⁴, J.M. Seixas^{24a},
 G. Sekhniaidze^{102a}, S.J. Sekula⁴⁰, K.E. Selbach⁴⁶, D.M. Seliverstov¹²¹, B. Sellden^{146a},
 G. Sellers⁷³, M. Seman^{144b}, N. Semprini-Cesari^{20a,20b}, C. Serfon⁹⁸, L. Serin¹¹⁵, L. Serkin⁵⁴,
 R. Seuster^{159a}, H. Severini¹¹¹, A. Sfyrla³⁰, E. Shabalina⁵⁴, M. Shamim¹¹⁴, L.Y. Shan^{33a},
 J.T. Shank²², Q.T. Shao⁸⁶, M. Shapiro¹⁵, P.B. Shatalov⁹⁵, K. Shaw^{164a,164c}, D. Sherman¹⁷⁶,
 P. Sherwood⁷⁷, S. Shimizu¹⁰¹, M. Shimojima¹⁰⁰, T. Shin⁵⁶, M. Shiyakova⁶⁴, A. Shmeleva⁹⁴,
 M.J. Shochet³¹, D. Short¹¹⁸, S. Shrestha⁶³, E. Shulga⁹⁶, M.A. Shupe⁷, P. Sicho¹²⁵, A. Sidoti^{132a},
 F. Siegert⁴⁸, Dj. Sijacki^{13a}, O. Silbert¹⁷², J. Silva^{124a}, Y. Silver¹⁵³, D. Silverstein¹⁴³,
 S.B. Silverstein^{146a}, V. Simak¹²⁷, O. Simard¹³⁶, Lj. Simic^{13a}, S. Simion¹¹⁵, E. Simioni⁸¹,
 B. Simmons⁷⁷, R. Simoniello^{89a,89b}, M. Simonyan³⁶, P. Sinervo¹⁵⁸, N.B. Sinev¹¹⁴, V. Sipica¹⁴¹,
 G. Siragusa¹⁷⁴, A. Sircar²⁵, A.N. Sisakyan^{64,*}, S.Yu. Sivoklokov⁹⁷, J. Sjölin^{146a,146b},
 T.B. Sjurson¹⁴, L.A. Skinnari¹⁵, H.P. Skottowe⁵⁷, K. Skovpen¹⁰⁷, P. Skubic¹¹¹, M. Slater¹⁸,
 T. Slavicek¹²⁷, K. Sliwa¹⁶¹, V. Smakhtin¹⁷², B.H. Smart⁴⁶, L. Smestad¹¹⁷, S.Yu. Smirnov⁹⁶,
 Y. Smirnov⁹⁶, L.N. Smirnova⁹⁷, O. Smirnova⁷⁹, B.C. Smith⁵⁷, D. Smith¹⁴³, K.M. Smith⁵³,
 M. Smizanska⁷¹, K. Smolek¹²⁷, A.A. Snegarev⁹⁴, S.W. Snow⁸², J. Snow¹¹¹, S. Snyder²⁵,
 R. Sobie^{169,k}, J. Sodomka¹²⁷, A. Soffer¹⁵³, C.A. Solans¹⁶⁷, M. Solar¹²⁷, J. Solc¹²⁷,
 E.Yu. Soldatov⁹⁶, U. Soldevila¹⁶⁷, E. Solfaroli Camillocci^{132a,132b}, A.A. Solodkov¹²⁸,
 O.V. Solovyanov¹²⁸, V. Solovyev¹²¹, N. Soni¹, A. Sood¹⁵, V. Sopko¹²⁷, B. Sopko¹²⁷, M. Sosebee⁸,
 R. Soualah^{164a,164c}, A. Soukharev¹⁰⁷, S. Spagnolo^{72a,72b}, F. Spanò⁷⁶, R. Spighi^{20a}, G. Spigo³⁰,
 R. Spiwok³⁰, M. Spousta^{126,ah}, T. Spreitzer¹⁵⁸, B. Spurlock⁸, R.D. St. Denis⁵³, J. Stahlman¹²⁰,
 R. Stamen^{58a}, E. Stanecka³⁹, R.W. Stanek⁶, C. Stanescu^{134a}, M. Stanescu-Bellu⁴²,
 M.M. Stanitzki⁴², S. Stapnes¹¹⁷, E.A. Starchenko¹²⁸, J. Stark⁵⁵, P. Staroba¹²⁵, P. Starovoitov⁴²,
 R. Staszewski³⁹, A. Staude⁹⁸, P. Stavina^{144a,*}, G. Steele⁵³, P. Steinbach⁴⁴, P. Steinberg²⁵,
 I. Stekl¹²⁷, B. Stelzer¹⁴², H.J. Stelzer⁸⁸, O. Stelzer-Chilton^{159a}, H. Stenzel⁵², S. Stern⁹⁹,
 G.A. Stewart³⁰, J.A. Stillings²¹, M.C. Stockton⁸⁵, K. Stoerig⁴⁸, G. Stoicea^{26a}, S. Stonjek⁹⁹,
 P. Strachota¹²⁶, A.R. Stradling⁸, A. Straessner⁴⁴, J. Strandberg¹⁴⁷, S. Strandberg^{146a,146b},
 A. Strandlie¹¹⁷, M. Strang¹⁰⁹, E. Strauss¹⁴³, M. Strauss¹¹¹, P. Strizenc^{144b}, R. Ströhmer¹⁷⁴,
 D.M. Strom¹¹⁴, J.A. Strong^{76,*}, R. Stroynowski⁴⁰, B. Stugu¹⁴, I. Stumer^{25,*}, J. Stupak¹⁴⁸,
 P. Sturm¹⁷⁵, N.A. Styles⁴², D.A. Soh^{151,u}, D. Su¹⁴³, H.S. Subramania³, R. Subramaniam²⁵,
 A. Succurro¹², Y. Sugaya¹¹⁶, C. Suhr¹⁰⁶, M. Suk¹²⁶, V.V. Sulim⁹⁴, S. Sultansoy^{4d}, T. Sumida⁶⁷,

X. Sun⁵⁵, J.E. Sundermann⁴⁸, K. Suruliz¹³⁹, G. Susinno^{37a,37b}, M.R. Sutton¹⁴⁹, Y. Suzuki⁶⁵,
Y. Suzuki⁶⁶, M. Svatos¹²⁵, S. Swedish¹⁶⁸, I. Sykora^{144a}, T. Sykora¹²⁶, J. Sánchez¹⁶⁷, D. Ta¹⁰⁵,
K. Tackmann⁴², A. Taffard¹⁶³, R. Tafirout^{159a}, N. Taiblum¹⁵³, Y. Takahashi¹⁰¹, H. Takai²⁵,
R. Takashima⁶⁸, H. Takeda⁶⁶, T. Takeshita¹⁴⁰, Y. Takubo⁶⁵, M. Talby⁸³, A. Talyshv^{107.9},
M.C. Tamsett²⁵, K.G. Tan⁸⁶, J. Tanaka¹⁵⁵, R. Tanaka¹¹⁵, S. Tanaka¹³¹, S. Tanaka⁶⁵,
A.J. Tanasijczuk¹⁴², K. Tani⁶⁶, N. Tannoury⁸³, S. Tapprogge⁸¹, D. Tardif¹⁵⁸, S. Tarem¹⁵²,
F. Tarrade²⁹, G.F. Tartarelli^{89a}, P. Tas¹²⁶, M. Tasevsky¹²⁵, E. Tassi^{37a,37b}, Y. Tayalati^{135d},
C. Taylor⁷⁷, F.E. Taylor⁹², G.N. Taylor⁸⁶, W. Taylor^{159b}, M. Teinturier¹¹⁵, F.A. Teischinger³⁰,
M. Teixeira Dias Castanheira⁷⁵, P. Teixeira-Dias⁷⁶, K.K. Temming⁴⁸, H. Ten Kate³⁰,
P.K. Teng¹⁵¹, S. Terada⁶⁵, K. Terashi¹⁵⁵, J. Terron⁸⁰, M. Testa⁴⁷, R.J. Teuscher^{158,k},
J. Therhaag²¹, T. Theveneaux-Pelzer⁷⁸, S. Thoma⁴⁸, J.P. Thomas¹⁸, E.N. Thompson³⁵,
P.D. Thompson¹⁸, P.D. Thompson¹⁵⁸, A.S. Thompson⁵³, L.A. Thomsen³⁶, E. Thomson¹²⁰,
M. Thomson²⁸, W.M. Thong⁸⁶, R.P. Thun⁸⁷, F. Tian³⁵, M.J. Tibbetts¹⁵, T. Tic¹²⁵,
V.O. Tikhomirov⁹⁴, Y.A. Tikhonov^{107.9}, S. Timoshenko⁹⁶, E. Tiouchichine⁸³, P. Tipton¹⁷⁶,
S. Tisserant⁸³, T. Todorov⁵, S. Todorova-Nova¹⁶¹, B. Toggerson¹⁶³, J. Tojo⁶⁹, S. Tokár^{144a},
K. Tokushuku⁶⁵, K. Tollefson⁸⁸, M. Tomoto¹⁰¹, L. Tompkins³¹, K. Toms¹⁰³, A. Tonoyan¹⁴,
C. Topfel¹⁷, N.D. Topilin⁶⁴, E. Torrence¹¹⁴, H. Torres⁷⁸, E. Torró Pastor¹⁶⁷, J. Toth^{83,ac},
F. Touchard⁸³, D.R. Tovey¹³⁹, T. Trefzger¹⁷⁴, L. Tremblet³⁰, A. Tricoli³⁰, I.M. Trigger^{159a},
S. Trincaz-Duvoid⁷⁸, M.F. Tripiana⁷⁰, N. Triplett²⁵, W. Trischuk¹⁵⁸, B. Trocmé⁵⁵, C. Troncon^{89a},
M. Trottier-McDonald¹⁴², P. True⁸⁸, M. Trzebinski³⁹, A. Trzupek³⁹, C. Tsarouchas³⁰,
J.C-L. Tseng¹¹⁸, M. Tsiakiris¹⁰⁵, P.V. Tsiareshka⁹⁰, D. Tsionou^{5,ai}, G. Tsipolitis¹⁰,
S. Tsiskaridze¹², V. Tsiskaridze⁴⁸, E.G. Tskhadadze^{51a}, I.I. Tsukerman⁹⁵, V. Tsulaia¹⁵,
J.-W. Tsung²¹, S. Tsuno⁶⁵, D. Tsybychev¹⁴⁸, A. Tua¹³⁹, A. Tudorache^{26a}, V. Tudorache^{26a},
J.M. Tuggle³¹, M. Turala³⁹, D. Turecek¹²⁷, I. Turk Cakir^{4e}, E. Turlay¹⁰⁵, R. Turra^{89a,89b},
P.M. Tuts³⁵, A. Tykhonov⁷⁴, M. Tylmad^{146a,146b}, M. Tyndel¹²⁹, G. Tzanakos⁹, K. Uchida²¹,
I. Ueda¹⁵⁵, R. Ueno²⁹, M. Ugland¹⁴, M. Uhlenbrock²¹, M. Uhrmacher⁵⁴, F. Ukegawa¹⁶⁰,
G. Unal³⁰, A. Undrus²⁵, G. Unel¹⁶³, Y. Unno⁶⁵, D. Urbaniec³⁵, P. Urquijo²¹, G. Usai⁸,
M. Uslenghi^{119a,119b}, L. Vacavant⁸³, V. Vacek¹²⁷, B. Vachon⁸⁵, S. Vahsen¹⁵, J. Valenta¹²⁵,
S. Valentineti^{20a,20b}, A. Valero¹⁶⁷, S. Valkar¹²⁶, E. Valladolid Gallego¹⁶⁷, S. Vallecorsa¹⁵²,
J.A. Valls Ferrer¹⁶⁷, R. Van Berg¹²⁰, P.C. Van Der Deijl¹⁰⁵, R. van der Geer¹⁰⁵,
H. van der Graaf¹⁰⁵, R. Van Der Leeuw¹⁰⁵, E. van der Poel¹⁰⁵, D. van der Ster³⁰, N. van Eldik³⁰,
P. van Gemmeren⁶, I. van Vulpen¹⁰⁵, M. Vanadia⁹⁹, W. Vandelli³⁰, A. Vaniachine⁶, P. Vankov⁴²,
F. Vannucci⁷⁸, R. Vari^{132a}, E.W. Varnes⁷, T. Varol⁸⁴, D. Varouchas¹⁵, A. Vartapetian⁸,
K.E. Varvell¹⁵⁰, V.I. Vassilakopoulos⁵⁶, F. Vazeille³⁴, T. Vazquez Schroeder⁵⁴, G. Vegni^{89a,89b},
J.J. Veillet¹¹⁵, F. Veloso^{124a}, R. Veness³⁰, S. Veneziano^{132a}, A. Ventura^{72a,72b}, D. Ventura⁸⁴,
M. Venturi⁴⁸, N. Venturi¹⁵⁸, V. Vercesi^{119a}, M. Verducci¹³⁸, W. Verkerke¹⁰⁵, J.C. Vermeulen¹⁰⁵,
A. Vest⁴⁴, M.C. Vetterli^{142,e}, I. Vichou¹⁶⁵, T. Vickey^{145b,aj}, O.E. Vickey Boeriu^{145b},
G.H.A. Viehhauser¹¹⁸, S. Viel¹⁶⁸, M. Villa^{20a,20b}, M. Villaplana Perez¹⁶⁷, E. Vilucchi⁴⁷,
M.G. Vincter²⁹, E. Vinek³⁰, V.B. Vinogradov⁶⁴, M. Virchaux^{136,*}, J. Virzi¹⁵, O. Vitells¹⁷²,
M. Viti⁴², I. Vivarelli⁴⁸, F. Vives Vaque³, S. Vlachos¹⁰, D. Vladoiu⁹⁸, M. Vlasak¹²⁷, A. Vogel²¹,
P. Vokac¹²⁷, G. Volpi⁴⁷, M. Volpi⁸⁶, G. Volpini^{89a}, H. von der Schmitt⁹⁹, H. von Radziewski⁴⁸,
E. von Toerne²¹, V. Vorobel¹²⁶, V. Vorwerk¹², M. Vos¹⁶⁷, R. Voss³⁰, J.H. Vossebeld⁷³,
N. Vranjes¹³⁶, M. Vranjes Milosavljevic¹⁰⁵, V. Vrba¹²⁵, M. Vreeswijk¹⁰⁵, T. Vu Anh⁴⁸,
R. Vuillermet³⁰, I. Vukotic³¹, W. Wagner¹⁷⁵, P. Wagner¹²⁰, H. Wahlen¹⁷⁵, S. Wahrmund⁴⁴,
J. Wakabayashi¹⁰¹, S. Walch⁸⁷, J. Walder⁷¹, R. Walker⁹⁸, W. Walkowiak¹⁴¹, R. Wall¹⁷⁶,
P. Waller⁷³, B. Walsh¹⁷⁶, C. Wang⁴⁵, H. Wang¹⁷³, H. Wang⁴⁰, J. Wang¹⁵¹, J. Wang^{33a},
R. Wang¹⁰³, S.M. Wang¹⁵¹, T. Wang²¹, A. Warburton⁸⁵, C.P. Ward²⁸, D.R. Wardrope⁷⁷,
M. Warsinsky⁴⁸, A. Washbrook⁴⁶, C. Wasicki⁴², I. Watanabe⁶⁶, P.M. Watkins¹⁸, A.T. Watson¹⁸,

I.J. Watson¹⁵⁰, M.F. Watson¹⁸, G. Watts¹³⁸, S. Watts⁸², A.T. Waugh¹⁵⁰, B.M. Waugh⁷⁷, M.S. Weber¹⁷, J.S. Webster³¹, A.R. Weidberg¹¹⁸, P. Weigell⁹⁹, J. Weingarten⁵⁴, C. Weiser⁴⁸, P.S. Wells³⁰, T. Wenaus²⁵, D. Wendland¹⁶, Z. Weng^{151,u}, T. Wengler³⁰, S. Wenig³⁰, N. Vermes²¹, M. Werner⁴⁸, P. Werner³⁰, M. Werth¹⁶³, M. Wessels^{58a}, J. Wetter¹⁶¹, C. Weydert⁵⁵, K. Whalen²⁹, A. White⁸, M.J. White⁸⁶, S. White^{122a,122b}, S.R. Whitehead¹¹⁸, D. Whiteson¹⁶³, D. Whittington⁶⁰, F. Wicek¹¹⁵, D. Wicke¹⁷⁵, F.J. Wickens¹²⁹, W. Wiedenmann¹⁷³, M. Wielers¹²⁹, P. Wienemann²¹, C. Wiglesworth⁷⁵, L.A.M. Wiik-Fuchs²¹, P.A. Wijeratne⁷⁷, A. Wildauer⁹⁹, M.A. Wildt^{42,r}, I. Wilhelm¹²⁶, H.G. Wilkens³⁰, J.Z. Will⁹⁸, E. Williams³⁵, H.H. Williams¹²⁰, W. Willis³⁵, S. Willocq⁸⁴, J.A. Wilson¹⁸, M.G. Wilson¹⁴³, A. Wilson⁸⁷, I. Wingerter-Seez⁵, S. Winkelmann⁴⁸, F. Winklmeier³⁰, M. Wittgen¹⁴³, S.J. Wollstadt⁸¹, M.W. Wolter³⁹, H. Wolters^{124a,h}, W.C. Wong⁴¹, G. Wooden⁸⁷, B.K. Wosiek³⁹, J. Wotschack³⁰, M.J. Woudstra⁸², K.W. Wozniak³⁹, K. Wraight⁵³, M. Wright⁵³, B. Wrona⁷³, S.L. Wu¹⁷³, X. Wu⁴⁹, Y. Wu^{33b,ak}, E. Wulf³⁵, B.M. Wynne⁴⁶, S. Xella³⁶, M. Xiao¹³⁶, S. Xie⁴⁸, C. Xu^{33b,y}, D. Xu¹³⁹, L. Xu^{33b}, B. Yabsley¹⁵⁰, S. Yacoob^{145a,al}, M. Yamada⁶⁵, H. Yamaguchi¹⁵⁵, A. Yamamoto⁶⁵, K. Yamamoto⁶³, S. Yamamoto¹⁵⁵, T. Yamamura¹⁵⁵, T. Yamanaka¹⁵⁵, T. Yamazaki¹⁵⁵, Y. Yamazaki⁶⁶, Z. Yan²², H. Yang⁸⁷, U.K. Yang⁸², Y. Yang¹⁰⁹, Z. Yang^{146a,146b}, S. Yanush⁹¹, L. Yao^{33a}, Y. Yao¹⁵, Y. Yasu⁶⁵, G.V. Ybeles Smit¹³⁰, J. Ye⁴⁰, S. Ye²⁵, M. Yilmaz^{4c}, R. Yoosoofmiya¹²³, K. Yorita¹⁷¹, R. Yoshida⁶, K. Yoshihara¹⁵⁵, C. Young¹⁴³, C.J. Young¹¹⁸, S. Youssef²², D. Yu²⁵, D.R. Yu¹⁵, J. Yu⁸, J. Yu¹¹², L. Yuan⁶⁶, A. Yurkewicz¹⁰⁶, B. Zabinski³⁹, R. Zaidan⁶², A.M. Zaitsev¹²⁸, Z. Zajacova³⁰, L. Zanello^{132a,132b}, D. Zanzi⁹⁹, A. Zaytsev²⁵, C. Zeitnitz¹⁷⁵, M. Zeman¹²⁵, A. Zemla³⁹, C. Zender²¹, O. Zenin¹²⁸, T. Ženis^{144a}, Z. Zinonos^{122a,122b}, D. Zerwas¹¹⁵, G. Zevi della Porta⁵⁷, D. Zhang^{33b,am}, H. Zhang⁸⁸, J. Zhang⁶, X. Zhang^{33d}, Z. Zhang¹¹⁵, L. Zhao¹⁰⁸, Z. Zhao^{33b}, A. Zhemchugov⁶⁴, J. Zhong¹¹⁸, B. Zhou⁸⁷, N. Zhou¹⁶³, Y. Zhou¹⁵¹, C.G. Zhu^{33d}, H. Zhu⁴², J. Zhu⁸⁷, Y. Zhu^{33b}, X. Zhuang⁹⁸, V. Zhuravlov⁹⁹, A. Zibell⁹⁸, D. Zieminska⁶⁰, N.I. Zimin⁶⁴, R. Zimmermann²¹, S. Zimmermann²¹, S. Zimmermann⁴⁸, M. Ziolkowski¹⁴¹, R. Zitoun⁵, L. Živković³⁵, V.V. Zmouchko^{128,*}, G. Zobernig¹⁷³, A. Zoccoli^{20a,20b}, M. zur Nedden¹⁶, V. Zutshi¹⁰⁶, L. Zwalinski³⁰.

¹ School of Chemistry and Physics, University of Adelaide, Adelaide, Australia

² Physics Department, SUNY Albany, Albany NY, United States of America

³ Department of Physics, University of Alberta, Edmonton AB, Canada

⁴ (a) Department of Physics, Ankara University, Ankara; (b) Department of Physics, Dumlupinar University, Kutahya; (c) Department of Physics, Gazi University, Ankara; (d) Division of Physics, TOBB University of Economics and Technology, Ankara; (e) Turkish Atomic Energy Authority, Ankara, Turkey

⁵ LAPP, CNRS/IN2P3 and Université de Savoie, Annecy-le-Vieux, France

⁶ High Energy Physics Division, Argonne National Laboratory, Argonne IL, United States of America

⁷ Department of Physics, University of Arizona, Tucson AZ, United States of America

⁸ Department of Physics, The University of Texas at Arlington, Arlington TX, United States of America

⁹ Physics Department, University of Athens, Athens, Greece

¹⁰ Physics Department, National Technical University of Athens, Zografou, Greece

¹¹ Institute of Physics, Azerbaijan Academy of Sciences, Baku, Azerbaijan

¹² Institut de Física d'Altes Energies and Departament de Física de la Universitat Autònoma de Barcelona and ICREA, Barcelona, Spain

¹³ (a) Institute of Physics, University of Belgrade, Belgrade; (b) Vinca Institute of Nuclear Sciences, University of Belgrade, Belgrade, Serbia

¹⁴ Department for Physics and Technology, University of Bergen, Bergen, Norway

¹⁵ Physics Division, Lawrence Berkeley National Laboratory and University of California, Berkeley CA, United States of America

- ¹⁶ *Department of Physics, Humboldt University, Berlin, Germany*
- ¹⁷ *Albert Einstein Center for Fundamental Physics and Laboratory for High Energy Physics, University of Bern, Bern, Switzerland*
- ¹⁸ *School of Physics and Astronomy, University of Birmingham, Birmingham, United Kingdom*
- ¹⁹ ^(a) *Department of Physics, Bogazici University, Istanbul;* ^(b) *Division of Physics, Dogus University, Istanbul;* ^(c) *Department of Physics Engineering, Gaziantep University, Gaziantep;* ^(d) *Department of Physics, Istanbul Technical University, Istanbul, Turkey*
- ²⁰ ^(a) *INFN Sezione di Bologna;* ^(b) *Dipartimento di Fisica, Università di Bologna, Bologna, Italy*
- ²¹ *Physikalisches Institut, University of Bonn, Bonn, Germany*
- ²² *Department of Physics, Boston University, Boston MA, United States of America*
- ²³ *Department of Physics, Brandeis University, Waltham MA, United States of America*
- ²⁴ ^(a) *Universidade Federal do Rio De Janeiro COPPE/EE/IF, Rio de Janeiro;* ^(b) *Federal University of Juiz de Fora (UFJF), Juiz de Fora;* ^(c) *Federal University of Sao Joao del Rei (UFSJ), Sao Joao del Rei;* ^(d) *Instituto de Fisica, Universidade de Sao Paulo, Sao Paulo, Brazil*
- ²⁵ *Physics Department, Brookhaven National Laboratory, Upton NY, United States of America*
- ²⁶ ^(a) *National Institute of Physics and Nuclear Engineering, Bucharest;* ^(b) *University Politehnica Bucharest, Bucharest;* ^(c) *West University in Timisoara, Timisoara, Romania*
- ²⁷ *Departamento de Física, Universidad de Buenos Aires, Buenos Aires, Argentina*
- ²⁸ *Cavendish Laboratory, University of Cambridge, Cambridge, United Kingdom*
- ²⁹ *Department of Physics, Carleton University, Ottawa ON, Canada*
- ³⁰ *CERN, Geneva, Switzerland*
- ³¹ *Enrico Fermi Institute, University of Chicago, Chicago IL, United States of America*
- ³² ^(a) *Departamento de Física, Pontificia Universidad Católica de Chile, Santiago;* ^(b) *Departamento de Física, Universidad Técnica Federico Santa María, Valparaíso, Chile*
- ³³ ^(a) *Institute of High Energy Physics, Chinese Academy of Sciences, Beijing;* ^(b) *Department of Modern Physics, University of Science and Technology of China, Anhui;* ^(c) *Department of Physics, Nanjing University, Jiangsu;* ^(d) *School of Physics, Shandong University, Shandong;* ^(e) *Physics Department, Shanghai Jiao Tong University, Shanghai, China*
- ³⁴ *Laboratoire de Physique Corpusculaire, Clermont Université and Université Blaise Pascal and CNRS/IN2P3, Clermont-Ferrand, France*
- ³⁵ *Nevis Laboratory, Columbia University, Irvington NY, United States of America*
- ³⁶ *Niels Bohr Institute, University of Copenhagen, Kobenhavn, Denmark*
- ³⁷ ^(a) *INFN Gruppo Collegato di Cosenza;* ^(b) *Dipartimento di Fisica, Università della Calabria, Arcavata di Rende, Italy*
- ³⁸ *AGH University of Science and Technology, Faculty of Physics and Applied Computer Science, Krakow, Poland*
- ³⁹ *The Henryk Niewodniczanski Institute of Nuclear Physics, Polish Academy of Sciences, Krakow, Poland*
- ⁴⁰ *Physics Department, Southern Methodist University, Dallas TX, United States of America*
- ⁴¹ *Physics Department, University of Texas at Dallas, Richardson TX, United States of America*
- ⁴² *DESY, Hamburg and Zeuthen, Germany*
- ⁴³ *Institut für Experimentelle Physik IV, Technische Universität Dortmund, Dortmund, Germany*
- ⁴⁴ *Institut für Kern- und Teilchenphysik, Technical University Dresden, Dresden, Germany*
- ⁴⁵ *Department of Physics, Duke University, Durham NC, United States of America*
- ⁴⁶ *SUPA - School of Physics and Astronomy, University of Edinburgh, Edinburgh, United Kingdom*
- ⁴⁷ *INFN Laboratori Nazionali di Frascati, Frascati, Italy*
- ⁴⁸ *Fakultät für Mathematik und Physik, Albert-Ludwigs-Universität, Freiburg, Germany*
- ⁴⁹ *Section de Physique, Université de Genève, Geneva, Switzerland*
- ⁵⁰ ^(a) *INFN Sezione di Genova;* ^(b) *Dipartimento di Fisica, Università di Genova, Genova, Italy*
- ⁵¹ ^(a) *E. Andronikashvili Institute of Physics, Iv. Javakishvili Tbilisi State University, Tbilisi;* ^(b) *High Energy Physics Institute, Tbilisi State University, Tbilisi, Georgia*
- ⁵² *II Physikalisches Institut, Justus-Liebig-Universität Giessen, Giessen, Germany*

- 53 *SUPA - School of Physics and Astronomy, University of Glasgow, Glasgow, United Kingdom*
- 54 *II Physikalisches Institut, Georg-August-Universität, Göttingen, Germany*
- 55 *Laboratoire de Physique Subatomique et de Cosmologie, Université Joseph Fourier and CNRS/IN2P3 and Institut National Polytechnique de Grenoble, Grenoble, France*
- 56 *Department of Physics, Hampton University, Hampton VA, United States of America*
- 57 *Laboratory for Particle Physics and Cosmology, Harvard University, Cambridge MA, United States of America*
- 58 ^(a) *Kirchhoff-Institut für Physik, Ruprecht-Karls-Universität Heidelberg, Heidelberg;* ^(b) *Physikalisches Institut, Ruprecht-Karls-Universität Heidelberg, Heidelberg;* ^(c) *ZITI Institut für technische Informatik, Ruprecht-Karls-Universität Heidelberg, Mannheim, Germany*
- 59 *Faculty of Applied Information Science, Hiroshima Institute of Technology, Hiroshima, Japan*
- 60 *Department of Physics, Indiana University, Bloomington IN, United States of America*
- 61 *Institut für Astro- und Teilchenphysik, Leopold-Franzens-Universität, Innsbruck, Austria*
- 62 *University of Iowa, Iowa City IA, United States of America*
- 63 *Department of Physics and Astronomy, Iowa State University, Ames IA, United States of America*
- 64 *Joint Institute for Nuclear Research, JINR Dubna, Dubna, Russia*
- 65 *KEK, High Energy Accelerator Research Organization, Tsukuba, Japan*
- 66 *Graduate School of Science, Kobe University, Kobe, Japan*
- 67 *Faculty of Science, Kyoto University, Kyoto, Japan*
- 68 *Kyoto University of Education, Kyoto, Japan*
- 69 *Department of Physics, Kyushu University, Fukuoka, Japan*
- 70 *Instituto de Física La Plata, Universidad Nacional de La Plata and CONICET, La Plata, Argentina*
- 71 *Physics Department, Lancaster University, Lancaster, United Kingdom*
- 72 ^(a) *INFN Sezione di Lecce;* ^(b) *Dipartimento di Matematica e Fisica, Università del Salento, Lecce, Italy*
- 73 *Oliver Lodge Laboratory, University of Liverpool, Liverpool, United Kingdom*
- 74 *Department of Physics, Jožef Stefan Institute and University of Ljubljana, Ljubljana, Slovenia*
- 75 *School of Physics and Astronomy, Queen Mary University of London, London, United Kingdom*
- 76 *Department of Physics, Royal Holloway University of London, Surrey, United Kingdom*
- 77 *Department of Physics and Astronomy, University College London, London, United Kingdom*
- 78 *Laboratoire de Physique Nucléaire et de Hautes Energies, UPMC and Université Paris-Diderot and CNRS/IN2P3, Paris, France*
- 79 *Fysiska institutionen, Lunds universitet, Lund, Sweden*
- 80 *Departamento de Física Teórica C-15, Universidad Autónoma de Madrid, Madrid, Spain*
- 81 *Institut für Physik, Universität Mainz, Mainz, Germany*
- 82 *School of Physics and Astronomy, University of Manchester, Manchester, United Kingdom*
- 83 *CPPM, Aix-Marseille Université and CNRS/IN2P3, Marseille, France*
- 84 *Department of Physics, University of Massachusetts, Amherst MA, United States of America*
- 85 *Department of Physics, McGill University, Montreal QC, Canada*
- 86 *School of Physics, University of Melbourne, Victoria, Australia*
- 87 *Department of Physics, The University of Michigan, Ann Arbor MI, United States of America*
- 88 *Department of Physics and Astronomy, Michigan State University, East Lansing MI, United States of America*
- 89 ^(a) *INFN Sezione di Milano;* ^(b) *Dipartimento di Fisica, Università di Milano, Milano, Italy*
- 90 *B.I. Stepanov Institute of Physics, National Academy of Sciences of Belarus, Minsk, Republic of Belarus*
- 91 *National Scientific and Educational Centre for Particle and High Energy Physics, Minsk, Republic of Belarus*
- 92 *Department of Physics, Massachusetts Institute of Technology, Cambridge MA, United States of America*
- 93 *Group of Particle Physics, University of Montreal, Montreal QC, Canada*
- 94 *P.N. Lebedev Institute of Physics, Academy of Sciences, Moscow, Russia*

- 95 *Institute for Theoretical and Experimental Physics (ITEP), Moscow, Russia*
 96 *Moscow Engineering and Physics Institute (MEPhI), Moscow, Russia*
 97 *Skobeltsyn Institute of Nuclear Physics, Lomonosov Moscow State University, Moscow, Russia*
 98 *Fakultät für Physik, Ludwig-Maximilians-Universität München, München, Germany*
 99 *Max-Planck-Institut für Physik (Werner-Heisenberg-Institut), München, Germany*
 100 *Nagasaki Institute of Applied Science, Nagasaki, Japan*
 101 *Graduate School of Science and Kobayashi-Maskawa Institute, Nagoya University, Nagoya, Japan*
 102 ^(a) *INFN Sezione di Napoli;* ^(b) *Dipartimento di Scienze Fisiche, Università di Napoli, Napoli, Italy*
 103 *Department of Physics and Astronomy, University of New Mexico, Albuquerque NM, United States of America*
 104 *Institute for Mathematics, Astrophysics and Particle Physics, Radboud University Nijmegen/Nikhef, Nijmegen, Netherlands*
 105 *Nikhef National Institute for Subatomic Physics and University of Amsterdam, Amsterdam, Netherlands*
 106 *Department of Physics, Northern Illinois University, DeKalb IL, United States of America*
 107 *Budker Institute of Nuclear Physics, SB RAS, Novosibirsk, Russia*
 108 *Department of Physics, New York University, New York NY, United States of America*
 109 *Ohio State University, Columbus OH, United States of America*
 110 *Faculty of Science, Okayama University, Okayama, Japan*
 111 *Homer L. Dodge Department of Physics and Astronomy, University of Oklahoma, Norman OK, United States of America*
 112 *Department of Physics, Oklahoma State University, Stillwater OK, United States of America*
 113 *Palacký University, RCPTM, Olomouc, Czech Republic*
 114 *Center for High Energy Physics, University of Oregon, Eugene OR, United States of America*
 115 *LAL, Université Paris-Sud and CNRS/IN2P3, Orsay, France*
 116 *Graduate School of Science, Osaka University, Osaka, Japan*
 117 *Department of Physics, University of Oslo, Oslo, Norway*
 118 *Department of Physics, Oxford University, Oxford, United Kingdom*
 119 ^(a) *INFN Sezione di Pavia;* ^(b) *Dipartimento di Fisica, Università di Pavia, Pavia, Italy*
 120 *Department of Physics, University of Pennsylvania, Philadelphia PA, United States of America*
 121 *Petersburg Nuclear Physics Institute, Gatchina, Russia*
 122 ^(a) *INFN Sezione di Pisa;* ^(b) *Dipartimento di Fisica E. Fermi, Università di Pisa, Pisa, Italy*
 123 *Department of Physics and Astronomy, University of Pittsburgh, Pittsburgh PA, United States of America*
 124 ^(a) *Laboratorio de Instrumentacao e Fisica Experimental de Particulas - LIP, Lisboa, Portugal;*
^(b) *Departamento de Fisica Teorica y del Cosmos and CAFPE, Universidad de Granada, Granada, Spain*
 125 *Institute of Physics, Academy of Sciences of the Czech Republic, Praha, Czech Republic*
 126 *Faculty of Mathematics and Physics, Charles University in Prague, Praha, Czech Republic*
 127 *Czech Technical University in Prague, Praha, Czech Republic*
 128 *State Research Center Institute for High Energy Physics, Protvino, Russia*
 129 *Particle Physics Department, Rutherford Appleton Laboratory, Didcot, United Kingdom*
 130 *Physics Department, University of Regina, Regina SK, Canada*
 131 *Ritsumeikan University, Kusatsu, Shiga, Japan*
 132 ^(a) *INFN Sezione di Roma I;* ^(b) *Dipartimento di Fisica, Università La Sapienza, Roma, Italy*
 133 ^(a) *INFN Sezione di Roma Tor Vergata;* ^(b) *Dipartimento di Fisica, Università di Roma Tor Vergata, Roma, Italy*
 134 ^(a) *INFN Sezione di Roma Tre;* ^(b) *Dipartimento di Fisica, Università Roma Tre, Roma, Italy*
 135 ^(a) *Faculté des Sciences Ain Chock, Réseau Universitaire de Physique des Hautes Energies - Université Hassan II, Casablanca;* ^(b) *Centre National de l'Energie des Sciences Techniques Nucleaires, Rabat;* ^(c) *Faculté des Sciences Semlalia, Université Cadi Ayyad, LPHEA-Marrakech;*
^(d) *Faculté des Sciences, Université Mohamed Premier and LPTPM, Oujda;* ^(e) *Faculté des*

- sciences, Université Mohammed V-Agdal, Rabat, Morocco
- 136 DSM/IRFU (Institut de Recherches sur les Lois Fondamentales de l'Univers), CEA Saclay
(Commissariat à l'Energie Atomique), Gif-sur-Yvette, France
- 137 Santa Cruz Institute for Particle Physics, University of California Santa Cruz, Santa Cruz CA,
United States of America
- 138 Department of Physics, University of Washington, Seattle WA, United States of America
- 139 Department of Physics and Astronomy, University of Sheffield, Sheffield, United Kingdom
- 140 Department of Physics, Shinshu University, Nagano, Japan
- 141 Fachbereich Physik, Universität Siegen, Siegen, Germany
- 142 Department of Physics, Simon Fraser University, Burnaby BC, Canada
- 143 SLAC National Accelerator Laboratory, Stanford CA, United States of America
- 144 ^(a) Faculty of Mathematics, Physics & Informatics, Comenius University, Bratislava; ^(b)
Department of Subnuclear Physics, Institute of Experimental Physics of the Slovak Academy of
Sciences, Kosice, Slovak Republic
- 145 ^(a) Department of Physics, University of Johannesburg, Johannesburg; ^(b) School of Physics,
University of the Witwatersrand, Johannesburg, South Africa
- 146 ^(a) Department of Physics, Stockholm University; ^(b) The Oskar Klein Centre, Stockholm, Sweden
- 147 Physics Department, Royal Institute of Technology, Stockholm, Sweden
- 148 Departments of Physics & Astronomy and Chemistry, Stony Brook University, Stony Brook NY,
United States of America
- 149 Department of Physics and Astronomy, University of Sussex, Brighton, United Kingdom
- 150 School of Physics, University of Sydney, Sydney, Australia
- 151 Institute of Physics, Academia Sinica, Taipei, Taiwan
- 152 Department of Physics, Technion: Israel Institute of Technology, Haifa, Israel
- 153 Raymond and Beverly Sackler School of Physics and Astronomy, Tel Aviv University, Tel Aviv,
Israel
- 154 Department of Physics, Aristotle University of Thessaloniki, Thessaloniki, Greece
- 155 International Center for Elementary Particle Physics and Department of Physics, The University
of Tokyo, Tokyo, Japan
- 156 Graduate School of Science and Technology, Tokyo Metropolitan University, Tokyo, Japan
- 157 Department of Physics, Tokyo Institute of Technology, Tokyo, Japan
- 158 Department of Physics, University of Toronto, Toronto ON, Canada
- 159 ^(a) TRIUMF, Vancouver BC; ^(b) Department of Physics and Astronomy, York University, Toronto
ON, Canada
- 160 Faculty of Pure and Applied Sciences, University of Tsukuba, Tsukuba, Japan
- 161 Department of Physics and Astronomy, Tufts University, Medford MA, United States of America
- 162 Centro de Investigaciones, Universidad Antonio Narino, Bogota, Colombia
- 163 Department of Physics and Astronomy, University of California Irvine, Irvine CA, United States of
America
- 164 ^(a) INFN Gruppo Collegato di Udine; ^(b) ICTP, Trieste; ^(c) Dipartimento di Chimica, Fisica e
Ambiente, Università di Udine, Udine, Italy
- 165 Department of Physics, University of Illinois, Urbana IL, United States of America
- 166 Department of Physics and Astronomy, University of Uppsala, Uppsala, Sweden
- 167 Instituto de Física Corpuscular (IFIC) and Departamento de Física Atómica, Molecular y Nuclear
and Departamento de Ingeniería Electrónica and Instituto de Microelectrónica de Barcelona
(IMB-CNM), University of Valencia and CSIC, Valencia, Spain
- 168 Department of Physics, University of British Columbia, Vancouver BC, Canada
- 169 Department of Physics and Astronomy, University of Victoria, Victoria BC, Canada
- 170 Department of Physics, University of Warwick, Coventry, United Kingdom
- 171 Waseda University, Tokyo, Japan
- 172 Department of Particle Physics, The Weizmann Institute of Science, Rehovot, Israel
- 173 Department of Physics, University of Wisconsin, Madison WI, United States of America

- 174 *Fakultät für Physik und Astronomie, Julius-Maximilians-Universität, Würzburg, Germany*
- 175 *Fachbereich C Physik, Bergische Universität Wuppertal, Wuppertal, Germany*
- 176 *Department of Physics, Yale University, New Haven CT, United States of America*
- 177 *Yerevan Physics Institute, Yerevan, Armenia*
- 178 *Centre de Calcul de l'Institut National de Physique Nucléaire et de Physique des Particules (IN2P3), Villeurbanne, France*
- ^a *Also at Laboratorio de Instrumentacao e Fisica Experimental de Particulas - LIP, Lisboa, Portugal*
- ^b *Also at Faculdade de Ciencias and CFNUL, Universidade de Lisboa, Lisboa, Portugal*
- ^c *Also at Particle Physics Department, Rutherford Appleton Laboratory, Didcot, United Kingdom*
- ^d *Also at Department of Physics, University of Johannesburg, Johannesburg, South Africa*
- ^e *Also at TRIUMF, Vancouver BC, Canada*
- ^f *Also at Department of Physics, California State University, Fresno CA, United States of America*
- ^g *Also at Novosibirsk State University, Novosibirsk, Russia*
- ^h *Also at Department of Physics, University of Coimbra, Coimbra, Portugal*
- ⁱ *Also at Department of Physics, UASLP, San Luis Potosi, Mexico*
- ^j *Also at Università di Napoli Parthenope, Napoli, Italy*
- ^k *Also at Institute of Particle Physics (IPP), Canada*
- ^l *Also at Department of Physics, Middle East Technical University, Ankara, Turkey*
- ^m *Also at Louisiana Tech University, Ruston LA, United States of America*
- ⁿ *Also at Dep Fisica and CEFITEC of Faculdade de Ciencias e Tecnologia, Universidade Nova de Lisboa, Caparica, Portugal*
- ^o *Also at Department of Physics and Astronomy, University College London, London, United Kingdom*
- ^p *Also at Department of Physics, University of Cape Town, Cape Town, South Africa*
- ^q *Also at Institute of Physics, Azerbaijan Academy of Sciences, Baku, Azerbaijan*
- ^r *Also at Institut für Experimentalphysik, Universität Hamburg, Hamburg, Germany*
- ^s *Also at Manhattan College, New York NY, United States of America*
- ^t *Also at CPPM, Aix-Marseille Université and CNRS/IN2P3, Marseille, France*
- ^u *Also at School of Physics and Engineering, Sun Yat-sen University, Guanzhou, China*
- ^v *Also at Academia Sinica Grid Computing, Institute of Physics, Academia Sinica, Taipei, Taiwan*
- ^w *Also at School of Physics, Shandong University, Shandong, China*
- ^x *Also at Dipartimento di Fisica, Università La Sapienza, Roma, Italy*
- ^y *Also at DSM/IRFU (Institut de Recherches sur les Lois Fondamentales de l'Univers), CEA Saclay (Commissariat a l'Energie Atomique), Gif-sur-Yvette, France*
- ^z *Also at Section de Physique, Université de Genève, Geneva, Switzerland*
- ^{aa} *Also at Departamento de Fisica, Universidade de Minho, Braga, Portugal*
- ^{ab} *Also at Department of Physics and Astronomy, University of South Carolina, Columbia SC, United States of America*
- ^{ac} *Also at Institute for Particle and Nuclear Physics, Wigner Research Centre for Physics, Budapest, Hungary*
- ^{ad} *Also at CERN, Geneva, Switzerland*
- ^{ae} *Also at California Institute of Technology, Pasadena CA, United States of America*
- ^{af} *Also at Institute of Physics, Jagiellonian University, Krakow, Poland*
- ^{ag} *Also at LAL, Université Paris-Sud and CNRS/IN2P3, Orsay, France*
- ^{ah} *Also at Nevis Laboratory, Columbia University, Irvington NY, United States of America*
- ^{ai} *Also at Department of Physics and Astronomy, University of Sheffield, Sheffield, United Kingdom*
- ^{aj} *Also at Department of Physics, Oxford University, Oxford, United Kingdom*
- ^{ak} *Also at Department of Physics, The University of Michigan, Ann Arbor MI, United States of America*
- ^{al} *Also at Discipline of Physics, University of KwaZulu-Natal, Durban, South Africa*
- ^{am} *Also at Institute of Physics, Academia Sinica, Taipei, Taiwan*
- * *Deceased*